AN ABSTRACT OF THE DISSERTATION OF

Willem J. van Verseveld for the degree of Doctor of Philosophy in Forest Engineering presented on August 27, 2007

Title: Hydro-biogeochemical Coupling at the Hillslope and Catchment Scale

Abstract approved:_____

Jeffrey J. McDonnell

The specific objectives of this dissertation are to determine subsurface flow behaviors across different antecedent wetness conditions from a top-down perspective and to mechanistically assess the hydrological controls on DOC and N transport at the hillslope and catchment scale. The study area is a small catchment where hillslopes issue directly to the stream without any riparian zone modulation. Subsurface flow is measured from a 10 m wide trench. Streamflow is measured at the catchment outlet. Tree regression of subsurface flow and soil matric potential with controlling variables rainfall history and antecedent wetness show three different subsurface flow behaviors. Furthermore, unsaturated zone dynamics that follow the Darcy-Richard's equation are a dominant control on rainfall pulse propagation. DOC and DON concentrations in subsurface flow and in stream water decrease from the transition (Fall) period to the wet (Winter-Spring) period, suggesting supply-limited DOC and DON at the seasonal scale. Specific UV absorbance (SUVA), a tool to "fingerprint" sources, is always lower in subsurface flow compared to stream water, suggesting

transient groundwater (high SUVA) mixes differently with seepage groundwater (low SUVA) at the hillslope and catchment scale, even when subsurface flow and stream water are ‘in sync’ with respect to DOC and N during the wet period. The dominant flushing mechanism at the hillslope and catchment scale is vertical transport of nutrients, by ‘preferential flow’ to the soil-bedrock interface and then laterally downslope with limited supply of nutrients in the organic horizon, and higher contributions of deep soil water/seepage groundwater during the falling limb compared to the rising limb of the hydrograph. Two dominant flowpaths: vertical flow and then lateral along the soil-bedrock interface, mass transfer between a small mobile zone and a large immobile zone, and dispersive mixing, in combination with supply-limited DOC in the organic horizon/shallow layer lead to a conceptual model that resolves the double paradox: rapid mobilization of old water but variable runoff chemistry. Overall these findings result in a mechanistically plausible conceptual model how DOC and N are transported at the hillslope and catchment scale.

HYDRO-BIOGEOCHEMICAL COUPLING AT THE HILLSLOPE AND CATCHMENT SCALE

by

Willem J. van Verseveld

A DISSERTATION

submitted to

Oregon State University

in partial fulfillment of
the requirements of the
degree of

Doctor of Philosophy

Presented August 27, 2007

Commencement June 2008

Doctor of Philosophy dissertation of Willem J. van Verseveld presented on August 27, 2007.

APPROVED:

Major Professor, representing Forest Engineering

Head of the Department of Forest Engineering

Dean of the Graduate School

I understand that my dissertation will become part of the permanent collection of Oregon State University libraries. My signature below authorizes release of my dissertation to any reader upon request.

Willem J. van Verseveld, Author

ACKNOWLEDGEMENTS

First of all I would like to thank my advisor Jeff McDonnell for his encouragement, guidance and (financial) support during the last 4.5 years. His positive and enthusiastic attitude kept me going and motivated. I would like to express my sincere thanks to my co-advisor Kate Lajtha who provided lab space for running water samples and cleaning sample bottles and biogeochemical expertise. I am indebted to Susan Crow for her much needed explanation about running the auto-analyzer, acid-washing of bottles and filtering samples in Kate Lajtha's lab. I also would like to thank my committee members Steve Wondzell, Stephen Schoenholtz and John Selker for their helpful comments.

I would like to thank Kevin McGuire very much, for re-initiating the hydrological work in Watershed 10, H. J Andrews Experimental Forest, Oregon, that was started in the '70s, by constructing the trench in Watershed 10. Without this work, this dissertation would no have been possible. Also, thanks to John Moreau for field assistance and keeping those data-loggers running. Many thanks to Kevin McGuire, Ilja Tromp-van Meerveld, Markus Weiler, Kellie Vaché, April James, Chris Graham, Holly Barnard, Adam Mazurkiewicz and Luisa Hopp, I enjoyed working, discussing science, sprinkler-experimenting, playing tennis (Danish Hammer), mountain biking, skiing, drinking beer and sailing with you.

Of course, a special thanks to family and friends for their support. Especially, I would like to thank Marloes very much for her encouragement and support at home in

the field or lab with ‘chasing’ storms, filtering samples and running a sprinkler experiment for 24 days.

CONTRIBUTION OF AUTHORS

Jeff McDonnell was involved in the writing, design and data interpretation of all the chapters. Kate Lathja was involved in the writing and data interpretation of Chapters 3, 4 and 5.

Several other authors were involved in Chapter 5. Chris Graham and Holly Barnard helped with collection of field data, Holly Barnard and Renee Brooks provided isotopic analysis.

TABLE OF CONTENTS

TABLE OF CONTENTS (Continued)

TABLE OF CONTENTS (Continued)

TABLE OF CONTENTS (Continued)

TABLE OF CONTENTS (Continued)

LIST OF FIGURES

LIST OF FIGURES (Continued)

LIST OF FIGURES (Continued)

LIST OF FIGURES (Continued)

LIST OF TABLES

LIST OF TABLES (Continued)

1 Introduction

1.1 Introduction

Hillslopes are the fundamental units of upland catchments and subsurface flow is the dominant runoff mechanism in many forested upland catchments around the world (Bonell, 1998). Subsurface flow processes not only control the quantity of runoff from upland forested catchments but also the flushing of soluble nutrients into surface waters (Creed et al., 1996; Hill et al., 1999; McHale et al., 2002). Subsurface flow during and between rainfall events is complex and a myriad of different behaviors have been revealed since the first hillslope hydrological investigations in the 1940s by Hursh and Brater (1941). Recent reviews by Weiler et al. (2005) and Beven (2006) show that it has been difficult to generalize hydrological behavior from individual field studies that focus on only a handful of storm events. Studies have been almost exclusively reductionist in their approach and rules for hillslope behavior based on measurable rainfall or antecedent wetness conditions, even at well-studied sites, have not been developed (Uchida et al., 2005). Determining subsurface flow behaviors across different antecedent wetness conditions from a top-down perspective is major research need in hydrology (Sivalapan, 2003) and is a blueprint for identifying dominant hydrological controls on stream nutrient patterns.

The term flushing mechanism has been used in the hydrological literature to describe the movement of solutes in relation to hydrological processes (Burns, 2005). To date, the flushing of nutrients has been explained qualitatively by (1) a rising water table that intersects high nutrient concentrations in the upper soil layer (Hornberger et al., 1994; Boyer et al., 1997), (2) vertical transport of nutrients, by preferential or

matrix flow through the (deeper less bio-active) soil to the soil-bedrock interface and then laterally downslope (Hill et al., 1999; Buttle et al., 2001; Creed et al., 1996), and (3) vertical transport of nutrients into the soil and then laterally within the soil profile (e.g. Gaskin et al., 1989). In each of these conceptual models, an unlimited supply of nutrients during storms is assumed, although no hydro-biogeochemical studies to date have tested this explicitly. These flushing mechanisms have some commonality in the sense that flushing of soluble nutrients is conceptualized two dimensionally—where water flowpaths intersect the distinct vertical soil solution chemistry profile. Recent research has attempted to move away from this two-dimensional view of catchments and has focused on spatial sources of stream nutrients by dissecting the catchment into different geomorphic units (for example hillslopes vs. riparian areas). Because it is difficult to observe hydro-(bio)geochemical expressions of hillslopes in the stream (Hooper, 2001), due to chemical transformations in the riparian zone (Hedin et al., 1998) or infrequent episodic flow into the riparian zone (McGlynn and McDonnell, 2003), research has been mostly focused on the riparian zone (Cirmo and McDonnell, 1997). Consequently, sources of soluble nutrients from the hillslope component that make up the largest part of catchments, are more poorly understood compared than those from the riparian zone.

Flushing of soluble nutrients like dissolved organic carbon (DOC) typically results in a stream DOC pattern during storm events where DOC concentrations are higher on the rising limb of the storm hydrograph compared to the falling limb. This and other variable runoff chemistry patterns, in combination with the observation of

rapid mobilization of stored, pre-event water to the stream, has been coined the double paradox by Kirchner (2003). The double paradox in catchment hydrology and (bio)-geochemistry is a source of major debate and discussion in hydrology at present (Bishop et al, 2004; Jones et al., 2006; Kienzler and Naef, 2007). Resolving the double paradox is essential to improve our understanding of flowpaths and predicting transport of natural (bio)-geochemical solutes at the hillslope and catchment scale.

The main objective of this dissertation is to mechanistically assess the hydrological controls on DOC and N transport at the hillslope and catchment scale. The research site at the HJ Andrews Experimental Forest provides a somewhat controlled natural experiment for this work where debris flows in 1986 and 1996 evacuated riparian zone almost entirely. As such, hillslopes now issue directly into the stream without riparian zone modulation. This makes for potentially major research advancements whereby we can study directly how hillslope hydrological processes control stream hydro-biogeochemical response. A 10 meter wide trenched hillslope enables comparison between the single highly instrumented study hillslope and the ensemble of hillslopes that comprise the complete catchment. We use a combination of hydrometric data, natural tracers and artificial tracers to define the age, origin and flowpath of subsurface water movement and how these water fluxes control transport of dissolved constituents. A novel part of this work is the combination, for the first time that we are aware, of Specific UV absorbance SUVA (to “fingerprint” sources of dissolved organic matter), biogeochemical solutes of DOC and N (our soluble nutrients in question), and deuterium labeled water (in a controlled sprinkler

experiment). We used these data to develop a conceptual model with transport modeling and end member mixing analysis. We develop a mechanistically plausible conceptual model that explains the hydrological controls on DOC and N transport at the hillslope and catchment scale.

1.2 Thesis outline

Chapter 2 examines subsurface flow behavior using a top-down, tree regression approach. It focuses on analysis of subsurface flow and matric potential patterns in response to mean rainfall intensity over different lengths of time (minutes to months) across different antecedent wetness conditions. Wetting front velocities are calculated and regressed against mean rainfall intensity, and modeled with Hydrus-2D (Simunek et al., 1999) to test the hypothesis that wetting front advancement follows the Darcy-Richard's equation. These analyses, in combination with groundwater level measurements and the unsaturated hydraulic conductivity function are used to develop a conceptual model of subsurface flow behavior. Understanding dominant subsurface flow behaviors across different antecedent wetness conditions is important for the prediction of flushing of soluble nutrients into surface waters (e.g. Creed et al., 1996).

Chapters 3 and 4 focus on the hydrological controls on DOC and N transport at the hillslope and catchment scale. In chapter 3, the hydro-biogeochemical dynamics of the hillslope component are isolated (lateral subsurface flow from the 10 meter wide trenched hillslope) from the hydro-biogeochemical catchment response (stream water) by comparing the two responses during the transition (Fall) period and wet (Winter-

Spring) period under different flow conditions (rain-driven vs. non-driven). SUVA is used for "fingerprinting" water sources. In addition, the seasonal controls on lateral subsurface flow and stream water DOC and N concentrations are examined by comparing these patterns between the transition and wet period. Further, the role of antecedent wetness conditions at the storm event scale is investigated by relating antecedent wetness conditions to peak and flow averaged DOC and N concentrations. Lastly, annual patterns of DOC and N concentrations and dissolved organic matter quality (DOM) indices as DOC:DON and SUVA in organic horizon water, shallow and deep soilwater, transient groundwater, seepage groundwater and lateral subsurface flow and stream water are investigated.

Chapter 4 focuses on two storm events in December 2004 and May 2005 to test three flushing mechanism hypotheses at the hillslope and catchment scale: (1) a rising water table that intersects high nutrient concentrations in the upper soil layer (Hornberger et al., 1994; Boyer et al., 1997), (2) vertical transport of nutrients, by preferential or matrix flow through the (deeper less bio-active) soil to the soil-bedrock interface and then laterally downslope (Hill et al., 1999; Buttle et al., 2001; Creed et al., 1996), and (3) vertical transport of nutrients and then laterally within the soil profile (e.g. Gaskin et al., 1989). A combination of continuous fluorescence measurements at the hillslope and catchment scale, hydrometric data and chemical measurements (DOC, N, SUVA, Cl^- and SO_4^{2-}) of soil, groundwater, lateral subsurface flow and stream water, end-member mixing analysis are used to develop a mechanistic assessment of the flushing mechanism and the development of a

conceptual model of the dominant controls on DOC and N concentrations in lateral subsurface flow and stream water during storm events.

Chapter 5 presents a 24 day sprinkler experiment at the hillslope scale with the objective to mechanistically assess the double paradox of rapid mobilization of stored, pre-event water to the stream during storm events but variable runoff chemistry. Steady simulated rainfall was used in combination with the application of labeled (deuterium) in the sprinkler water at the start of the experiment to enable clear and unambiguous flowpath identification. Detailed measurements of DOC and N concentrations in organic horizon water, soil and groundwater and lateral subsurface flow, and weekly DOC and N soil extractions provide sources of DOC and N to lateral subsurface flow to answer whether DOC and N are supply-limited or not limited. Lastly, modeling the deuterium breakthrough curve with the advection-dispersion-first order mass transfer equation is used to constrain transport parameters to aid in the development of a plausible conceptual model of rapid mobilization of old water but with variable runoff chemistry.

1.3 References

Anderson, S. P., W. E. Dietrich, D. R. Montgomery, M. E. Conrad, and K. Loague (1997a), Subsurface flow paths in a steep, unchanneled catchment., *Water Resour. Res., 33*, 2637-2653.

Anderson, S. P., W. E. Dietrich, R. Torres, D. R. Montgomery and K. Loague (1997b), Concentration-discharge relationships in runoff from a steep, unchanneled catchment, flow, *Water Resour. Res., 33*, 211-225.

Beven,, K. J. (2006), Benchmark Papers in Hydrology, Streamflow generation processes, Selection, Introduction and Commentary by Keith J. Beven, IAHS Benchmark Papers in Hydrology Series, Editor: J. J. McDonnell.

Bishop, K., J. Seibert, S. Kölhler, and H. Laudon (2004), Resolving the double paradox of rapidly old water with variable responses in runoff chemistry, *Hydrol. Processes, 18,*185-189.

Bonell, M. (1998), Selected challenges in runoff generation research in forests from the hillslope to headwater drainage basin scale, *Journal of the American Water Resources Association, 34,* 765-785.

Boyer, E. W., G. M. Hornberger, K. E. Bencala, and D. M. McKnight (1997), Response characteristics of DOC flushing in an Alpine catchment, *Hydrol. Processes, 11,* 1635-1647.

Burns, D., (2005),What do hydrologists mean when they use the term flushing?, *Hydr. Processes, 19,* 1325–1327.

Buttle, J. M., S. W. Lister and A. R. Hill (2001), Controls on runoff components on a forested slope and implications for N transport, *Hydrol. Processes, 15,* 1065–1070.

Cirmo, C. P., and J. J. McDonnell (1997), Linking the hydrologic and biochemical controls of nitrogen transport in near-stream zones of temperate-forested catchments: A review, *J. Hydrol., 199,* 88-120.

Creed, I. F., L. E. Band, N. W. Foster, I. K. Morrison, J. A. Nicolson, R. S. Semkin, and D. S. Jeffries (1996), Regulation of nitrate-N release from temperate forests: A test of the N flushing hypothesis, Water *Resour. Res., 32,* 3337–3354.

Gaskin, J. W., J. W. Dowd, W. L. Nutter and W. T. Swank (1989), Vertical and Lateral Components of Soil Nutrient Flux in a Hillslope, *J. Environ. Qual., 18*: 403-410.

Hedin, L. O., Fischer, von, J. C., Ostrom, N. E., Kennedy, B. P., Brown, M. G., and G. P. Robertson (1998), Thermodynamic constraints on nitrogen transformations and other biogeochemical processes at soil-stream interfaces, *Ecology, 79,* 684-703.

Hill, A. R., W. A. Kemp, J. M. Buttle, and D. Goodyear (1999), Nitrogen chemistry of subsurface storm runoff on forested Canadian Shield hillslopes, *Water Resour. Res., 35,* 811 –821.

Hooper, R. B. (2001), Applying the scientific method to small catchment studies: a review of the Panola Mountain experience, *Hydr. Processes, 15,* 2039–2050

Hornberger, G. M., K. E. Bencala, and D. M. McKnight (1994), Hydrological controls on dissolved organic carbon during snowmelt in the Snake River near Montezuma, Colorado, *Biogeochemistry, 25,* 147– 165.

Hursh, C. R., and E. F. Brater (1941), Separating storm-hydrographs from small drainage-areas into surface- and subsurfaceflow, *Transactions of the American Geophysical Union, 3,* 863–871.

Jones, J. P., E. A. Sudicky, A. E. Brookfield, and Y.-J. Park (2006), An assessment of the tracer-based approach to quantifying groundwater contributions to streamflow, *Water Resour. Res., 42,* W02407, doi:10.1029/2005WR004130.

Kienzler, P. M., and F. Naef (2007), Subsurface storm flow formation at different hillslopes and implications for the ‘old water paradox’, *Hydrol. Processes*, (in press).

Kirchner, J. W., (2003), A double paradox in catchment hydrology and geochemistry, *Hydrol. Processes*, *17*, 871-874.

McGlynn, B. L., and J. J. McDonnell, Role of discrete landscape units in controlling catchment dissolved organic carbon dynamics, *Water Resour. Res., 39(4),* 1090, doi:10.1029/2002WR001525, 2003.

McHale, M. R., J. J. McDonnell, M. J. Mitchell, and C. P. Cirmo (2002), A field-based study of soil water and groundwater nitrate release in an Adirondack forested watershed, *Water Resour. Res., 38,*1031,doi:10.1029/2000WR000102.

Simunek, J., M. Sejna, and M. Th. van Genuchten (1999), The HYDRUS-2D software package for simulating two-dimensional movement of water, heat, and multiple solutes in variably saturated media. Version 2.0, *IGWMC - TPS - 53,* International Ground Water Modeling Center, Colorado School of Mines, Golden, Colorado, 251pp.

Sivapalan, M. (2003), Process complexity at hillslope scale, process simplicity at the watershed cale: is there a connection? *Hydrol. Processes*, *17,* 1037-1041.

Uchida, T., I. Tromp-van Meerveld and J. J. McDonnell (2005), The role of lateral pipe flow in hillslope runoff response : an intercomparison of non-linear hillslope response, *J. Hydrol.*, 311, 117-133.

Weiler, M., J. McDonnell, H. J. Tromp-van Meerveld and T. Uchida (2005), Subsurface Stormflow. Encyclopedia of Hydrological Sciences.Wiley and Sons.Whipkey.

2 The role of rainfall history on hillslope runoff behavior: A tree regression approach

Van Verseveld, W. J.

McDonnell, J. J.

2.1 Introduction

Understanding the link between rainfall and runoff is fundamental to hydrology. Hillslopes are the fundamental units of upland catchments and subsurface flow is the dominant runoff mechanism in many forested upland catchments around the world (Bonell, 1998). Subsurface flow processes not only control the quantity of runoff from upland forested catchments, understanding subsurface flow processes is also important for predicting landslide initiation (Iverson, 2000; Montgomery et al., 2002) and flushing of soluble nutrients into surface waters (e.g. Creed et al., 1996; McHale et al., 2002; Hill et al., 1999).

The subsurface flow response within hillslopes to rainfall has revealed a myriad of different behaviors from reductionist, bottom-up, experimental field investigations and modeling studies, between different sites and under different antecedent wetness conditions since the first hillslope hydrological investigations in the 1940s by Hursh and Brater (1941). These observed and modeled processes at the hillslope scale, recently reviewed by Weiler et al., (2005) and Beven (2006), included (1) transient saturation at the soil bedrock interface (Weyman, 1973; Dunne and Black, 1970) or transient saturation at soil horizon contacts (Whipkey, 1965; Mosley, 1979), (2) matrix- and vertical and lateral macropore flow (Mosley, 1982; McDonnell, 1990; Tsuboyama, 1994), (3) the observation that subsurface flow is dominated by pre-event water (Pearce et al., 1986; Sklash et al., 1986, McDonnell, 1990) and (4) unsaturated zone dynamics control subsurface flow response following field (Hewlitt and Hibbert, 1963; Harr, 1977; Torres et al, 1998; Retter et al., 2006) and modeling

studies (McCord et al., 1991 and Jackson, 1992). Notwithstanding these important observations, it has been difficult to generalize hydrological behavior from individual field studies that focused on a handful of storm events guided by a bottom-up approach. Hillslopes are complex (Sivalapan, 2003), and generalization of hillslope behavior based on measurable rainfall or antecedent wetness conditions, even at well-studied sites has not been developed (Uchida et al., 2005). Putting measured subsurface flow in a rainfall historical perspective allows us to generalize hillslope behavior.

We define historical rainfall as mean rainfall intensity over different lengths of time periods (from minutes to months) prior to the subsurface flow measurement. We realize the importance of antecedent wetness conditions and include that as a second variable controlling subsurface flow response. In contrast to most studies that have focused on subsurface flow and considered only storm events and storm subsurface flow, we consider all subsurface flow measurements from dry to wet conditions. Through this approach we make use of all the available subsurface flow and rainfall data and are able to identify the role of historical rainfall across a large variety of antecedent wetness conditions. Attempts that have been made to explore the role of rainfall history on subsurface flow behavior to date have been largely qualitative. Whipkey (1965) applied artificial rain through a sprinkler set up and showed that subsurface flow was affected by antecedent wetness conditions; total seepage outflow after dry conditions (> 4 days of no rain) was always lower than total seepage outflow after wet conditions (< 4 days of rain). Hewlett et al. (1977) analyzed the relation

between rainfall patterns and stormflow at the watershed scale and found that maximum rainfall intensity had little effect on the magnitude of peak discharge. On the other hand, Haga et al. (2005) showed that lag time between rainfall and runoff were controlled by antecedent wetness conditions, rainfall amount and intensity. Several hillslope studies have found that preferential flow through macropores is a function of antecedent wetness conditions, rainfall magnitude and intensity (Uchida et al., 2001; Sidle et al., 1995). Furthermore, work by Tani (1997) showed that soil matric potential on a steep forested hillslope increased linearly with an exponential increase in rainfall intensity and that under very wet conditions almost all rainfall contributed to storm subsurface flow.

Although past studies improved our understanding of rainfall subsurface flow relationships across different antecedent wetness conditions, these have been mostly qualitative and focused only on a handful of storm events. Thus, how can we link historical rainfall patterns across different antecedent wetness conditions to subsurface flow through a top-down approach, in a more quantitative way and by making use of all the available data? Tree regression is an approach that includes these features. Tree regression is a data-mining approach that does not need information about the complex rainfall subsurface flow relationship in parametric form. Through the use of historical variables (i.e. rainfall or antecedent wetness conditions), regression trees divide the dataset into smaller subsets and apply a simple model (i.e. average or linear regression) to each subset (e.g. Solomatine and Xue, 2004; Iorgulescu and Beven, 2004). Furthermore, tree regression results are easy to interpret, while other regression

techniques are often difficult to interpret (Loh, 2006). Because of these features, tree regression can be a pathway to new learning about subsurface flow processes.

Tree regression can only find relationships that are contained in the data (Iorgulescu and Beven, 2004) and thus needs extensive continuous datasets. We have collected extensive datasets that allow us to apply tree regression to the relation between rainfall and both soil matric potential and subsurface flow. This enables us to link unsaturated zone dynamics and subsurface flow from a historical rainfall perspective. Furthermore, we determine wetting front velocities from the matric potential dataset and relate these wetting front velocities to rainfall history by simple linear regression to examine how the unsaturated zone controls propagation of the rainfall pulse. Despite several studies that have shown the significant control of unsaturated zone dynamics (e.g. Torres et al., 1998; Tani, 1997) on the subsurface flow response, the link between unsaturated zone dynamics and subsurface flow remains poorly understood. Water table dynamics are available but are not as extensive as the other datasets and thus we do not use water table dynamics in the tree regression analysis. Rather, we plot water table dynamics (and soil matric potential dynamics) against subsurface flow to reveal different subsurface flow behaviors and link these to the subsurface flow tree regression results. All our analyses are ultimately aimed at exploring the role of rainfall history on subsurface flow behavior. We address the following questions: (1) What is the relationship between rainfall history and soil matric potential at different depths in the soil profile across different antecedent wetness conditions? (2) What is the relationship between rainfall history and wetting

front velocity? (3) How does rainfall history control hillslope scale subsurface flow across different antecedent wetness conditions?

2.2 Site description

The study hillslope is located in Watershed 10 (WS10, 10.2 ha), at the H. J. Andrews Experimental Forest (HJA), in the western Cascades, Oregon, USA (44.2° N, 122.25° W) (Figure 2.1). The study hillslope area is located on the south aspect of WS10, 91 m upstream from the stream gauging station. The 125 m long stream-to-ridge slope has an average gradient of 37º, ranging from 27º near the ridge to 48º adjacent to the stream (McGuire, 2007). Elevation at the study hillslope area ranges from 480 to 565 m.

During the 1970s, hydrological studies in WS10 (Harr, 1977; Ranken, 1974) were completed as part of the U.S. International Biological Program's Coniferous Forest Biome project. McGuire (2007) re-established this infrastructure with a 10 m wide trench to measure subsurface throughflow at the location of a seep that had been previously gauged in the early to mid-1970s (Harr, 1977). Ranken (1974) collected soil cores from seven soil pits at depths, 10, 30, 70, 110, 150 and 200 and 250 cm. Soil cores (in total 452) were analyzed for particle-size distributions, soil moisture release curves, stone content and saturated hydraulic conductivity. Mean values of the six replicated cores were reported in archived data records (Forest Service Data Bank, maintained by the HJA Long Term Ecological Research program).

The HJA climate has dry summers and wet winters and an annual precipitation of 2340 mm (averaged from 1995 to 2005). The wet winters are characterized by long and low intensity storms. Snow accumulation is not uncommon, and rarely persists for more than two weeks (Sollins, 1981). Elevations range from 470 m at the watershed flume to 680 m at the watershed divide. The vegetation is dominated by a naturally regenerated second growth Douglas-fir (*Pseudotsuga menziesii*) stand resulting from a 1975 clear-cut harvest.

Soil textures range from gravelly, silty clay loam to very gravelly clay loam. Surface soils are well aggregated, but lower depths (70-110 cm) exhibit more massive blocky structure with less aggregation than surface soils (Harr, 1977). Beneath the weakly developed A and B horizons is relatively low permeability, partially weathered parent material (saprolite) ranging in thickness from 1 to 7 meters (Ranken, 1974; Sollins et al., 1981). The depth to unweathered bedrock ranges from 0.3 to 0.6 m at the stream-hillslope interface and increases gradually toward the ridge to approximately 3 to 8 m. Soils are underlain by bedrock of volcanic origin, including andesitic tuffs and breccia (James, 1978). Soils, formed either in residual parent material or in colluvium originating from these deposits are highly andic and vary across the landscape as either Typic Hapludands or as Andic Dystrudepts (Yano et al., 2005).

2.3 Methods

2.3.1 Infrastructure

The hillslope trench for capturing lateral subsurface flow was constructed by McGuire (2007) and consists of steel sheeting that was anchored 5 cm into exposed bedrock and then sealed with cement. Bulk intercepted subsurface water was routed to a calibrated 30º V-notch weir that recorded stage at 10-minute time intervals using a 1-mm resolution capacitance water level recorder (TruTrack, Inc., model WT-HR). Precipitation was measured with a tipping bucket and storage gauge in a small canopy opening on the hillslope. The drainage area of the hillslope to the trench was delineated from a total station topographic survey of the entire hillslope (Figure 2.1). We used a rounded value of 0.2 ha in all subsequent analyses.

Soil matric potential was measured by 7 fast responding tensiometers (type: UMS T4, 1 bar porous cup), that were installed vertically in a triangle pattern (two sets of three tensiometers at 30 and 70 cm depth, and one tensiometer at 100 cm depth). The tensiometer triangle was located 25 m upslope from the hillslope base (Figure 2.1). We installed the tensiometers close to each other (horizontal distance downlslope was ~0.9 m) in a triangle to calculate unsaturated flow vectors without bias of an elevation gradient. This enabled us to investigate the possible occurrence of an unsaturated lateral flow component during storms.

Transient saturation was measured with 69 maximum rise cork wells (32 mm diameter). However only four wells showed (consistent) transient saturation . These were equipped with 1-mm resolution capacitance water level recorders (TruTrack,

Inc., model WT-HR). We had continuous data available for seepage well (A01) and well (E04) that showed transient groundwater, and used these groundwater datasets for our analysis (Figure 2.1). All the wells were installed until refusal (hand auger).

2.3.2 Regression tree approach

The selection of the appropriate historical input variables in tree regression is a difficult task. Most studies that have predicted runoff through tree regression have used both antecedent runoff and rainfall conditions as input variables over a given number of previous time steps (Sudheer et al., 2002; Solomatine and Xue, 2004). Iorgulescu and Beven (2004) adopted an alternative approach considering only variables that were actual inputs to the system (e.g. cumulative precipitation and evapotranspiration) at a given number of previous time steps.

We used cross-correlation to choose the appropriate maximum time step for the input variable. The maximum time step is the "memory" window of the system: the timescale over which the input to the system is still related to the system response. We used historical rainfall expressed as mean rainfall intensity over different lengths of time before subsurface flow observation (time lag) as the input variable. Mean rainfall intensity was cross-correlated to our output variables, subsurface flow and matric potential at 30, 70 and 100 cm depth, over different time lags. The time lags were calculated as follows. We incremented the time lags progressively with a geometric progression:

$$T(i) = 10 \times 1.02^{(i+1)} \quad (1)$$

where T is the time lag and i refers to the time step (1 min). The original precipitation dataset consisted of rainfall totals at a 10 minute time step. The sequence of calculated time lags T, with time lags < 10 minutes, was converted to a time lag sequence with time intervals of $k \cdot 10$, where $k = 1, 2, \ldots . n$. We used the second value (20 minutes) and then every other value from this final sequence and also considered a time lag of 0 minutes in our tree regression analysis. The calculated value of an input variable at a given time lag included the input at the current time step. The cross correlation indicated a maximum time lag of 60 days. This method resulted in 155 different variables (mean rainfall intensity over 155 different time lags), which we define as our predictor variables.

2.3.3 GUIDE regression tree algorithm

We used the GUIDE regression tree algorithm (Loh, 2002), to recursively split the WS10 hillslope dataset. We used the GUIDE option to fit a linear model to the observations in each tree partition. GUIDE is similar to the more common classification and regression trees (CART) approach of Breiman et al. (1984) in the sense that it also constructs a sequence of nested trees and then uses cross validation to select the optimal tree size (Loh, 2006). We used three-cross-validation in our analysis. The optimal tree was the smallest tree within 0.5 times the smallest prediction mean square error (PMSE) found in the cross-validation. GUIDE used the least squares error criterion to choose the predictor variable in the linear regression. At each split, GUIDE performed lack-of-fit tests of the residuals to choose a predictor

variable to split the data (Loh, 2006). At each node, it used the signs of the residuals to separate the observations into two classes and then used curvature and variable interaction tests to choose the best split variable (Loh, 2002). GUIDE has the option to define a predictor variable as a fitting variable, a splitting variable or both. A splitting variable is used only to split the data, and a fitting variable is used only as a regressor in the nodes.

We applied the GUIDE tree regression to each dataset by using 1/4 of the dataset to validate the tree regression model. The rest of the dataset was used to train the tree-regression model. The regression tree algorithm was applied to the rainfall-subsurface flow record and the three rainfall-soil matric potential records from 30, 70 and 100 cm depth. The rainfall – subsurface flow record available for this study was almost 455 days of 10 minute rainfall and subsurface flow measurements over two main periods: April 2002-January 2003 and December 2004-July 2005. Gaps in the subsurface flow record existed in the second period because of problems with the water level recorder. The rainfall-matric potential record was 10 minute data collected continuously from November 2004 to July 2005. The soil matric potential records at 30 and 70 cm depth were averaged for the tree regression analysis.

We used simple linear models in the partitions to model each rainfall-soil matric potential record and the rainfall-subsurface flow record. The fitting variable was mean rainfall intensity at 155 different time steps previous to each soil matric potential measurement. We used the splitting variable “soil matric potential 6-hours previous to each soil matric potential measurement” to approximate antecedent

wetness conditions. We used the same method for the rainfall-subsurface flow record. We used mean rainfall intensity at 155 different time steps before each subsurface flow measurement as a fitting variable. We used the splitting variable subsurface flow 6-hours before each subsurface flow measurement as an approximation for antecedent wetness conditions. Splitting variables were constrained to 6 hour time lags. A preliminary analysis of other time lags (3, 12, 24 hours) for subsurface flow and matric potential showed that time lags of more than 6 hours resulted in splits in the tree regression that were difficult to interpret. With time lags of more than 6 hours similar mean values in the left and right nodes of a partition occurred.

Figure 2.2 illustrates in a schematic way how the GUIDE tree regression algorithm works. X_1 is the splitting variable (in our case subsurface flow or matric potential 6-hour before observation) that splits the dataset (Figure 2.2.a) into data partitions based on the statistical rules used in the GUIDE algorithm (Figure 2.2.b). Each final data partition is modeled with a linear regression model, with X_2 (in our case mean rainfall intensity at different time lags ? t) as the independent variable. The result is an easy to interpret regression tree (Figure 2.2.c), that splits the dataset into partitions through simple rules. The end nodes represent the final partitions of the tree (squares).

2.3.4 Wetting front analysis

The arrival time of the wetting front at each tensiometer was determined following a method similar to the method used by Tymchak and Torres (2007). The

first significant decrease in soil matric potential after the start of rainfall (t_r) was defined as the arrival time (t_w) of the wetting front. Standard deviations of soil matric potential during 3-hour intervals of no rainfall were calculated for soil matric potentials < 4 kPa at 30 cm and soil matric potentials < 3 kPa at 70 and 100 cm depth. A significant change in soil matric potential was defined as a decrease that exceeded the 90% quartile standard deviation of the calculated standard deviations (0.06 kPa). Average wetting front velocity was calculated as follows:

$$v_w = \frac{d}{(t_w - t_r)} \tag{2}$$

where, d [mm] is the tensiometer depth, and v_w [mm h^{-1}] is the average wetting velocity. Average wetting front velocities were analyzed for storm events that were separated by at least 3 hours of no rainfall and with a wetting front response at depths 30, 70 and 100 cm. This resulted in a total of 27 storm events. Mean rainfall intensities were calculated during periods between start of rainfall and wetting front arrival time for each tensiometer. Average wetting front velocities were linearly regressed to corresponding mean rainfall intensities.

2.4 Results

2.4.1 Rainfall history and soil matric potential

We ran a tree regression for each soil matric potential dataset at 30, 70 and 100 cm to determine the relation between rainfall history and soil matric potential at different soil depths. Rainfall history was expressed as mean rainfall intensity (input

variable) over 155 different previous time steps (fitting variable) in the tree regression. The tree regression used matric potential with a 6 hour time lag as the splitting variable. The end nodes of the tree regression of matric potential at 30 cm depth (Figure 2.3.) represented the final partition of the dataset. In each end node, soil matric potential was fitted linearly to mean rainfall intensity at different time lags (fitting variable) and was positively related to mean rainfall intensity in each end node. End nodes with more negative soil matric potentials on average were correlated to mean rainfall intensities with longer time lags (Table 2.1). Figure 2.4 shows the observed and fitted matric potential time series at 30 cm depth. The tree regression model had 39 end nodes and the prediction appeared continuous with slight stepwise changes in matric potential. The linear regression in each end node made the prediction appear more continuous compared to a constant fit model. The tree regression model captured both the magnitude and timing of the soil matric potential response (Figure 2.3). The coefficient of determination (r^2) of the regression tree and mean square error (MSE) of the validated cases, were 0.94 and 0.95 respectively.

The regression trees for matric potential at 70 and 100 cm depth showed results similar to those of the 30-cm tensiometer. The tree regression result for 70 and 100 cm depth showed 40 and 23 end nodes respectively. The most important difference between the regression tree for 30 cm depth and the regression trees at 70 and 100 cm depth was that rainfall history in the end nodes of the two latter tree regressions was characterized by longer time lags (Figure 2.5). Mean soil matric potential values at 70 and 100 cm depth were linear regressed to similar fitting variables with respect to the

time lag of mean rainfall intensity (Figure 2.5). The r^2 of the regression tree and MSE of the validated cases were 0.94 and 5.96 x 10^{-2} for 70 cm depth, and 0.78 and 0.12 for 100 cm depth, respectively.

We extracted additional information from the tree regression analysis by examining the relationship between mean soil matric potential (the average of measured soil matric potential values in each end node) and average rainfall history (the average of mean rainfall intensity values used in the linear regression in each end node) of the regression tree. We ran a second tree regression for the depths 30, 70 and 100 cm for soil matric potential values that were = -1 kPa. Smallest time lags of rainfall history for soil matric potential = -1 kPa were 2 hours for 30 and 100 cm depths, and 20 minutes for 70 cm depth. These time lags indicate very fast response times of matric potential to rainfall inputs. Mean soil matric potential was exponentially related to average rainfall history in the end nodes of the regression tree for the three different depths (Figure 2.5). While the average mean rainfall intensity did not change much for soil matric potential values < -1kPa at all three depths, an increase in matric potential from -1 to 0 kPa was related to a very fast increase in average mean rainfall intensity.

2.4.2 Rainfall history and wetting front velocity

Initial conditions at depths 30, 70 and 100 cm measured by the 7 tensiometers, before the 27 storm events ranged between 0.48 and 5.68 kPa. Despite this variation in initial conditions, plotting these initial conditions against wetting front velocities

suggested wetting front velocities were not controlled by initial conditions. Each tensiometer nest showed progressive wetting front advancement with depth. This indicates bypass flow with depth did not occur at our site. Wetting front velocities ranged from 11.8– 163.7 mm h^{-1} (at 30 cm depth), 15.7– 135.4 mm h^{-1} (at 70 cm depth) and 22.6 – 153.7 mm h^{-1} (at 100 cm depth). During most storm events (19 out of 27) wetting front velocities increased with depth, while the remainder of storm events showed wetting front velocities decreasing with depth. The trend in wetting front velocities with depth appeared to be related to mean rainfall intensity calculated over the period between start of rainfall and wetting front arrival time for each depth and tensiometer. During storm events that showed increasing wetting front velocities with depth, 12 out of 19 of these storm events were characterized by increasing mean rainfall intensities over three time periods (time periods between start of rainfall and wetting front arrival time at 30, 70 and 100 cm depth respectively). Two out of these 19 storm events were characterized by constant rainfall intensities (changes were < 0.1 mm hr^{-1}). Six out of 8 storm events that showed decreasing wetting front velocities with depth were characterized by decreasing mean rainfall intensities. Furthermore, mean rainfall intensity largely controlled wetting front velocities as shown by the linear regression between these two variables (Figure 2.7).

2.4.3 Rainfall history and subsurface flow

Figure 2.8 illustrates the tree regression result for subsurface flow with mean rainfall intensity as a fitting variable and subsurface flow with a 6 hour time lag as a

splitting variable. The r^2 and MSE of the regression tree was 0.95 and 1.99×10^{-3}, respectively. Subsurface flow modeled with the regression tree captured both the magnitude and timing of the observed subsurface flow very well (Figure 2.9). The time lags of mean rainfall intensity ranged between 3.7 and 20.3 hours for all end nodes except one. This end node with the lowest mean subsurface flow value was correlated to mean rainfall intensities with a time lag of 11.7 days.

Three distinct hydrological behaviors were evident from this regression tree: (1) low discharge values ($Q = 0.0208$ L s^{-1}) were correlated with rainfall history with a time lag of 11.7 days, (2) intermediate discharge values ($0.0208 < Q = 0.13$ L s^{-1}) were correlated with rainfall history with short time lags (between 3.7 and 6.3 hours), and (3) high discharge values ($Q > 0.13$ L s^{-1}) correlated with rainfall history with short time lags (between 6 and 20.3 hours). We plotted mean subsurface flow against the average rainfall history value from each end node of the un-pruned regression tree to further examine the relation between these two variables (Figure 2.10). Average rainfall history for each end node was calculated as the average of the "mean rainfall intensities" that were used in the linear regression. Mean subsurface flow was the average of measured subsurface flow values included in each end node. The slope of the relation between mean subsurface flow and average mean rainfall intensity decreased with an increase in mean lateral subsurface flow from behavior 1 to 3, except for the highest mean subsurface flow value (Figure 2.10). This indicates that as the system wetness increased (higher subsurface flow values were related to higher antecedent wetness conditions (Figure 2.8)), the system became on average more

responsive to rainfall up till the highest mean subsurface flow value that was related to a high average mean rainfall intensity of 1.92 mm h^{-1}.

2.4.4 Testing the physical meaning of the subsurface flow tree regression

We used independent groundwater and soil matric potential data to test whether the three different behaviors from the subsurface flow tree regression result were consistent with internal hydrological hillslope dynamics. Subsurface flow was plotted against soil matric potential at 30 cm and groundwater height from well A01 (seepage) and well E04 (transient groundwater). The relation between subsurface flow and -70 and 100 cm depth soil matric potential respectively, were very similar to the relation between subsurface flow and 30 cm depth soil matric potential, so they are not shown here. These relationships were partitioned with the splitting rules (of the three different behaviors) of the subsurface flow regression tree (Figure 2.10). The range of groundwater heights and soil matric potential values decreased with an increase in subsurface flow values. Consequently, these ranges also decreased from subsurface flow hydrological behavior 1 to subsurface flow hydrological behavior 3. The rules that defined each hydrological behavior partitioned the subsurface flow– groundwater height and – soil matric potential relationships at points where the slope of these relationships changed. While the partitions for the seep well A01, well E04 and soil matric potential at 30 cm depth showed overlap, these results indicate that the rules we found in the subsurface flow regression tree were consistent with internal hillslope hydrological dynamics.

2.5 Discussion

While the rainfall runoff relationship is fundamental in hydrology, the link between rainfall and subsurface flow is still poorly understood. Observational bottom-up field studies of hillslope subsurface flow have shown a myriad of different runoff mechanisms recently reviewed by Weiler et al. (2005) and Beven (2006). While these studies have improved our understanding of subsurface flow processes it has been difficult to generalize hydrological behavior from individual field studies that focused on a handful of storm events guided by a bottom-up approach. Generalization of hillslope behavior at even well-studied sites based on measurable rainfall or antecedent wetness conditions, has not been developed (Uchida et al., 2005). This study showed that putting measured subsurface flow in a rainfall historical perspective allows us to generalize hillslope behavior.

We used the GUIDE tree regression algorithm as a pathway to new learning about subsurface flow processes by extracting information from the complete dataset. We used historical rainfall expresses as mean rainfall intensity at different time lags as an input variable that was only allowed to fit the data partitions of the tree. Subsurface flow and matric potential 6 hour prior to observation were used to split the dataset of subsurface flow and matric potential at 30, 70 and 100 cm depth respectively into partitions and as approximations of antecedent wetness conditions. This approach resulted in cleary interpretable tree regression results, and led to new insights in subsurface flow processes at our site. We found an exponential relationship between average matric potential and average rainfall history. This relationship had a threshold

effect near -1 kPa; a very fast increase in average rainfall history was related to a small decrease in matric potential from -1 to 0 kPa. In addition linear regression showed that wetting front velocities were significantly related to rainfall history. Furthermore, we were able to detect three different subsurface flow behaviors from the subsurface flow tree regression result.

We have put subsurface flow and soil matric potential dynamics in a historical rainfall perspective through tree regression. We are aware that evapotranspiration and intensity smoothing of rainfall patterns (i.e. throughfall) are important controls on subsurface flow (e.g. Keim et al., 2006) and soil matric potential dynamics. Accounting for evapotranspiration and throughfall patterns was outside the scope of this study, simply because throughfall data was not available and our main objective was to explore the rainfall subsurface flow relationship at our site. However, in the following sections we interpret the physical meaning of our tree regression result in the context of historical rainfall patterns in more detail. We consider briefly where throughfall and evapotranspiration may have played a role in the observed subsurface flow behaviors. Subsurface flow behavior 1 was characterized by low runoff values and related to historical rainfall with a time lag of 11.7 days. The physical interpretation of this time lag in relation to the time lags observed in the other two subsurface flow behaviors is difficult. Despite this, it indicates a disconnection between rainfall and subsurface flow. This interpretation is in agreement with a large range in groundwater levels and soil matric potential values during behavior 1. With respect to evapotranspiration and throughfall we can say that both were likely

significant controls on subsurface flow and internal hillslope dynamics during behavior 1. Subsurface flow behavior 3 was more sensitive to historical rainfall on average (i.e. subsurface flow increased rapidly to rainfall inputs) than subsurface flow behavior 2. We can explain this difference in response to historical rainfall by unsaturated zone dynamics. The vertical propagation of the rainfall input in the unsaturated zone was faster during subsurface flow behavior 3 than subsurface flow behavior 2 and we will discuss this in more detail in the next sections. Both subsurface flow behavior 2 and 3 are related to relatively high rainfall history values with short time lags (hours). This implies that evapotranspiration was not a dominant control during the time lag of rainfall history, since both subsurface flow behaviors were controlled by wet conditions. However, throughfall may have played an important role, and the combination of interception and canopy evaporation was likely besides unsaturated zone dynamics an additional control on the difference between subsurface flow behavior 2 and 3.

2.5.1 Three subsurface flow hydrological behaviors

This study clearly showed that subsurface flow is a function of antecedent wetness conditions (expressed as subsurface flow 6 hours before observation) and rainfall history. Above a threshold subsurface flow of 0.13 L s^{-1}, small changes in groundwater and soil matric potential caused substantial increases in subsurface flow. The tree regression result of subsurface flow showed that the slope of subsurface flow-average rainfall history for this subsurface flow domain was small compared to

subsurface flow = 0.13 L s^{-1}, if we don not consider the highest mean subsurface flow value. Furthermore, this subsurface flow domain was characterized by wet conditions, 93% of the time matric potential was = -1.5 kPa and 68% of the time matric potential was = -1 kPa at 30 cm depth. To link these matric potential patterns to unsaturated hydraulic conductivity at our site we modeled the unsaturated hydraulic conductivity function with the Brooks-Corey model using the method of Campbell (1974) for moisture release curves at 30, 70 and 100 cm depth:

$$y(z) = y_e(z)\left(\frac{q(z)}{q_s(z)}\right)^{-l(z)} \tag{3}$$

where z [cm] is soil depth, y [cm] is pore pressure, y_e [cm] is the air entry pressure, q [cm^3/cm^3] is water content, q_s [cm^3/cm^3] is the saturated water content and l [-] is the pore size distribution. The unsaturated hydraulic conductivity function was calculated with:

$$K(q,z) = K_s(z)\left(\frac{q(z)}{q_s(z)}\right)^{3+\frac{2}{l(z)}} \tag{4}$$

where $K(q,z)$ [mm h^{-1}] is the unsaturated hydraulic conductivity and $K_s(z)$ [mm h^{-1}] is the saturated hydraulic conductivity. Saturated hydraulic conductivity was estimated by (McGuire et al., 2007):

$$K_{sat} = 8.7 \cdot 10^3 \exp(-z/0.56) \tag{5}$$

where K_{sat} [mm h^{-1}] is saturated hydraulic conductivity and z [m] is soil depth. For matric potential > -1 kPa, $\partial K / \partial \Psi$ becomes significantly larger in the unsaturated hydraulic conductivity soil matric potential function (Figure 2.11). This indicates that

during the wet conditions characteristic for this subsurface flow domain the frequently observed fast increase in subsurface flow at our site was caused by a sudden increase in unsaturated hydraulic conductivity, while groundwater and soil matric potential showed small changes. The highest mean subsurface flow value was related to a relatively high average mean rainfall intensity, suggesting that besides wet conditions a substantial increase in mean rainfall intensity was necessary. Furthermore, the wetting front analysis showed that wetting front velocities increased linearly with mean rainfall intensity. This flow domain was characterized by high average rainfall history values. Consequently, this subsurface flow domain was characterized by fast wetting front velocities.

Low subsurface flow values were correlated to a historical rainfall with a time lag of 11.7 days and were characterized by a high range in matric potential values and groundwater levels, while subsurface flow values showed a small range. This part of the dataset was characterized by hillslope water deficits, and thus storage must be filled first before rainfall patterns and subsurface flow are more strongly connected. This disconnection between soilwater, groundwater and subsurface flow follows also from the larger time lags of historical rainfall found in the tree regression of soil matric potential compared to the tree regression results of hillslope runoff.

The intermediate subsurface flow values were clearly a transition state between dry conditions with high soil water deficits, and wet antecedent conditions where groundwater and soil matric potential were in a semi-steady-state condition. This transitional state was characterized by small soil water deficits. Nevertheless,

unsaturated fluxes during this state were relatively small because soil matric potentials were 73% of the time < -1 kPa. Thus, while on average soil matric potential increased substantially with small changes in mean rainfall intensity during the transitional state, the unsaturated zone tended to have a delaying effect on rainfall rates during the transitional state. In addition, wetting front velocities were likely smaller compared to wetting front velocities during higher subsurface flow conditions, because subsurface flow during the transitional state was related to lower historical rainfall values on average.

2.5.2 Conceptual model of subsurface flow based on tree regression

The three subsurface flow behaviors we extracted from the tree regression are illustrated in a simplified decision tree in Figure 2.13. The influence of antecedent wetness conditions expressed as subsurface flow 6 hour prior observation, on the subsurface flow response is obvious from this decision tree. Others (e.g. Whipkey, 1965; Tani, 1997; Haga et al., 2005) have also demonstrated the influence of antecedent wetness conditions on the subsurface flow response. The graphs below each hydrological behavior, demonstrate (1) the relations between groundwater, matric potential and subsurface flow, and (2) the sensitivity of subsurface flow to rainfall history on average that was typical for each hydrological behavior. The sensitivity of subsurface flow to average rainfall history was a function of (1) hillslope water deficits we inferred from antecedent wetness conditions and the relation between groundwater and matric potential and subsurface flow, and (2) the unsaturated

hydraulic conductivity function. For example under hydrological behavior 1, subsurface flow does not respond to rainfall inputs, while groundwater and matric potential show a large range in values, suggesting hillslope storage is filled during this behavior.

The long time lag of rainfall history (11.7 days) of hydrological behavior 1 compared to the time lags of the other two hydrological behaviors, and the lack of subsurface flow response to rainfall during hydrological behavior I indicates a threshold effect. Other studies have reported a threshold effect in the rainfall-subsurface flow relationship (e.g. Tani, 1997; Tromp-van Meerveld and McDonnell, 2006).

In our conceptual model of subsurface flow we also included the average "matric potential" – "rainfall history" relationship we extracted from the matric potential regression trees. Average matric potential increased linearly with an exponential increase in average "rainfall history". In addition, our conceptual model shows that the lag time of rainfall history regressed in each end node of the tree against matric potential decreased with a decrease in matric potential. Tani (1997) found an exponential relationship between peak matric potential at 10 cm soil depth and rainfall intensity averaged over a 3-hour period before the peak. These field experimental findings were related to a theoretical analysis of Rubin and Steinhardt (1963) based on the Darcy-Richard's equation. Their analysis showed that soil moisture contents would approach a definite limit when the rainfall intensity was less or equal the saturated hydraulic conductivity. Furthermore, Rubin et al. (1964) showed

that soil moisture contents at increasing soil depths tended to approach a constant level during steady state vertical infiltration in laboratory soil columns. They showed soil moisture increases linearly with an exponential increase in rainfall intensities. While the analysis of Rubin and Steinhardt (1963) and Rubin et al. (1964) were based on constant rainfall intensities and our matric potential-mean rainfall intensity relationship was based on an average relationship, it indicates that vertical flow at our site follows the Darcy-Richard's equation. Across the three different hydrological behaviors subsurface flow values were related to higher historical rainfall values on average, suggesting that wetting front velocities were increasing from behavior 1 to 3.

2.6 Conclusions

Our examination of subsurface flow through the use of regression trees uncovered three distinct behaviors: (1) a disconnection between rainfall and subsurface flow, characterized by soil moisture deficits and filling of storage, (2) a transitional phase, where the unsaturated zone damped the rainfall signal and (3) a wet phase, where groundwater and matric potential were in a semi-steady-state condition, and subsurface flow responded immediately to rainfall. Accounting for rainfall history and antecedent wetness conditions enabled us to quantitatively separate subsurface flow into different behavioral classes. We showed that on average the unsaturated hydraulic conductivity function controlled the different response of subsurface flow to rainfall history between behavior 2 and 3. Behavior 3, in contrast to behavior 2, was characterized by conditions where $\partial K / \partial \Psi$ becomes significantly larger in the

unsaturated hydraulic conductivity soil matric potential function, which made subsurface flow more responsive to historical rainfall, except for the highest mean subsurface flow value that was related to relatively high average mean rainfall intensity. Throughfall likely played an additional role besides unsaturated zone dynamics in the different response to rainfall history between subsurface flow behavior 1 and 2. Tree regression of matric potential showed that average matric potential increased linearly with an exponential increase in average rainfall history, an indication that vertical flow at our site follows Darcy-Richard's equation. In addition we showed that wetting front velocities were largely controlled by mean rainfall intensity between the start of rainfall and wetting front arrival time, and not by initial conditions. This analysis demonstrated that tree regression of subsurface flow and matric potential patterns is a pathway to new learning about subsurface flow processes. Tree regression results are easily interpretable in comparison to other statistical techniques that are often difficult to interpret. Overall, our study showed that putting subsurface flow patterns in a historical rainfall perspective across different antecedent wetness conditions, allowed us to generalize hillslope behavior.

2.7 Acknowledgements

This work was supported through funding from the National Science Foundation (grant DEB 021-8088 to the Long-Term Ecological Research Program at the H. J. Andrews Experimental Forest) and Department of Forest Engineering at Oregon State University. We thank John Moreau for providing field assistance and K.

J. McGuire for providing additional subsurface flow and rainfall data. We also thank R. D. Harr and D. Ranken for initiating the hillslope studies at WS10, and K. J. McGuire for re-initiating this site and providing generously rainfall and subsurface flow data.

2.8 References

Beven,, K. J. (2006), Benchmark Papers in Hydrology, Streamflow generation processes, Selection, Introduction and Commentary by Keith J. Beven, IAHS Benchmark Papers in Hydrology Series, Editor: J. J. McDonnell.

Bonell, M. (1998), Selected challenges in runoff generation research in forests from the hillslope to headwater drainage basin scale, *Journal of the American Water Resources Association, 34,* 765-785.

Breiman, L., J. Friedman, R. Olshen and C. Stone (1984), *Classification and Regression Trees,* Wadsworth, Belmont, Calif. Richland, Wash.

Campbell, G.S., (1974), A simple method for determining unsaturated conductivity from moisture retention data, *Soil Science, 117,* 311-314.

Creed, I.F., L.E. Band, N.W. Foster, I.K. Morrison, J.A., Nicolson, R.S. Semkin and D.S. Jeffries (1996), Regulation of nitrate-N release from temperate forests: A test of the N flushing hypothesis, *Water Resour. Res., 32,* 3337-3354.

Dunne, T., and R. D. Black (1970), An experimental investigation of runoff production in permeable soils, *Water Resour. Res., 6,* 478– 490.

Haga, H., Y. Matsumoto, J. Matsutani, M. Fujita, K. Nishida, and Y. Sakamoto (2005), Flow paths, rainfall properties, and antecedent soil moisture controlling lags to peak discharge in a granitic unchanneled catchment, *Water Resour. Res., 41,* W12410, doi:10.1029/2005WR004236.

Harr, R. D., (1977), Water flux in soil and subsoil on a steep forested slope, *J. Hydrol., 33,* 37-58.

Hewlett, J. D., J. C. Fortson and G. B. Cunningham (1977), The effect of rainfall intensity on storm flow and peak discharge from forest land, *Water Resour. Res., 13,* 259-266.

Hewlett, J. D., and A. R. Hibbert (1963), Moisture and energy conditions within a sloping soil mass during drainage, *Journal of Geophysical Research, 68,* 1081-1087.

Hill, A. R., W. A. Kemp, J. M. Buttle, and D. Goodyear (1999), Nitrogen chemistry of subsurface storm runoff on forested Canadian Shield hillslopes, *Water Resour. Res., 35,* 811 –821.

Hursh, C. R., and E. F. Brater (1941), Separating storm-hydrographs from small drainage-areas into surface- and subsurfaceflow, *Transactions of the American Geophysical Union, 3,* 863–871.

Iorgulescu, I., and K. J. Beven (2004), Nonparametric direct mapping of rainfall-runoff relationships: An alternative approach to data analysis and modeling?, *Water Resour. Res.*, 40, W08403, doi:10.1029/2004WR003094.

Iverson R.M. (2000), Landslide triggering by rain infiltration, *Water Resour. Res., 36,* 1897-1910.

Jackson, C. R., (1992), Hillslope infiltration and lateral downslope unsaturated flow, *Water Resour. Res., 28,* 2533-2539.

James, M. E., (1978), Rock weathering in the central western Cascades, M.S., University of Oregon, Eugene.

Keim, R., H. J. Tromp-van Meerveld and J. J. McDonnell (2006), A virtual experiment on the effects of evaporation and intensity smoothing by canopy interception on subsurface stormflow generation, *J. Hydr., 327,* 352-364.

Loh, W. Y. (2002), Regression trees with unbiased variable selection and interaction detection. *Statistica Sinica,* 12, 361-386

Loh, W. Y. (2006), Regression by Parts: Fitting Visually Interpretable Models with GUIDE, *Handbook of Computational Statistics,* vol. III, Springer, (in press)

McCord, J. T., D. B. Stephens, and J. L. Wilson (1991), Hysteresis and state-dependent anisotropy in modeling unsaturated hillslope hydrologic processes, *Water Resour. Res., 27,* 1501–1518.

McHale, M. R., J. J. McDonnell, M. J. Mitchell, and C. P. Cirmo (2002), A field-based study of soil water and groundwater nitrate release in an Adirondack forested watershed, *Water Resour. Res., 38,*1031,doi:10.1029/2000WR000102.

McDonnell, J. J. (1990), A rational for old water discharge through macropores in a steep, humid catchment, *Water Resour. Res., 26,* 2821-2832

McGuire, K. J., J. J. McDonnell, M. Weiler (2007), Integrating tracer experiments with modeling to infer water transit times. *Advances in Water Resources, 30,* 824-837.

Montgomery D.R., W. E. Dietrich and J. T. Heffner (2002), Piezometric response in shallow bedrockat CB1: Implications for runoff generation and landsliding, *Water Resour, Res., 38,* 101-1018.

Mosley, M.P., (1982), Subsurface flow velocities through selected forest soils, South Island, New Zealand, *J. Hydrol., 55,* 65-92

Mosley, M.P., (1979), Streamflow generation in a forested watershed, *Water Resour. Res., 15,* 795-806.

Ranken, D. W., (1974), Hydrologic properties of soil and subsoil on a steep, forested slope, M.S., Oregon State University, Corvallis.

Retter, M., P. Kienzler and P. F. Germann (2006), Vectors of subsurface stormflow in a layered hillslope during runoff initiation, *Hydrology and Earth System Sciences, 10,* 309-320.

Rubin, J. and R. Steinhardt (1963), "Soil water relation during rain infiltration: I. Theory." *Soil Sci. Soc. Am. Proc.*, 27, 246–251

Rubin. J.. R. Steinhardt and P. Reiniger (1964), "Soil-water relations during rain infiltration II: moisture content profiles during rains of low intensities." *Proc., Soil Sci. Soc. of Am., 28,* 1-5.

Pearce, A. J., M. K. Stewart, and M. G. Sklash (1986), Storm runoff generation in humid headwater catchments, 1, Where does the water come from?, *Water Resour. Res., 22,* 1263–1271.

Sidle, R. C., Y. Tsuboyama, S. Noguchi, I. Hosoda, M. Fujieda, and T. Shimizu (1995), Seasonal hydrologic response at various spatial scales in a small forested catchment, Hitachi Ohta, Japan, *J. Hydrol., 168,* 227-250.

Sivapalan, M. (2003), Process complexity at hillslope scale, process simplicity at the watershed cale: is there a connection? *Hydrol. Processes, 17,* 1037-1041.

Sklash, M.G., M.K. Stewart, and A.J. Pearce (1986), Storm runoff generation in humid headwater catchments: A case study of hillslope and low-order stream response, *Water Resour. Res., 22,* 1273-1282.

Sollins, P., K. J. Cromack, F. M. McCorison, R. H. Waring, and R. D. Harr, (1981). Changes in nitrogen cycling at an old-growth Douglas-fir site after disturbance. *Journal of Environmental Quality,* 10: 37-42.

Solomatine, D. P. and Y. Xue (2004), M5 Model Trees and Neural Networks: Application to Flood Forecasting in the Upper Reach of the Huai River in China *Journal of Hydrologic Engineering, 9,* 491-501

Sudheer, K. P, A. K. Gosain, K. S. Ramasastri (2002), A data-driven algorithm for constructing artificial neural network rainfall-runoff models, *Hydrol. Process.,* 16, 1325–1330

Tani, M. (1997), Runoff generation processes estimated from hydrological observations on a steep forested hillslope with a thin soil layer, *J. Hydrol.,* 200, 84-109.

Torres, R., W. E. Dietrich, D. R. Montgomery, S. P. Anderson, and K. Loague, (1998), Unsaturated zone processes and the hydrologic response of a steep, unchanneled catchment, *Water Resour. Res., 34,* 1865-1879.

Tsuboyama Y, R. C. Sidle, S. Noguchi, and I. Hosoda (1994), Flow and solute transport through the soil matrix and macropores of a hillslope segment. *Water Resour. Res., 30,* 879–880.

Tromp-van Meerveld, H. J., and J. J. McDonnell (2006), Threshold relations in subsurface stormflow: 2. The fill and spill hypothesis, *Water Resour. Res., 42,* W02411, doi:10.1029/2004WR003800.

Tymchak, M. P., and R. Torres (2007), Effects of variable rainfall intensity on the unsaturated zone response of a forested sandy hillslope, *Water Resour. Res., 43,* W06431, doi:10.1029/2005WR004584.

Uchida, T., Kosugi, K. and T. Mizuyama (2001), Effects of pipeflow on hydrological process and its relation to landslide: a review of pipeflow studies in forested headwater catchments, *Hydrol. Processes, 15,* 2151-2174

Uchida, T., I. Tromp-van Meerveld and J. J. McDonnell (2005), The role of lateral pipe flow in hillslope runoff response : an intercomparison of non-linear hillslope response, *J. Hydrol.,* 311, 117-133.

Van Verseveld, W. J. (2007), Hydro-biogeochemical coupling at the hillslope and catchment scale, Ph.D., Oregon State University, Corvallis.

Weiler, M., J. McDonnell, H. J. Tromp-van Meerveld and T. Uchida (2005), Subsurface Stormflow. Encyclopedia of Hydrological Sciences.Wiley and Sons.Whipkey.

Weyman, D.R. (1973), Measurements of the downslope flow of water in a soil, *J. Hydrol., 20*, 267-288.

Whipkey, R.Z. (1965), Subsurface stormflow from forested slopes, *Int. Ass. Sci. Hydrol. Bull.,10*, 74-85.

Yano, Y., K. Lajtha, P. Sollins and B. A. Caldwell (2005), Chemistry and Dynamics of Dissolved Organic Matter in a Temperate Coniferous Forest on Andic Soils: Effects of Litter Quality, *Ecosystems, 8,* 286-300.

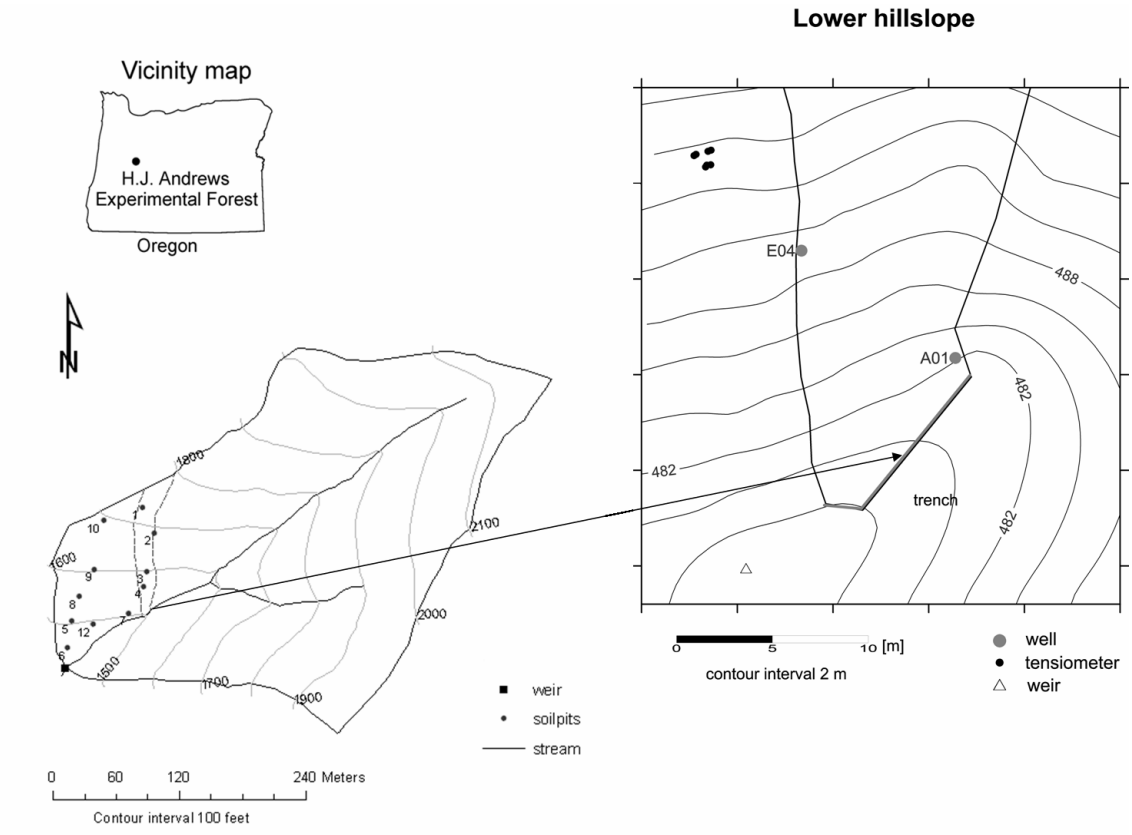

Figure 2.1. Map of study area showing WS10 with the soilpits (Ranken, 1974). It also shows the hillslope drainage area, and the lower hillslope study area with instrumentation.

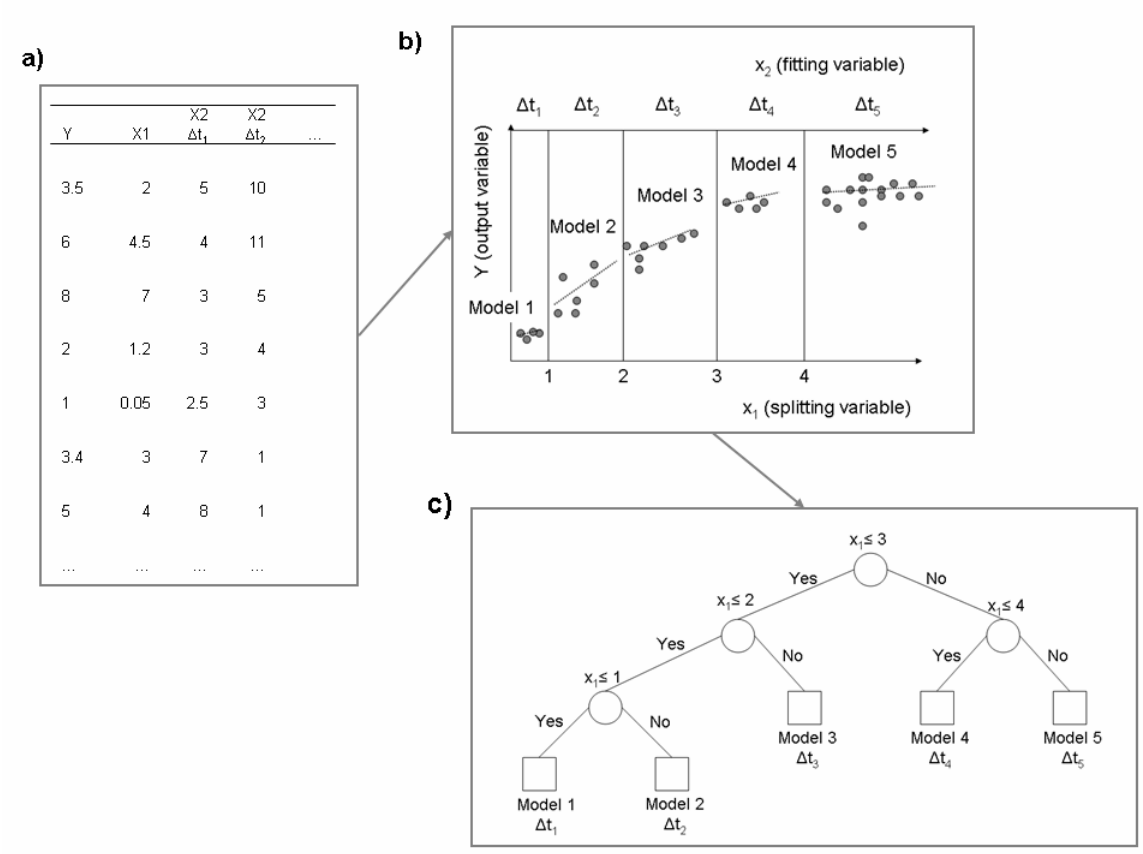

Figure 2.2. Example of tree regression result with GUIDE algorithm in a schematic diagram (adapted from Fig.1 in Solomatine and Xue, 2004), a) input data in matrix form, b) partition of dataset with GUIDE algorithm, and c) visualization of tree regression result

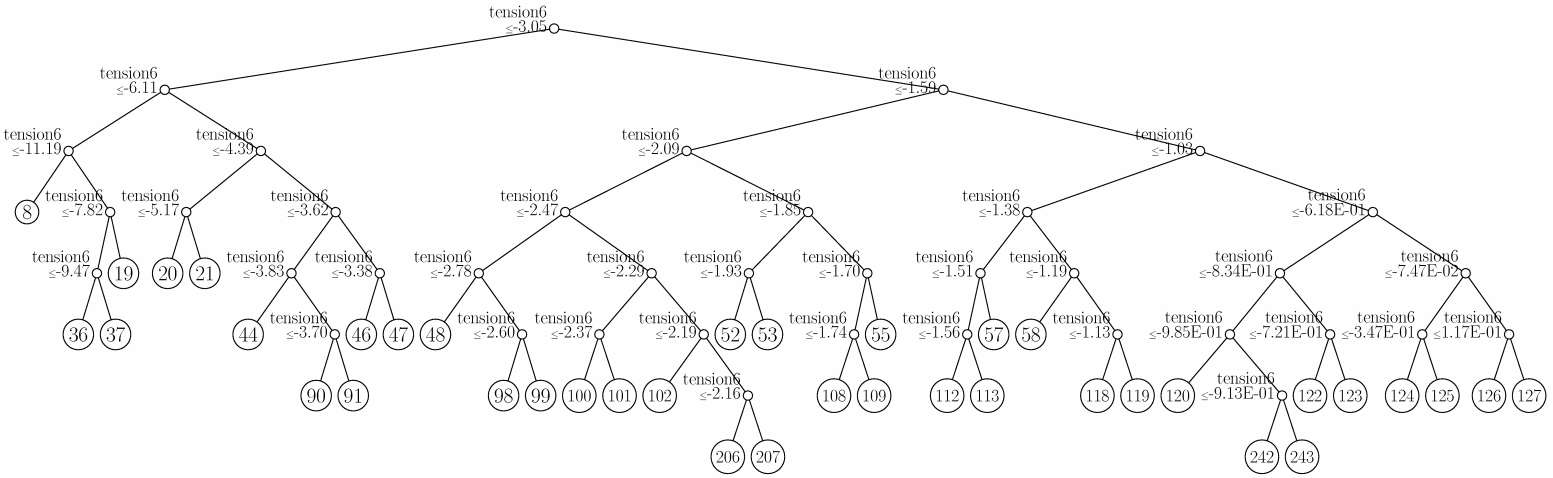

Figure 2.3. GUIDE piecewise simple linear least-squares model of matric potential (kPa) at 30 cm depth. The nodes with numbers are the end-nodes, tension6 means matric potential 6 hours before the observation

Table 2.1. Results for the end nodes in the regression tree of Figure 2.2.

Node label	No. of cases	Cases fitted	Mean node	MSE node	Node R^2	Fit variable (time lag (hr) of mean rainfall intensity)
8	601	410	-12.45	0.37	0.53	1364.17
36	588	322	-10.33	0.09	0.83	327.67
37	620	457	-8.53	0.18	0.52	815.17
19	554	386	-6.90	0.18	0.73	229.33
20	731	344	-5.50	0.03	0.98	173.83
21	672	299	-4.66	0.05	0.95	78.67
44	983	467	-4.12	0.02	0.49	450.00
90	404	298	-3.73	0.01	0.56	415.67
91	372	276	-3.62	0.01	0.74	35.50
46	836	485	-3.52	0.02	0.65	22.00
47	847	474	-3.26	0.02	0.64	11.17
48	833	374	-3.01	0.01	0.86	14.83
98	595	401	-2.76	0.01	0.52	34.17
99	526	326	-2.24	0.07	0.89	10.33
100	592	437	-2.10	0.09	0.78	10.67
101	502	432	-2.30	0.04	0.67	8.83
102	844	773	-2.26	0.01	0.34	9.83
206	819	743	-2.09	0.02	0.88	9.83
207	454	374	-2.13	0.03	0.58	25.83
52	1379	1055	-2.04	0.01	0.74	22.83
53	840	735	-1.82	0.03	0.80	21.17
108	1709	1339	-1.77	0.02	0.80	23.83
109	559	429	-1.69	0.03	0.67	13.67
55	1506	1256	-1.57	0.02	0.88	38.50
112	622	571	-1.48	0.03	0.82	8.00
113	557	460	-1.42	0.03	0.81	4.67
57	1745	1194	-1.43	0.03	0.58	26.83
58	1820	1434	-1.32	0.01	0.84	16.67
118	521	401	-1.13	0.02	0.82	20.33
119	964	826	-1.07	0.02	0.83	10.33
120	575	472	-0.92	0.06	0.45	7.67
242	887	600	-1.05	0.01	0.71	8.83
243	1115	929	-0.93	0.02	0.76	11.17
122	1274	1000	-0.86	0.01	0.77	11.17
123	1219	994	-0.68	0.02	0.77	9.83
124	2206	1817	-0.57	0.03	0.54	4.67
125	1204	1033	-0.40	0.04	0.47	4.33
126	606	561	-0.19	0.03	0.55	3.67
127	352	341	0.02	0.02	0.58	2.00

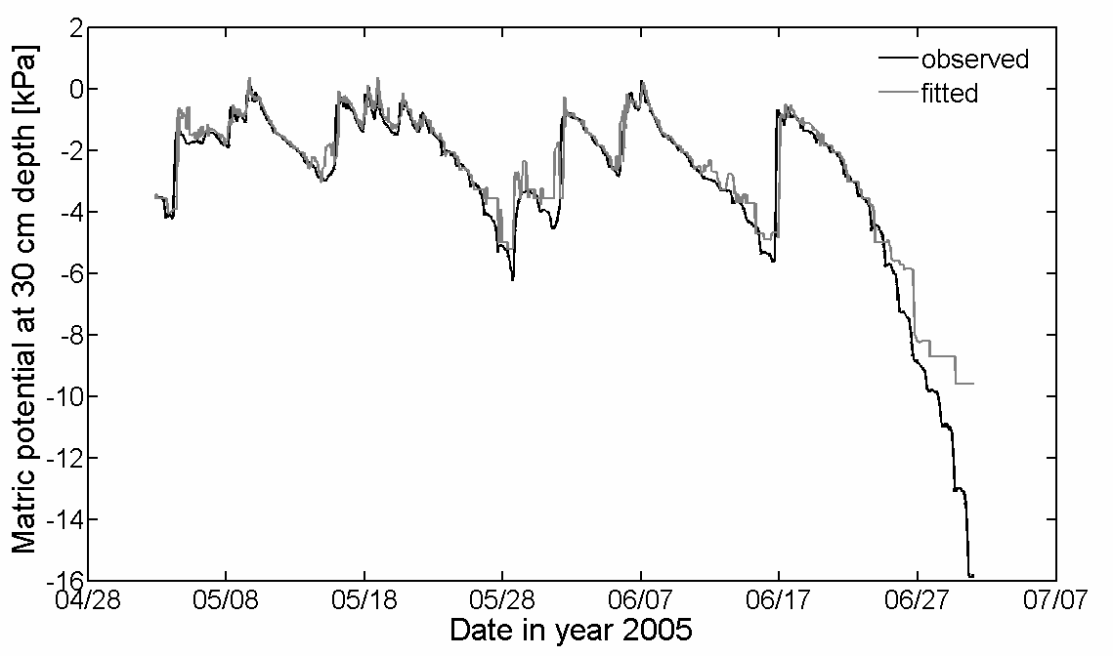

Figure 2.4. Observed and modeled time series of matric potential at 30 cm depth during the validation period.

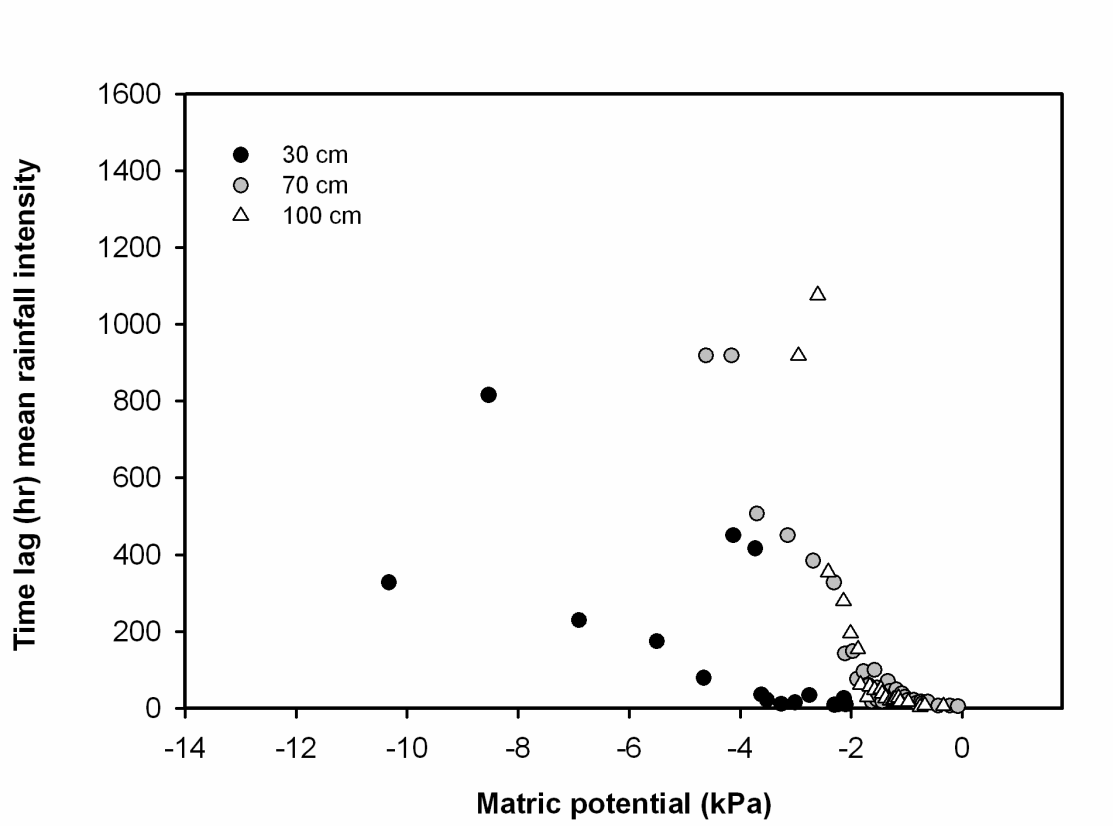

Figure 2.5. Time lags of matric potential for 30, 70 and 100 cm depth, extracted from the tree regression.

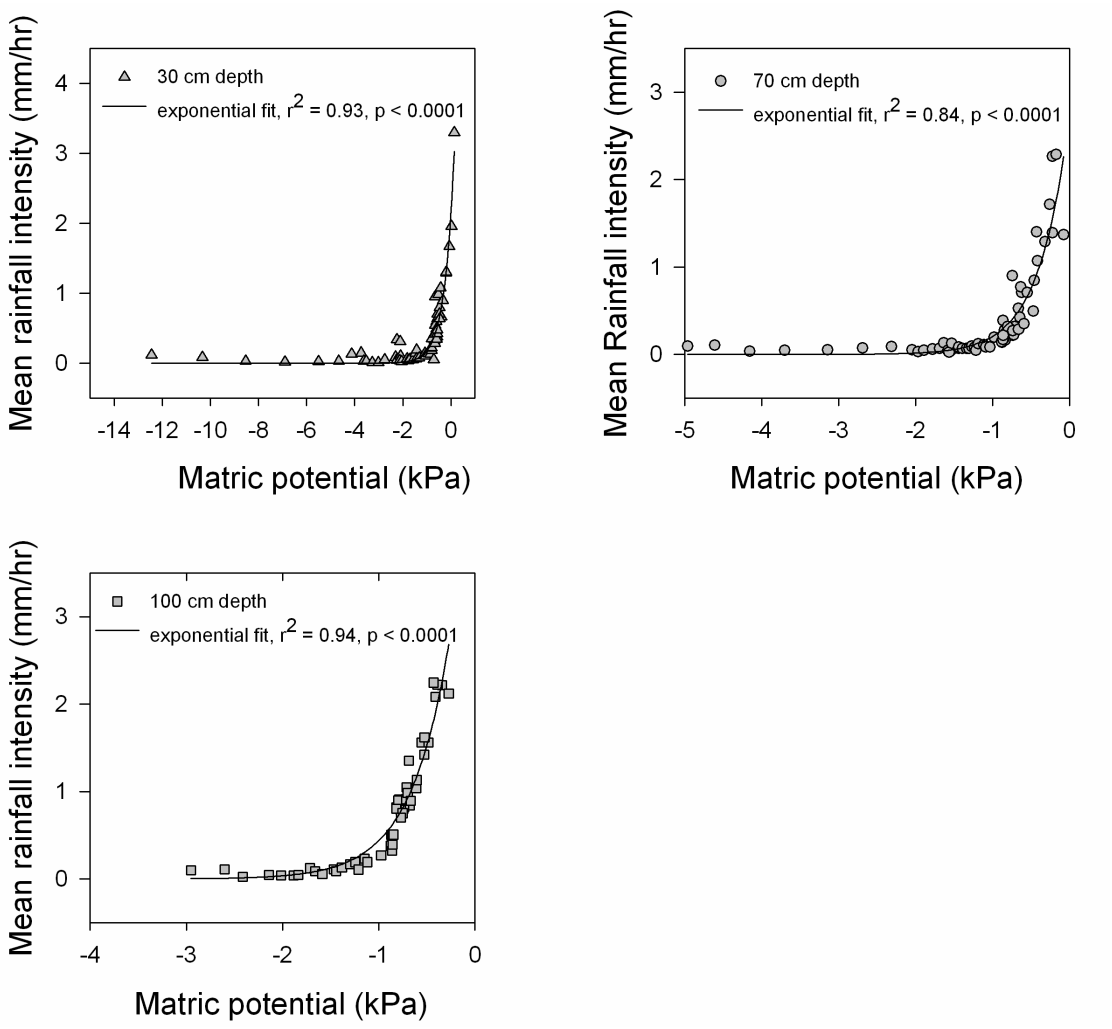

Figure 2.6. The relation between average mean rainfall intensity and average matric potential from the end nodes in each tree regression, for 30, 70 and 100 cm depth.

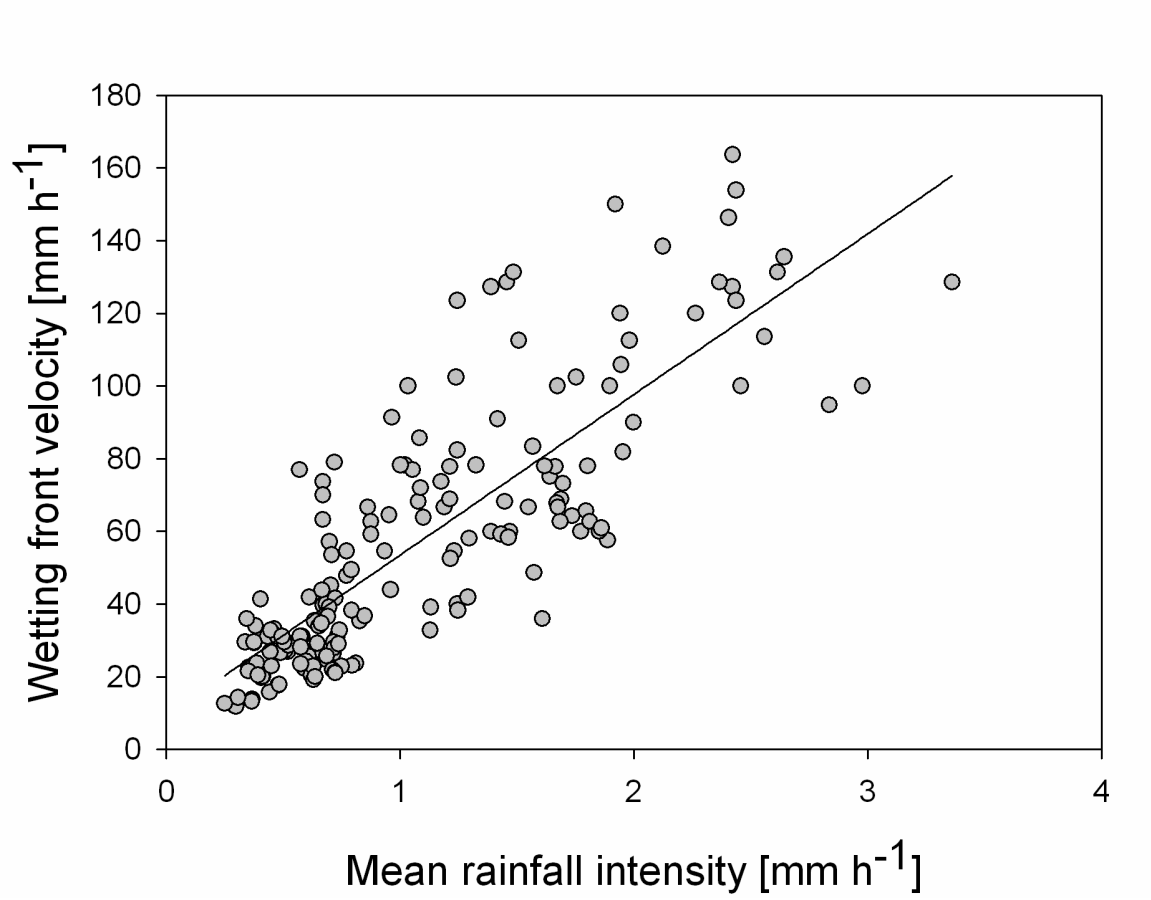

Figure 2.7. Relation between mean rainfall intensity and wetting front velocity, line in the graph is a linear fit (R^2=0.68, p<0.0001).

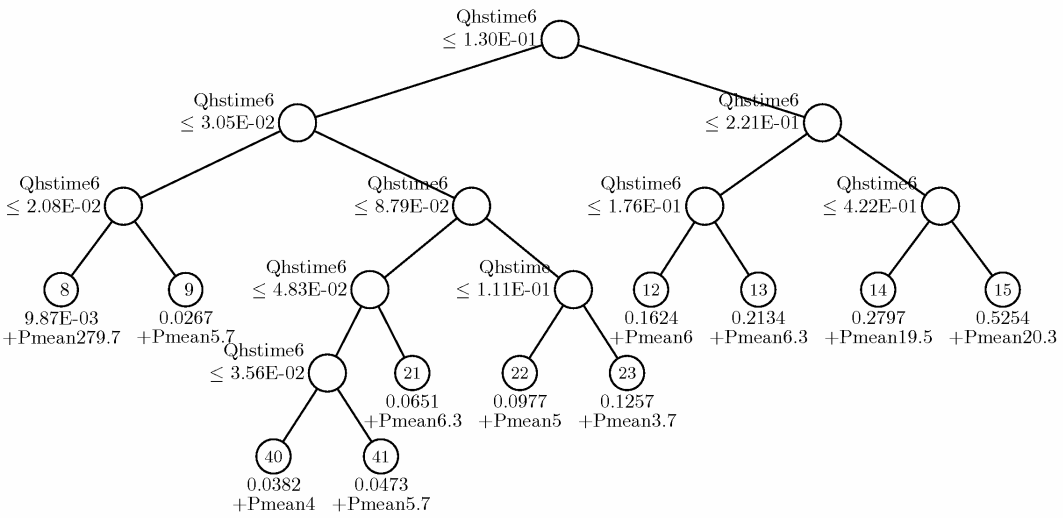

Figure 2.8. GUIDE piecewise simple linear least-squares model of subsurface flow (L s^{-1}). Beneath each end node are the sample mean of subsurface flow and the sign and name of the regressor (Pm=mean rainfall intensity, numbers after subsurface flow and Pm are time lags in hours, Qhstime6 is subsurface flow 6 hours before the observation).

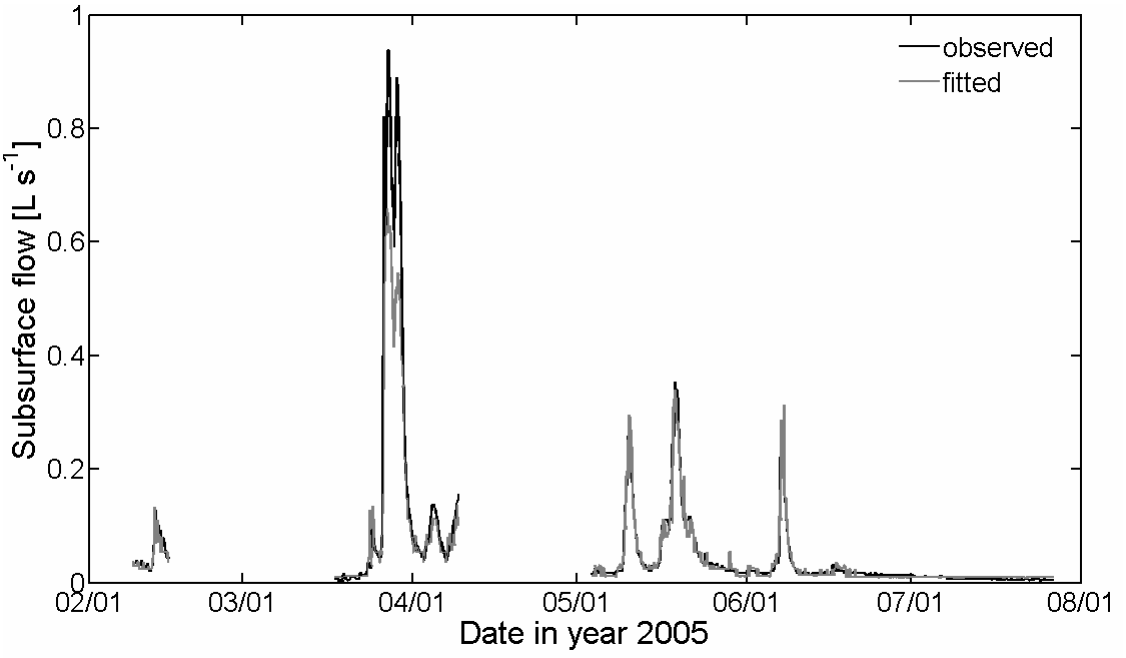

Figure 2.9. Observed and modeled subsurface flow hydrograph for the validation period .

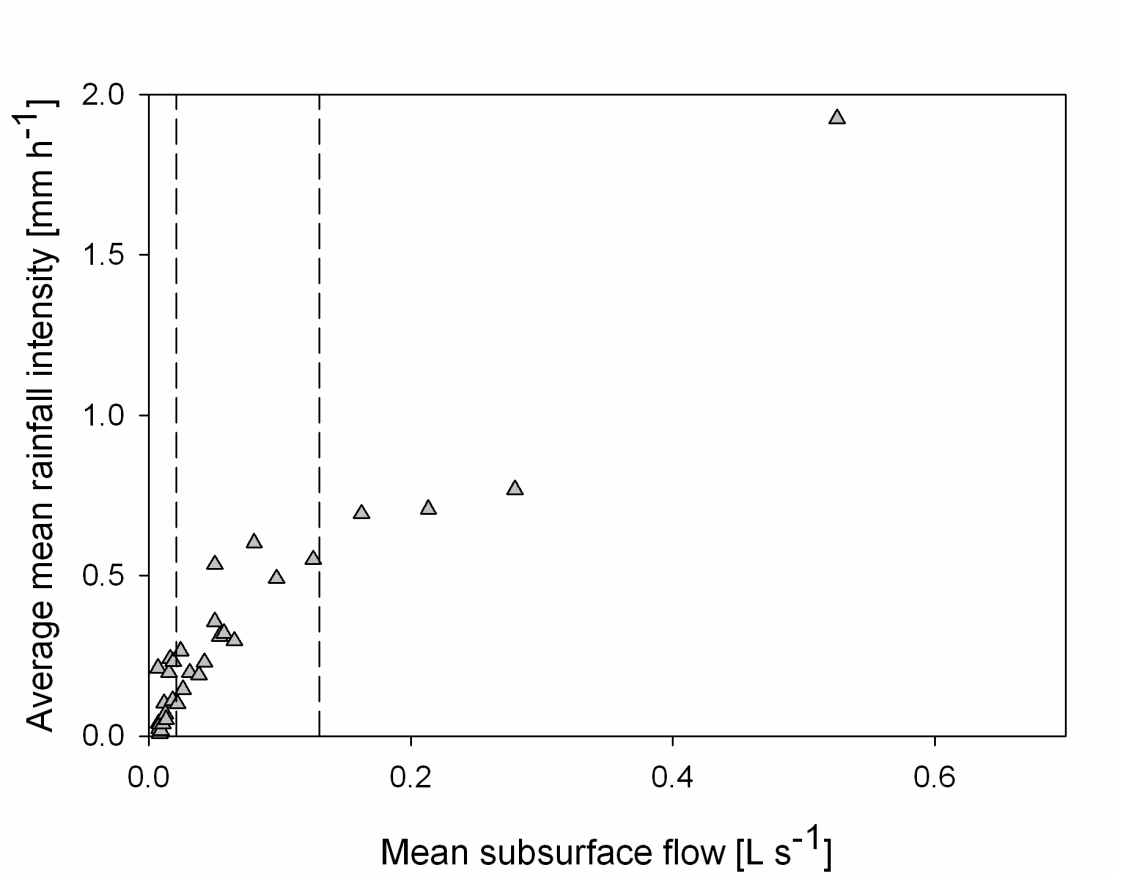

Figure 2.10. The relation between mean subsurface flow and average mean rainfall intensity in the end nodes of the un-pruned regression tree of subsurface flow. The dashed lines in the graph represent the boundaries between subsurface flow behavior 1, 2 and 3.

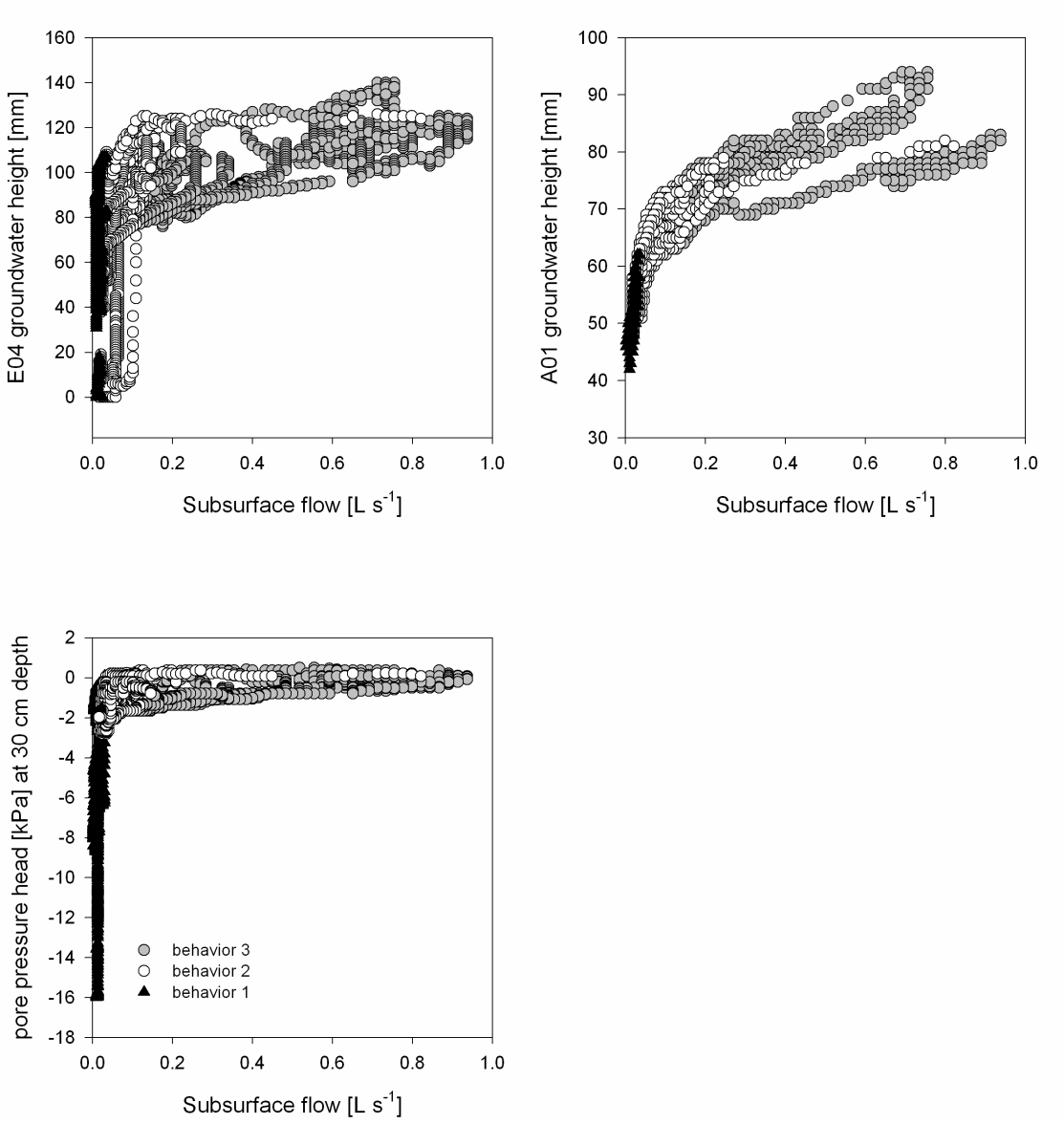

Figure 2.11. The three different hydrological behaviors found in the subsurface flow regression tree applied to the groundwater-subsurface flow and matric potential-subsurface flow relationship.

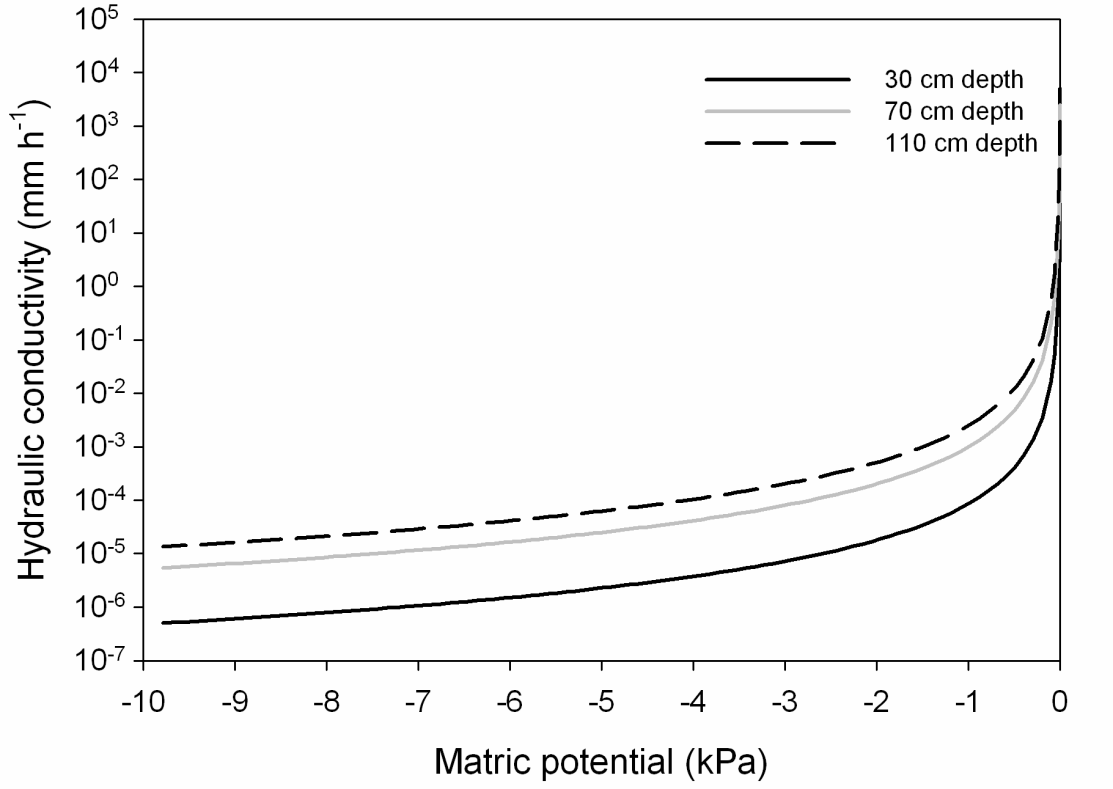

Figure 2.12. The unsaturated hydraulic conductivity function determined with the Brooks-Corey model applied to soilpit 3.

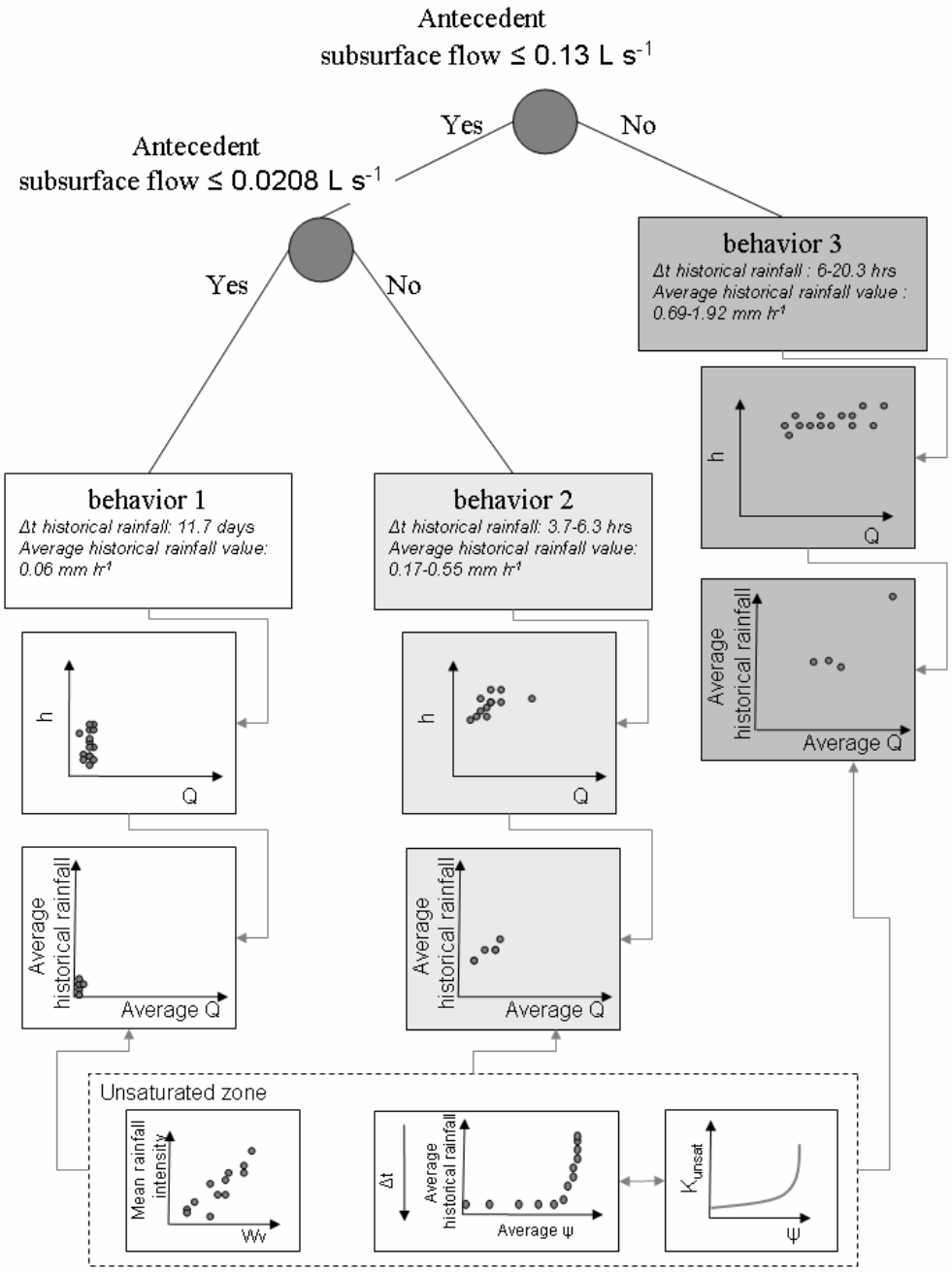

Figure 2.13. Decision tree of subsurface flow tree regression result. The graphs underneath each behavior are the relationships typical for each behavior. h and Q represent pore pressure or groundwater height and subsurface flow respectively. The unsaturated zone, with results from the matric potential tree regression, unsaturated hydraulic conductivity (K_{unsat}) function, and linear regression between mean rainfall intensity and wetting front velocity (Wv) is also included in the conceptual model, and linked to the three subsurface flow behaviors.

3 The role of hillslope hydrology in controlling nutrient loss

Van Verseveld, W. J.

McDonnell, J. J.

Lajtha, K.

3.1 Introduction

Controls on dissolved organic matter (DOM) losses at the catchment scale are poorly understood, and yet DOM fluxes may have important consequences for both terrestrial and aquatic ecosystem function. DOM has the ability to form complexes with metals, and thus plays an important role in metal toxicity and transport (Leenheer et al,, 1998). Dissolved organic nitrogen (DON) can represent a significant loss of nitrogen (N) (Sollins et al., 1980; Hedin et al., 1995; Perakis and Hedin, 2002; Vanderbilt et al., 2003) in unpolluted forested ecosystems, and may be a critical factor in maintaining N-limitation in these systems (Vitousek et al., 1998). In addition, dissolved organic carbon (DOC) is an important energy source to bacteria and some algae in streams (Kaplan and Newbold, 1993) and absorbs UV-radiation (Scully and Lean, 1994; Morris et al., 1995) that can damage aquatic organisms.

Recent research has focused on the hydrological controls on stream concentrations and quality of dissolved organic carbon (DOC) (McKnight et al., 2002, McGlynn and McDonnell., 2003; Inamdar and Mitchell, 2006; Park et al., 2007), dissolved organic nitrogen (DON) (Hill et al, 1999; Hagedorn et al., 2000, Buffam et al., 2001; Bernal et al., 2005), and nitrate (NO_3-N) (McHale et al, 2002; Ocampo et al., 2006). While these studies have improved our understanding of flushing and draining processes of nutrients at the catchment scale (as described by Hornberger et al., 1994; Boyer, et al. 1997, Creed et al, 1996), quantifying spatial sources of these nutrients during storm events and across seasons remain poorly understood. The main reason is that it is difficult to separate different geomorphic units of the catchment. While

hillslopes make up the largest part of catchments, research has been mostly focused on the riparian zone (Cirmo and McDonnell, 1997), such that sources of nutrients from the hillslope component are more poorly understood compared than those from riparian zone.

One approach to increase our understanding of spatial sources of DOM and N at the catchment scale, is to isolate discrete landscape units and to understand their individual hydro-biogeochemical dynamics. While some studies have done this for the riparian zone (e.g. Hill, 1993; McDowell et al., 1992; Vidon and Hill, 2004) few studies have been able to isolate the hillslope hydro-biogeochemical response (McGlynn and McDonnell, 2003). It is difficult to observe hydro-biogeochemical expressions of hillslopes in the stream (Hooper, 2001), due to chemical transformations in the riparian zone (Hedin et al., 1998) or infrequent episodic flow into the riparian zone (McGlynn and McDonnell, 2003). An approach to quantify the hillslope response directly, without any riparian zone modulation, is to trench experimental hillslopes. A few trenched experimental hillslopes exist around the world (Woods and Rowe, 1996 (Maimai, New Zealand); Tromp-van Meerveld and McDonnell, 2006 (Panola, USA);Uchida et al., 2003 (Fudoji, Japan)) but these experiments have typically monitored only a handful of storms to work with (Tromp-van Meerveld and McDonnell, 2003), and often lack detailed biogeochemical data.

While isolating the hillslope or riparian zone has led to new insights into spatial sources of nutrients, questions remain about the hydrological controls on DOM and N export from the hillslope component at seasonal and storm event scales. It is especially

important to understand the role of hillslopes in DOM and N export across different antecedent wetness conditions because several studies have suggested that seasonal variation in stream DOC, DON and NO_3-N is related to antecedent wetness conditions (Triska et al., 1984; Vanderbilt et al., 2003; Bernal et al., 2005) and many studies have reported significant increases in DON, DOC and NO_3-N during individual storm events (Creed et al., 1996; McHale et al., 2002; Boyer et al., 1997).

We report on work from a small well-studied hillslope trench within a headwater catchment at the H. J. Andrews Experimental Forest (HJA), Oregon. The catchment is well-suited for exploring questions of how hillslope hydrological processes control stream DOC and N concentrations. This study site has a unique feature: hillslopes that issue directly into the headwater stream without any riparian zone modulation. Riparian zone water storage was effectively removed from the site due to 1986 and 1996 debris flows that evacuated the valley bottom. This setup made it possible to isolate lateral subsurface flow from the hillslope trench and compare the hydro-biogeochemical response from this hillslope to the response of the whole array of hillslopes that make up this watershed. Furthermore, we explored the use of different indices of DOM quality (specific UV absorbance (SUVA) and DOC:DON) to fingerprint terrestrial sources of DOM. Recent studies have demonstrated that SUVA can be used as a surrogate for the aromatic carbon content and molecular weight of DOC (Chin et al., 1997; McKnight et al., 1997; Weishaar et al., 2003; Hood et al., 2005). The chemical character of DOM (DOC:DON, (SUVA)) has been used to identify terrestrial sources of DOM at seasonal scales (Hood et al., 2003, 2005;

McKnight et al., 1997, 2001) and during storms at the catchment (Hagedorn et al., 2000; Hood et al., 2006; Katsuyama and Ohte, 2002) and plot scale (Kaiser and Guggenberger, 2005).

Our study builds upon a wealth of previous hydrological (Harr, 1977; McGuire, 2004) and biogeochemical (Sollins et al., 1980; Sollins et al., 1981; Triska et al., 1984) research at the site. The H. J. Andrews Experimental Forest is characterized by dry summers, a gradual wet up between October and December (transition period), and from December through late spring the watershed is persistently wet. This steady and progressive shift from dry to very wet conditions allowed us to explore the role of antecedent wetness and flow conditions on DOC and nitrogen (N) patterns at seasonal and storm event scales. Monitoring and sampling of lateral subsurface flow from the hillslope trench, and stream water at the catchment outlet between August 2004 and June 2005 during and between storm events allowed us to compare DOC and N concentrations and SUVA values between the transition period and the wet period at the hillslope and catchment scale, and between these two scales, during baseflow and stormflow conditions. In addition, sampling storm events at the hillslope and catchments scale during the transition and wet period enabled us to examine the role of antecedent wetness conditions on DOC and N concentrations and compare export rates between these two scales.

We address the following questions to improve our understanding of the hydrological controls on DOM and N fluxes from hillslopes in a small watershed: (1) What is the variation in DIN, DON and DOC concentrations and DOM quality

(SUVA and DOC:DON) among sources from the plot scale, lateral subsurface flow and stream water on an annual scale? (2) What is the influence of flow conditions at the seasonal scale (transition vs. wet period) on the variation of solutes and DOM quality in lateral subsurface flow and stream water during baseflow and stormflow conditions? (3) What is the role of timing (transition vs. wet period) and under what flow conditions are the single gauged hillslope and catchment response similar with respect to the solutes and DOM quality? (4) Do peak and flow averaged DOC and N concentrations during storms at the catchment and hillslope scale increase with a decrease in antecedent soil moisture and antecedent precipitation conditions? (5) Is the total carbon and nitrogen-export at the hillslope and catchment scale during storm events the same?

3.2 Site description

The study was conducted in Watershed 10 (WS10), a 10.2 ha headwater catchment located in the H. J. Andrews Experimental Forest (HJA), in the western-central Cascade Mountains of Oregon, USA (44.2° N, 122.25° W) (Figure 3.1). Elevations range from 470 m at the watershed flume to a maximum watershed elevation of 680 m. HJA has a Mediterranean climate, with dry summers and wet winters characterized by long, low intensity storms. Average annual rainfall is 2220 mm and about 80% falls between October and April. Snow accumulation in WS10 seldom exceeds 30 cm, and seldom persists for more than 2 weeks (Sollins et al., 1981). Atmospheric total bulk N deposition is low compared to other sites in USA and

averages 1.6 – 2 kg N ha^{-1} yr^{-1} (Vanderbilt et al., 2003). The watershed was harvested in 1975 and is now dominated by a naturally regenerated second growth Douglas-fir (*Pseudotsuga menziesii*) stand. Seep areas along the stream have been observed (Harr, 1977; Triska, 1984), which are related to the local topography of bedrock and/ or saprolite, or to the presence of vertical, andesitic dikes approximately 5 meters wide, located within the south-facing hillslope (Swanson and James, 1975; Harr, 1977).

The hillslope study area is located on the south aspect of WS10, 91 m upstream from the stream gauging station (Figure 3.1). The 125 m long stream-to-ridge slope has an average gradient of 37º, ranging from 27º near the ridge to 48º adjacent to the stream (McGuire, 2004). Elevation at the hillslope ranges from 480 to 565 m. The bedrock is of volcanic origin, including andesitic and dacitic tuff and coarse breccia (Swanson and James, 1975). The depth to unweathered bedrock ranges from 0.3 to 0.6 m at the stream-hillslope interface and increases gradually toward the ridge to approximately 3 to 8 m. Soils are about 1 m deep, and formed either in residual parent material or in colluvium originating from these deposits. The soils are highly andic and vary across the landscape as either Typic Hapludands or as Andic Dystrudepts (Yano et al., 2005) and are underlain by 1-8 m relatively low permeability subsoil (saprolite), formed in the highly weathered coarse breccia (Ranken, 1974; Sollins, 1981). Soil textures range from gravelly, silty clay loam to very gravelly clay loam. Surface soils are well aggregated, but lower depths (70-110 cm) exhibit more massive blocky structure with less aggregation than surface soils (Harr, 1977).

3.3 Methods

3.3.1 Infrastructure

A 10 m long trench was constructed to measure subsurface flow at a natural seepage face (McGuire, 2004). Intercepted subsurface water was routed to a calibrated 30º V-notch weir that recorded stage at 10-minute time intervals using a 1-mm resolution capacitance water-level recorder (TruTrack, Inc., model WT-HR). Rainfall was measured with a tipping bucket and storage gauge located in a small canopy opening on the hillslope. The drainage area of the hillslope was delineated topographically from a total station survey of the entire hillslope (0.17 ha, round to 0.2 ha in all analyses) and verified by a water balance calculation (McGuire, 2004). As part of the long term monitoring at the H.J. Andrews Experimental Forest, discharge at the WS10 outlet was measured with a trapezoidal flume. During the summer a V-notch weir was used to measure discharge at the WS10 outlet. Stage was measured with a Model 2 Stevens Instruments Position Analog Transmitter (PAT) (0.001 ft resolution).

Soil water content (θ) was measured with water content reflectometers (WCR) (CS615, Campbell Scientific, Inc.). The soil moisture probes were installed parallel to the slope at 3 depths (30, 70, and 100 cm) in three soil pits in the lower portion of the hillslope. The nests were located 15, 20 and 25 m upslope from the slope base (McGuire, 2004).

We installed six plastic 10 x 10 cm zero tension lysimeters just below (0.5 cm) the organic layer (Figure 3.1). Twenty seven superquartz (Prenart Equipment ApS)

tension (0.5 bar) lysimeters were installed at shallow (20 cm), middle (30-40 cm), and deep (70-110 cm) soil profile positions (Figure 3.1) at a 30º angle following the method described by Lajtha et al. (1999).

We installed 69 maximum cork rise wells (3.18 cm diameter), that were screened for the lower 25 cm, the maximum water height observed by Harr (1977). All wells were installed until refusal by a hand auger. We sampled five wells located outside the seepage area that showed transient saturation and one well (A01) located in the seepage area (Figure 3.1.).

3.3.2 Sampling and chemical analysis

Throughfall, lateral subsurface flow, WS10 stream water, soil water (zero tension and tension), transient and seepage groundwater samples were collected between August 2004 and June 2005 at three-week intervals, and prior to, during, and after selected storm events. Throughfall was captured using the technique of Keim and Skaugset (2004). Grab samples at three-week intervals and during storms were taken at the right fork during the transition period, and at the left fork during the whole study period. Prenart tension lysimeters were evacuated to -50 kPa and allowed to collect water for 24 hours. These samples were not filtered because initial experiments with filtered soil solutions demonstrated that tension lysimeter samples did not need to be filtered (Lajtha et al., 2005). Other samples were filtered through combusted Whatman GF/F glass fiber filters (nominal pore size = 0.7 µm) and stored frozen until analysis. The gauged hillslope and watershed outlet were sampled with ISCO samplers during

five storms, at 1 to 4 hour intervals. Samples were analyzed for DOC, total dissolved nitrogen (TDN), nitrate, ammonium and UV-absorbance at 254 nm (UV_{254}). DOC and TDN was measured with Pt-catalyzed high-temperature combustion (Shimadzu TOC-V CSH analyzer with TN unit). NO_3-N was measured with the hydrazine sulfate reduction method and NH_4^+-N was determined by the Berthelot reaction method with a an Orion Scientific AC 100 continuous flow auto-analyzer (Westco Scientific Instruments, Inc., Danbury, CT). DON was calculated as the difference between TDN and DIN (nitrate and ammonium). Because DON was calculated by difference, values sometimes fell slightly below 0 mg l^{-1}. Negative DON values were considered to be 0 mg l^{-1}. UV_{254} was measured with a Hitachi V-2001 spectrophotometer and SUVA is UV_{254} normalized by DOC concentration.

3.3.3 Data analysis

We divided the dataset into two periods: a transition period (transition from dry to wet conditions) and a wet period in order to investigate the influence of flow conditions on DIN, DOC, DON concentrations and SUVA. The transition and wet periods were defined by measurable hillslope discharge. The transition period was defined as the period with hillslope baseflow (between storm events) discharge = 0.01 L s^{-1}, and the wet period was defined as the period with hillslope baseflow discharge > 0.01 L s^{-1}. We subdivided the runoff record of these two periods into two different catchment response modes; baseflow and stormflow conditions. Stormflow conditions were defined as flow during and 12 hours after storm events. The remainder of the

runoff dataset was defined as baseflow conditions. A storm event was defined as a precipitation event of more than 10 mm and separated by at least 12 hour periods with rainfall intensities smaller than 0.1 mm/h. We used the Wilcoxon ranksum to test for significant differences ($p < 0.01$) in DOC and N concentrations and SUVA for flow conditions within and between the transition and wet period. Hillslope discharge before 12-02-2004 was estimated from stream discharge with a second order polynomial because the hillslope discharge gauge failed. Average 95% confidence bounds of the second order polynomial on predicted values during this period were ± 7.95 10^{-4} mm h^{-1}. Because of these small confidence bounds uncertainty resulting from calculations with estimated hillslope discharge was not quantified.

Pearson correlation coefficients (r) were calculated between antecedent wetness conditions as antecedent soil moisture at 30 cm depth and antecedent precipitation before a storm event and DOC, DON and DIN peak and flow weighted concentrations. The correlation was considered significant when $p < 0.1$. We used a 7-day, 14 day and 30 day average of soil moisture before a storm event as antecedent soil moisture indices (AMI_7, AMI_{14} and AMI_{30}) and a 7-day, 14 day and 30 day total precipitation before a storm event as antecedent precipitation indices (API_7, API_{14} and API_{30}). We used soil moisture data from the lower soil pit (Figure 3.1.), since that data was most reliable. All statistical and mathematical computations were made in MATLAB.

3.4 Results

3.4.1 Variation in DOC and N

To investigate variation in DOC and N concentrations between sources from the plot scale, lateral subsurface flow and stream water we compared average DOC, DON and DIN concentrations, and average SUVA and DOC:DON values from throughfall, below the organic horizon, in shallow, middle, and deep soil profile positions, transient and seepage groundwater, lateral subsurface flow and stream water. Furthermore, through this analysis we are able to identify sources that contributed to high DOC and N concentrations in lateral subsurface flow and stream water.

DOC and DON concentrations were low in throughfall, highest from just below the organic layer and then progressively decreased with depth into the soil profile (Table 3.1.). This suggests a net release of both DOC and DON from the organic layer, and net removal of DON and DOC from solution below the organic layer. DOC and DON concentrations in transient groundwater were higher than soil water DOC and DON concentrations observed at the deep soil profile position. In addition, DOC and DON concentrations in transient groundwater were higher than the groundwater seep concentrations. DON and DOC concentrations of lateral subsurface flow and stream water were most similar to soil water DON and DOC concentrations at the middle soil profile depth.

SUVA values showed a maximum in the organic layer and transient groundwater solution (Table 3.1.). SUVA values increased from throughfall to the

organic horizon, and decreased from the organic layer to the deep soil layer (70-110 cm). SUVA values in stream water were most similar to SUVA values from deep soil water. Lateral subsurface flow showed a much lower SUVA value than WS10 stream water and was most similar to SUVA values from the groundwater seep.

DOC:DON did not show a clear trend with soil depth. Soil water from the middle soil profile position had the greatest DOC:DON ratio, while organic horizon, shallow and deep soil water had lower ratios. DOC:DON increased from deep soil water to seepage and transient groundwater. Lateral subsurface flow showed the greatest DOC:DON ratio, similar to the DOC:DON ratio of the groundwater seep. Stream water showed the second highest DOC:DON ratio. The DOC:DON ratio of throughfall was similar to the shallow soil water.

DIN was the dominant form of total dissolved nitrogen (TDN) in transient groundwater, while DON was the dominant form of TDN in the other solutions. DON as a fraction of TDN ranged from 0.70 to 0.92 in all solutions, while the fraction was 0.35 in transient groundwater. NO_3-N concentrations decreased with depth from the organic horizon to the deep soil profile position, but NH_4-N concentrations did not show a trend with depth. Low NO_3-N and NH_4-N concentrations (= 0.01 mg l^{-1}) were found in throughfall, seep groundwater, lateral subsurface flow and WS10 stream water.

3.4.2 DON and N during transition and wet period

First, we compared DOC concentrations, DOC quality and N concentrations between the transition and wet period during baseflow conditions in lateral subsurface flow and stream water. NH_4-N and NO_3-N concentrations, DOC quality (expressed as DOC:DON and SUVA) in lateral subsurface flow during baseflow conditions were not different between the transition and wet period (Figure 3.2a). Stream water during baseflow conditions followed the same pattern as lateral subsurface flow, except that NH_4-N was significantly higher during the wet period. DOC and DON concentrations during baseflow conditions in stream water were significantly lower during the wet period, while in lateral subsurface flow only DOC was significantly lower during the wet period ($p>0.01$ for hillslope water DON).

Secondly, we compared DOC concentrations, DOC quality and N concentration between lateral subsurface flow and stream water under baseflow conditions, during the transition and wet period. During the wet period under non-driven conditions, SUVA values of lateral subsurface flow were significantly lower than SUVA values of stream water, while DOC, DON and DIN concentrations and DOC:DON ratios of lateral subsurface flow and stream water were similar. During the transition period and baseflow conditions, DOM quality (DOC:DON and SUVA) between lateral subsurface flow and stream water was different; lateral subsurface flow had higher DOC:DON ratios and lower SUVA values. In addition, non-driven DON concentrations in lateral subsurface flow were lower than stream water during this period.

Thirdly, we compared DOC concentrations, DOC quality and N concentrations between the transition and wet period during stormflow conditions in lateral subsurface flow and stream water. During stormflow conditions, stream water SUVA values were not different between the transition and wet period, while DOC and DON concentrations were lower, NH_4-N concentrations were higher, and DOC:DON ratios were higher during the wet period (Figure 3.2b). Lateral subsurface flow followed the same pattern as stream water except for SUVA values that were significantly higher during the wet period, and DOC:DON ratios that were not different between the transition and wet period in lateral subsurface flow.

Finally, we compared DOC concentrations, DOC quality and N concentrations between lateral subsurface flow and stream water under stormflow conditions, during the transition and wet period. During the wet period and stormflow conditions SUVA values and NH_4-N concentrations were significantly different between lateral subsurface flow and stream water. Stormflow DOC and DON concentrations and SUVA values during the transition period were each lower in lateral subsurface flow than stream water, while DOC:DON ratios were higher in lateral subsurface flow.

3.4.3 Antecedent wetness conditions and stormflow DOC and N

We used five sampled storms (Figure 3.2.) to examine the influence of antecedent wetness conditions on peak and flow weighted DOC, DON and DIN in stream water and lateral subsurface flow (Table 3.3.). Three antecedent soil moisture indices were used: the 7-day, 14-day and 30-day antecedent soil moisture index

(AMI_7, AMI_{14} and AMI_{30}), and three antecedent precipitation indices were used: the 7-day, 14-day and 30-day antecedent precipitation index (API_7, API_{14} and API_{30}).

The storm characteristics of these events as well as DOC, DON, DIN peak and flow weighted concentrations are summarized in Table 3.2. API_7, API_{14} and API_{30} were not significantly related to peak and flow weighted DOC, DON and DIN concentrations. AMI_7, AMI_{14} and AMI_{30} were similar (Table 3.3.), and thus we calculated pearson correlations between AMI_7 and peak and flow weighted DOC, DON and DIN in stream water and lateral subsurface flow. The concentration of all solutes except DIN decreased with an increase in AMI_7 at 30 cm depth. DOC, DON peak and flow weighted concentrations in stream water were more weakly correlated to AMI_7 than these solutes in lateral subsurface flow. Both DIN peak and flow weighted DIN in stream water and lateral subsurface flow were not significantly related to AMI_7. In addition DON peak in stream water was not significantly related to AMI_7.

3.4.4 Storm event export rates of C and N at hillslope and catchment scale

The export rates of DOC, DON and DIN for all five storms were smaller at the hillslope than watershed scale (Figure 3.4.a-c). DON was the dominant form of total nitrogen export during all storms. The DON:TDN ratios during storms 4 and 5, both storms during the wet period, were 0.84 and 0.87 at the watershed scale for storm 4 and 5 respectively, and 0.84 and 0.90 at the hillslope scale for storm 4 and 5

respectively. In contrast DON:TDN ratios for storms during the transition period were > 0.94.

The highest DOC, DON and DIN export rates were observed during storm 4. For the watershed and hillslope scale during storm 4, export rates of DOC were 4.4 and 3.0 kg/ha/storm respectively. Rates of DON export for the watershed and hillslope scale were 0.11 and 0.08 kg/ha/storm respectively. Rates of DIN export for the watershed and hillslope scale were 0.020 and 0.014 kg/ha/storm respectively.

3.5 Discussion

Quantifying spatial sources of soluble nutrients at the catchments scale is one of the greatest challenges faced in hydro-biogeochemical research. Isolating the hillslope component has been difficult in past studies because so few trenched experimental hillslopes exist around the world in catchments where active biogeochemical research is done. These trenched experimental hillslopes often lack detailed hydro-biogeochemical data across a wide range of antecedent wetness conditions. In addition, it is extremely difficult to quantify the representativeness of a single experimental hillslope for the whole array of hillslopes that make up a catchment. Single gauged hillslopes only sample part (tens of meters) of the hillslope component and, more importantly, most catchments have a riparian zone that transforms the biogeochemical signal of the hillslope component en route to the stream channel.

Our work exploits a rather unique experimental design where a trenched hillslope is compared to the stream response in a headwater cacthment without a riparian zone. This natural experimental design allowed us to study the hydrological controls on DOM and N export from the hillslope component at seasonal and storm event scales unimpeded by riparian dynamics. Because of the installation of a ten meter wide trench to capture lateral subsurface flow, we were also able to compare the hydro-biogeochemical signal from the single gauged hillslope to the overall hydro-biogeochemical response of the whole array of hillslopes that make up the catchment, by examining when the study hillslope acted in concert with the stream and when hillslope dynamics were different from the stream response. This comparison allowed us to examine when the single gauged hillslope hydro-biogeochemical signal is representative of the whole array of hillslopes that make up the catchment. During the wet period the hydro-biogeochemical signal from the gauged hillslope was not significantly different from the catchment response, except for DOM quality expressed as SUVA and NH_4-N concentrations that were lower in lateral subsurface flow. During the transition period the hydro-biogeochemical signal from the gauged hillslope was significantly different from the catchment response. Furthermore, organic horizon water and transient groundwater were high DOC, DON and DIN contributors to lateral subsurface flow and stream water, emphasizing the need to sample ‘below’ the root zone to accurately determine DOC, DON and DIN sources to the stream. High DOC, DON and DIN concentrations in transient groundwater, suggested a vertical preferential flow mechanism at our site. Antecedent wetness

conditions controlled DOC and DON concentrations in lateral subsurface flow and stream water during storm events; more prior flushing (expressed as AMI_7) resulted in lower DOC and DON peak and flow weighted concentrations during storms. In addition, DOC and DON concentrations in lateral subsurface flow in stream water during stormflow conditions were lower during the wet period compared to the transition period. Both of these results suggest that the production of DOC and DON in soils lagged behind the flushing of these nutrients. If DOC and DON production is seasonally (and storm) limited, this has important consequences for the interpretation of soil solution concentrations in end-member mixing analysis (EMMA) and annual calculations of solute losses from limited soil solution data. Since EMMA requires conservative behavior of tracers and time invariance of end-member compositions, limitation of DOC and DON on a seasonal (and storm) scale violates the EMMA assumptions.

3.5.1 What were the high DOC and N sources at the plot scale?

DOC and DON profiles with depth during the study period showed that the organic horizon (including the upper mineral soil) was the largest DOC and DON source. This result is similar to findings of Yano et al. (2004) in a nearby site in the H. J. Andrews Experimental Forest, where the upper mineral soil (0-10 cm) appeared to be the most significant source of DOM. In addition the organic horizon had the highest DIN concentrations.

Transient groundwater was high in DON, DOC and DIN concentrations, and was the only water source where DON was not the dominant form of TDN. Average values of DOC, DON and DOM quality (SUVA) in transient groundwater were similar to observed values in organic horizon and shallow soil water, suggesting a vertical preferential flow mechanism without much soil matrix interaction. Jardine et al. (1989b) found that if preferential flow at the pedon scale was dominant, DOC was non-reactive with the solid phase because it bypassed the soil matrix. DOM and DIN concentrations and SUVA in deep soil water was lower than transient groundwater, indicating that flow paths with significant soil matrix interaction undergo preferential retention of aromatic DOM and loss of DIN. Many other studies (Hagedorn et al., 2000; Yano et al., 2004; Kaiser and Guggenberger, 2005; Jardine et al., 1989a) have found preferential retention of aromatic DOM with depth.

3.5.2 Were DIN concentrations in transient groundwater biogeochemically controlled?

It is not likely that the high DIN concentrations in transient groundwater were caused exclusively by a preferential flow mechanism. Transient groundwater DIN concentrations were higher than organic horizon DIN concentrations, indicating net production of nitrate and ammonium in transient groundwater. Sollins et al. (1981) also found higher nitrate concentrations in suction lysimeters at 2 m depth than at 0.3 m depth at the same location in WS10. They hypothesized that this difference may have been caused by a decrease in bio-available C compounds below the rooting zone such that nitrifiers were able to compete for reduced N with heterotrophic bacteria. We

observed high DOC and DON concentrations in transient groundwater 'below' the rooting zone, suggesting that a significant C source was available below the rooting zone, although the lability of this DOM is unknown. Transient groundwater was only sampled frequently from one well (E04) during storm 5 within the study period. NO_3-N increased until 5/17/05 during the rising limb of the storm, while NH_4-N decreased until 5/17/05 (Figure 3.5.). This indicates that during this period of the storm autotrophic and/or heterotrophic nitrification occurred. After 5/17/05, NO_3-N began to decrease during the remainder of the storm while at the same time NH_4-N increased until 5/20/05. The increase in NH_4-N may have been caused by dissimilatory nitrate reduction to ammonium (DNRA). DNRA is an anaerobic microbial pathway that transforms NO_3-N to NH_4-N and has been documented in soils and sediments (Buresh and Patrick, 1978; Tiedje, 1988; Silver et al., 2001). Conditions that favor DNRA are available NO_3-N, (labile) C and a low redox potential and could have occurred after 5/17/05 during the storm. Thus, the high NO_3-N and NH_4-N concentrations in transient groundwater we observed could be the result of the co-occurrence of nitrification and DNRA. Another explanation we cannot rule out is that the pattern of NO_3-N and NH_4-N in transient groundwater was simply caused by ammonification and nitrification. Since groundwater was transient, and thus the soil at this depth was likely not sufficient anoxic to favor DNRA, the observed NO_3-N and NH_4-N concentration patterns were most likely caused by ammonification and nitrification.

3.5.3 Patterns of DOC and N in lateral subsurface flow and stream water

3.5.3.1 Baseflow conditions

SUVA, DON:DOC and NO_3-N concentrations in lateral subsurface flow and stream water did not show a difference between the transition and wet period. Stability in NO_3-N concentrations represented its biological control. NH_4-N in stream water did show a seasonal pattern, with higher concentrations during the wet period. Lack of DOM quality difference between the transition and wet period indicated that sources of baseflow did not change significantly during the year in stream water and lateral subsurface flow. However, DOC and DON concentrations in stream water and DOC concentrations in lateral subsurface flow decreased from the transition to the wet period. The high DOC and DON concentrations during the transition period were probably the result of low antecedent wetness conditions with a build up of labile organic material in the upper soil layer due to incomplete decomposition and the lack of flushing in combination with leaf fall during the autumn. Triska et al. (1984) and Vanderbilt et al., (2003) found a similar DON pattern in WS10 and in six small watersheds at the HJA.

3.5.3.2 Stormflow conditions

NH_4-N during the wet period was higher in lateral subsurface flow and stream water compared to the transition period. NO_3-N did not show any seasonal pattern at the hillslope and watershed scale. These findings are similar to Vanderbilt et al. (2003) who did not find a seasonal pattern in NO_3-N concentrations at the HJA. The observed

NH_4-N seasonal pattern could have been caused by less biological and more hydrological control of NH_4-N flushing during stormflow conditions in the winter. DOC and DON concentrations were highest during the transition period in lateral subsurface flow and stream water. Lower DOC and DON concentrations during the wet period compared to the transition period illustrated that the DOC and DON source was depleted over time and DOC and DON export was supply limited over seasonal scales.

3.5.4 The single gauged hillslope and catchment hydro-biogeochemical response during the wet period.

The single gauged hillslope response was not significantly different from the catchment response (with respect to DOC, DON and NO_3-N concentrations and DOC:DON ratios) during the wet period, during both baseflow and stormflow conditions. This result indicates that DOC and DON in stream and lateral subsurface flow water during the wet period during both flow conditions were derived from the same allochthonous source, and that in stream processes that may cause differences in DOC and DON patterns between lateral subsurface flow and stream water were not significant during the wet period. However, SUVA in lateral subsurface flow was significantly lower than SUVA in stream water during the wet period during both baseflow and stormflow conditions. The difference in SUVA we observed in lateral subsurface flow and stream water suggests that sources of DOM at the single gauged hillslope and catchment scale were not similar during the wet period and illustrates the value of using SUVA as a fingerprinting tool. An explanation could be that the lower

observed SUVA in lateral subsurface flow was caused by bio-available carbon compounds with a low aromatic and nitrogen content that were rapidly processed in the WS10 stream. However, this does not explain the observed low SUVA values in stream water (range: 0.17-0.88) and lateral subsurface flow (range: 0.14-0.41) before storm 1 during low flow conditions. During these conditions flow paths are characterized by long residence times and thus processing of these bio-available carbon compounds within the hillslope would occur. Another more likely explanation is that the hydrological flowpaths of the single gauged hillslope are not representative of the integrated flowpaths at the watershed scale. The observed high DOC and N concentrations and high SUVA values in transient groundwater indicate vertical preferential flow. Transient groundwater represents one source of lateral subsurface flow and stream water. Another source of lateral subsurface flow and stream water is seepage groundwater. Stream water during summer low flow conditions is sustained by different seeps in WS10 (e.g. Triska et al. (1984) identified five different seeps in WS10). These seepage areas are characterized by low SUVA values during summer low flow conditions. During the transition period the contribution of transient groundwater will increase and SUVA values in stream water and lateral subsurface flow reflect the ratio between the two water sources. We argue that the ratio of seep groundwater to transient groundwater from vertical preferential flow at the single gauged hillslope was larger than the ratio at the catchment scale during the whole study period.

3.5.5 The single gauged hillslope and catchment hydro-biogeochemical response during the transition period.

Lateral subsurface flow during the transition period was characterized by lower DON concentrations and higher DOC:DON than stream water during baseflow conditions, while DIN and DOC concentrations showed no difference. Algae were observed in the bedrock channel of WS10, are characterized by low C:N ratios, and higher stream DON concentrations may have been caused by by-products of in-stream production. In addition, N_2-fixing alder was present in the right fork of watershed 10, which can influence stream N concentrations (Compton et al., 2003; Cairns and Lajtha, 2005). During low flow conditions, when in-stream processes as by-products of algae production (autochthonous input) and leaching of leaf litter (allochthonous input) (Meyer et al., 1998) are likely more important than transport of DOM from the terrestrial to the stream environment (Mulholland and Hill, 1997; Hagedorn et al., 2000) these sources likely contributed significantly to elevated stream DON concentrations. Lateral subsurface flow DON and DOC concentrations were lower than stream water concentrations during stormflow conditions within the transition period. The lower observed concentrations in lateral subsurface flow may have resulted from in-stream processes or different mixing of sources between the hillslope and catchment scale. While there was a difference in mixing of sources between the hillslope and catchment scale during the transition period inferred from SUVA measurements, we argue that in-stream processes were the dominant control on higher DOC and DON concentrations in stream water. Grab samples during stormflow conditions from the hillslope trench, right fork and left fork during the transition

period showed that average DOC and DON concentrations were higher at the right fork (DOC: 9.7; DON: 0.28 mg l^{-1}, $n = 4$) and left fork (DOC: 7.3; DON: 0.17 mg l^{-1}, $n = 4$) compared to the hillslope trench (DOC: 5.0; DON: 0.11 mg l^{-1}, $n = 4$). This indicates that sources more upstream in the catchment caused the higher DOC and DON concentrations during stormflow conditions at the WS10 stream outlet compared to lateral subsurface flow. Average SUVA values from the right and left fork were 3.54 and 2.13 respectively and average DOC:DON ratios were 37 and 44 respectively, suggesting a terrestrial source of DOM. Grab samples ($n = 58$, during the wet period) were taken from the left fork (DOC: 3.8 mg l^{-1}; DON: 0.10 mg l^{-1}, $n =58$) during the whole study period that were not different in DOC and DON concentrations compared to lateral subsurface flow (DOC: 4.1 mg l^{-1}; DON: 0.09 mg l^{-1}, $n =56$) and stream water (DOC: 3.9 mg l^{-1}; DON: 0.10 mg l^{-1}, $n =56$) at the catchment outlet during the wet period. This lack of difference indicates that DOC and N concentrations were controlled mainly by lateral subsurface flow and not in-stream processes during the wet period with storms characterized by high runoff ratios (Table 3.2.), consistent with the findings of Mulholland and Hill (1997). During the transition period storms were characterized by small runoff coefficients (Table 3.2.) and a lower discharge regime (Figure 3.2.b). In addition, DOC and DON concentrations were higher at the left, right fork and catchment outlet compared to lateral subsurface flow during the transition period. We can not rule out that the difference in mixing at the hillslope scale compared to the catchment scale inferred from SUVA measurements partly caused the difference in DOC and DON concentrations between lateral subsurface flow and

stream water during the transition period. However, the hydrological observations as runoff coefficients and discharge regime and spatial sampling within the catchment indicated that in-stream processes were the dominant control during the transition period.

3.5.6 What caused lower C and N export rates at the hillslope scale?

We used mean flow weighted DOC, DON and DIN concentrations and storm flow totals to assess what caused lower C and N export rates at the hillslope scale compared to the catchment scale. The difference in DOC export between the catchment and hillslope was an effect of lower mean flow weighted concentrations during storms 1-4 in lateral subsurface flow and lower storm totals at the hillslope scale. The difference in DOC export for storm 5 was caused by a storm difference since flow weighted mean DOC concentration were lower in stream water. The difference in DON export between the watershed and hillslope was an effect of lower mean flow weighted concentrations during all storms in hillslope water and lower storm totals at the hillslope scale. As already mentioned, higher DOC and DON concentrations in stream water at the WS10 outlet likely resulted from in-stream processes.

McGlynn and McDonnell (2003) found that hillslope DOC export accounted for 22-36% of total catchment DOC export in a Maimai catchment, New Zealand. The remaining 64-78% originated in riparian and channel zones. At our site we observed that hillslope DOC export during five storm events accounted for a range of 56-82%

of total WS10 catchment DOC export. In WS10 hillslopes issue water directly into the stream without significant riparian zone modulation and this caused very likely higher hillslope DOC export contributions to total catchment DOC export than reported by McGlynn and McDonnell (2003).

3.5.7 Antecedent wetness conditions control C and N storm- event concentrations

High solute (DOC, DON) concentrations during storms after dry antecedent wetness conditions have been reported by others (Grieve, 1991; Vanderbilt et al., 2003; Cooper et al., 2007; Inamdar et al, 2006). We did not find a significant relationship between AMI_7 and DIN concentrations during storms. This is likely caused by the high biological demand of nitrate and ammonium in this environment. Storm DOC and DON peak and flow weighted concentrations at the hillslope and catchment scale generally decreased during the sequence of storms (Table 3.2.), with an increase in antecedent soil moisture. The AMI_7 at 30 cm soil depth can be considered as an index of how much flushing in the soil profile occurred prior to a storm event. AMI_{14} and AMI_{30} were not different from AMI_7. Furthermore, API_7, API_{14} and API_{30} were not significantly related to DOC and N peak and flow weighted concentrations. This suggests that solute concentrations during storm events were not controlled by rainfall events and thus flushing in the soil profile up to a month prior to these events. Rather, our results indicate that DOC and DON in the soil profile were exhausted rapidly during the transition period and stayed ‘constant’ during the wet period as a result of long-term precipitation patterns reflected in the soil moisture

pattern at 30 cm depth. Thus the observed pattern of storm DOC and DON peak and flow weighted concentrations may have been caused by rapid exhaustion of DOC and DON during the transition period as a response to flushing during storm events over time.

3.6 Conclusions

DON was the dominant form of total dissolved nitrogen (TDN) in all sampled solutions, except in transient groundwater, where DIN was the dominant form. The organic horizon and upper mineral soil layer was an important DOC and N source during the study period. The high observed DOC and N concentrations in transient groundwater underscore the importance of measuring DOC and N concentrations at different depths within the soil profile. In addition high DO C and N concentrations and SUVA values in transient groundwater indicated the occurrence of vertical preferential flow at our site.

We found that lateral subsurface flow and stream water did not differ in DOC, DON and NO_3-N concentrations during the wet period during baseflow and stormflow. However, SUVA values during this period and as well during the transition period were in lateral subsurface flow significantly lower than SUVA values of stream water. We suggest that the ratio of seep groundwater that was characterized by low SUVA values to transient groundwater that was characterized by high SUVA values, originating from preferential flow was higher at the hillslope scale than the ratio at the watershed scale.

During the transition period we found higher DOC and DON concentrations in stream water compared to lateral subsurface flow, during stormflow conditions. Low runoff ratios of lateral subsurface flow and stream water and a low discharge regime during the transition period, indicate in-stream processes caused these differences. This pattern was also reflected in the lower C and N export rates at the hillslope scale compared to the catchment scale during the transition period that was partly explained by lower DOC and N concentrations in lateral subsurface flow than stream water.

DOC and DON concentrations in stream water and lateral subsurface flow were significantly lower during the wet period compared to the transition period during stormflow conditions. Thus, DOC and DON were a finite source (production of DOC and DON lagged behind flushing of these nutrients) at the seasonal time scale. Furthermore, flow weighted and peak DOC and DON concentrations in lateral subsurface flow and stream water during storm events were correlated to antecedent soil moisture and supported the finite source at the seasonal scale (more prior flushing resulted in lower storm peak and flow weighted DOC and DON concentrations).

3.7 Acknowledgements

This work was supported through funding from the National Science Foundation (grant DEB 021-8088 to the Long-Term Ecological Research Program at the H. J. Andrews Experimental Forest) and Department of Forest Engineering at Oregon State University. We thank Marloes Bakker and John Moreau for providing

field assistance. We also thank R. D. Harr and D. Ranken for initiating the hillslope studies at WS10, and K. J. McGuire for re-initiating this site.

3.8 References

Bernal, S., Butturini, A. and F. Sabater (2005), Seasonal variations of dissolved nitrogen and DOC:DON ratios in an intermittent Mediterranean stream, *Biogeochemistry, 75,* 351–372.

Boyer, E. W., G. M. Hornberger, K. E. Bencala, and D. M. McKnight (1997), Response characteristics of DOC flushing in an Alpine catchment, *Hydrol. Processes, 11,* 1635-1647.

Buffam, I., J. N. Galloway, L. K. Blum and K. J. McGlathery (2001), A stormflow/baseflow comparison of dissolved organic matter concentrations and bioavailability in an Appalachian stream, *Biogeochemistry, 53,* 269-306.

Buresh, R. J. and W. H. Jr. Patrick (1978), Nitrate reduction to ammonium in anaerobic soil, *Soil Sci. Soc. Am. J., 42,* 913–918.

Cairns, M.A. and K. Lajtha (2005), Effects of Succession on Nitrogen Export in the West-Central Cascades, Oregon, *Ecosystems, 8,* 583-601.

Chin Y. P., G. R. Aiken and E. O'Loughlin (1994), Molecular weight, polydispersivity, and spectroscopic properties of aquatic humic substances, *Environ. Sci. Technol. 28,* 1853–1858.

Cirmo, C. P., and J. J. McDonnell, (1997), Linking the hydrologic and biochemical controls of nitrogen transport in near-stream zones of temperate-forested catchments: A review, *J. Hydrol., 199,* 88-120.

Creed, I. F., L. E. Band, N. W. Foster, I. K. Morrison, J. A. Nicolson, R. S. Semkin, and D. S. Jeffries (1996), Regulation of nitrate-N release from temperate forests: A test of the N flushing hypothesis, Water *Resour. Res., 32,* 3337–3354.

Compton, J. E., R. M. Church, S. T. Larned and W. E. Hogsett (2003), Nitrogen export from forested watersheds in the Oregon coast range: The role of N_2-fixing Red Alder, *Ecosystems, 6,* 773-785.

Cooper, R., V. Thoss and H. Watson (2007), Factors influencing the release of dissolved organic carbon and dissolved forms of nitrogen from a small upland headwater during autumn runoff events, *Hydrol. Processes, 21,* 622–633

Grieve I. C. (1991), A model of dissolved organic carbon concentration in soil and stream waters, *Hydrol. Processes 5,* 301–307.

Jardine, P. M., N. L. Weber and J. F. McCarthy (1989a), Mechanisms of dissolved organic carbon adsorption by soil, *Soil Sci. Soc. Am. J., 53,*1378–1385.

Hagedorn, F., P. Schleppi, P. Waldner and H. Fluhler (2000), Export of dissolved organic carbon and nitrogen from Gleysol dominated catchments—The significance of water flow paths, *Biogeochemistry, 50,* 137–161.

Harr, R. D., (1977), Water flux in soil and subsoil on a steep forested slope, *J. Hydrol., 33,* 37-58.

Hedin, L. O., J. C. von Fischer, N. E. Ostrom, B. P. Kennedy., M. G. Brown and G. P. Robertson (1998), Thermodynamic constraints on nitrogen transformations and other biogeochemical processes at soil-stream interfaces, *Ecology, 79,* 684-703.

Hedin, L. O., J. J. Armesto and A. H. Johnson (1995), Patterns of nutrient loss from unpolluted, old-growth temperate forests: evaluation of biogeochemical theory, *Ecology, 76,* 493-509.

Hill, A. R., W. A. Kemp, J. M. Buttle, and D. Goodyear (1999), Nitrogen chemistry of subsurface storm runoff on forested Canadian Shield hillslopes, *Water Resour. Res., 35,* 811 –821.

Hill, A. R., (1993), Nitrogen dynamics of storm runoff in the riparian zone of a forested watershed, *Biogeochemistry, 20,* 19-44.

Hood, E., D. M. McKnight and M. W. Williams (2003), Sources and chemical character of dissolved organic carbon across an alpine/subalpine ecotone, Green Lakes Valley, Colorado Front Range, United States, *Water Resour. Res., 39,* 1188, doi:10.1029/2002WR001738.

Hood, E., M. W. Williams and D. M. McKnight (2005), Sources of dissolved organic matter (DOM) in a Rocky Mountain stream using chemical fractionation and stable isotopes, *Biogeochemistry, 74,* 231-255.

Hood, E., M. N. Gooseff, and S. L. Johnson (2006), Changes in the character of stream water dissolved organic carbon during flushing in three small watersheds, Oregon, *J. Geophys. Res., 111,* G01007, doi:10.1029/2005JG000082.

Hooper, R. B. (2001), Applying the scientific method to small catchment studies: a review of the Panola Mountain experience, *Hydr. Processes, 15,* 2039–2050

Hornberger, G. M., K. E. Bencala, and D. M. McKnight (1994), Hydrological controls on dissolved organic carbon during snowmelt in the Snake River near Montezuma, Colorado, *Biogeochemistry, 25,* 147– 165.

Inamdar, S. P., O'Leary, N., Mitchell, M. J., and J. T. Riley (2006), The impact of storm events on solute exports from a glaciated forested watershed in western New York, USA, *Hydrol. Process. 20,* 3423–3439

Inamdar, S. P., and M. J. Mitchell (2006), Hydrological and topographical controls on storm-event exports of dissolved organic carbon (DOC) and nitrate across catchment scales, *Water Resour. Res., 42,* W03421, doi:10.1029/2005WR004212.

Kaiser, K., and G. Guggenbergers (2005), Storm flow flushing in a structured soil changes the composition of dissolved organic matter leached into the subsoil, *Geoderma, 127,* 177-187.

Kaplan, L. A., and J. D. Newbold (1993), Biogeochemistry of dissolved organic carbon entering streams, in *Aquatic Microbiology: An Ecological Approach,* edited by T. E. Ford, pp. 139 – 165, Blackwell Sci., Malden,Mass.

Katsuyama, M. and N. Ohte (2002), Determining the sources of stormflow from the fluorescence properties of dissolved organic carbon in a forested catchment, *J. of Hydr.,* 268, 192-202.

Keim, R. F., and A. E. Skaugset (2004), A linear system model of dynamic throughfall rates beneath forest canopies, *Water Resour. Res., 40,* W05208 doi:10.1029/2003WR002875

Lajtha, K., W. M. Jarrell, D. W. Johnson and P. Sollins (1999), Collection of Soil Solution. In: Robertson G. P., and others, Eds. Standard Soil Methods for Long-Term Ecological Research. New York: Oxford, University Press, p 166–182.

Lajtha, K., S. E. Crow, Y. Yano, S. S. Kaushal, E. Sulzman, P. Sollins and J. D. H. Spears (2005), Detrital controls on soil solution N and dissolved organic matter in soils: a field experiment, *Biogeochemistry, 76,* 261-281.

Leenheer, J. A., Brown, G. K., MacCarthy, P., and S. E. Cabaniss (1998), Models of metal binding structures in fulvic acid from the Suwannee River, Georgia, *Environmental Science and Technology, 32,* 2410-2416

McDowell, W. H., W. B. Bowden and C. E. Asbury (1992), Riparian nitrogen dynamics in two geomorphologically distinct tropical rain forest watersheds: subsurface solute patterns, *Biogeochemistry, 18,* 53-75.

McGlynn, B. L., and J. J. McDonnell, Role of discrete landscape units in controlling catchment dissolved organic carbon dynamics, *Water Resour. Res., 39(4),* 1090, doi:10.1029/2002WR001525, 2003.

McGuire, K. J., (2004), Water residence time and runoff generation in the western Cascades of Oregon, Ph.D., Oregon State University, Corvallis.

McHale M. R., Mitchell M. J., McDonnell J. J. and C. P. Cirmo(2000), Nitrogen solutes in an Adirondack forested watershed: importance of dissolved organic nitrogen, *Biogeochemistry, 48,*165–184.

McHale, M. R., J. J. McDonnell, M. J. Mitchell, and C. P. Cirmo (2002), A field-based study of soil water and groundwater nitrate release in an Adirondack forested watershed, *Water Resour. Res., 38(4),* 1031,doi:10.1029/2000WR000102.

McKnight, D. M., R. Harnish, R. L. Wershaw, J. S. Baron, and S. Schiff (1997), Chemical characteristics of particulate, colloidal and dissolved organic material in Loch Vale Watershed, Rocky Mountain National Park, *Biogeochemistry, 36,* 99–124.

McKnight, D. M., E. W. Boyer, P. K. Westerhoff, P. T. Doran, T. Kulbe, and D. T. Anderson (2001), Spectrofluorometric characterization of dissolved organic matter for indication of precursor organic material and aromaticity, *Limnol. Oceanogr., 46,* 38– 48.

McKnight, D. M., G. M. Hornberger, K. E. Bencala and E. W. Boyer (2002), In-stream sorption of fulvic acid in an acidic stream: A stream-scale transport experiment *Water Resourc. Res. 38(1),* 10.1029/2001WR000269.

Meyer, J. L., B. J. Wallace and S. L. Eggert (1998), Leaf litter as a source of dissolved organic carbon in streams, *Ecosystems,1,* 240–249.

Morris, D., H. Zagarese, C. E. Williamson, E. G. Balseiro, B. R. Hargreaves, B. Modenutti, R. Moeller and C. Queimalinos (1995), The attenuation of solar UV radiation in lakes and the role of dissolved organic carbon, *Limnol. Oceanogr., 40*, 1381–1391.

Mulholland, P. J., and W. R. Hill (1997), Seasonal patterns in streamwater nutrient and dissolved organic carbon concentrations: Separating catchment flow path and in-stream effects, *Water Resour. Res., 33,*, 1297-1306.

Ocampo, C. J., C. E. Oldham, M. Sivapalan and J. V. Turner (2006), Hydrological versus biogeochemical controls on catchment nitrate export: a test of the flushing mechanism, *Hydrol. Processes, 20*, 4269 – 4286.

Park, J., J. Lee, S. Kang and S. Kim (2007), Hydroclimatic controls on dissolved organic matter (DOM) characteristics and implications for trace metal transport in Hwangryong River Watershed, Korea, during a summer monsoon period, *Hydrol. Processes, 21*.

Perakis S. S. and L. O. Hedin (2002), Nitrogen losses from temperate South American forests mainly as dissolved organic forms, *Nature, 415,* 416- 419.

Ranken, D. W. (1974), Hydrologic properties of soil and subsoil on a steep, forested slope, M.S., Oregon State University, Corvallis.

Scully, N. M., and D. R. S. Lean (1994), The attenuation of ultraviolet light in temperate lakes, *Ergeb. Limnol., 43*, 101-114.

Silver, W. L., D. J. Herman and M. K. Firestone (2001), Dissimilatory nitrate reduction to ammonium in upland tropical forest soils, *Ecology, 82(9)*, 2410-2416.

Sollins, P., K. J. Cromack, F. M. McCorison, R. H. Waring, and R. D. Harr, (1981), Changes in nitrogen cycling at an old-growth Douglas-fir site after disturbance, *J. Enivron. Qual.,, 10*, 37-42.

Sollins P., C. C. Grier, F. M. McCorison, K. J. Cromack, R. Fogel and R. L. Fredriksen (1980), The internal element cycles of an oldgrowth Douglas-fir ecosystem in western Oregon. *Ecol. Monogr. 50*, 261–285.

Swanson, F. J., and M. E. James, (1975), Geology and geomorphology of the H.J. Andrews Experimental Forest, western Cascades, Oregon., Res. Pap. PNW-188, U.S. Department of Agriculture, Forest Service, Pacific Northwest Forest and Range Experiment Station, Portland, OR.

Tiedje, J. M., (1988), Ecology of denitrification and dissimilatory nitrate reduction to ammonium, in: Zehnder AJB (ed) Biology of Anaerobic Microorganisms, pp 179–244. John Wiley and Sons, New York

Triska, F. J., J. R. Sedell, K. Cromack, S. V. Gregory, and F. M. McCorison, (1984), Nitrogen budget for a small coniferous forest stream, *Ecological Monographs, 54*, 119-140.

Tromp-van Meerveld, H. J., and J. J. McDonnell (2006), Threshold relations in subsurface stormflow: 1. A 147-storm analysis of the Panola hillslope, *Water Resour. Res., 42*, W02410, doi:10.1029/2004WR003778.

Uchida, T., Y. Asano, N. Ohte, and T. Mizuyama (2003), Seepage area and rate of bedrock groundwater discharge at a granitic unchanneled hillslope, *Water Resouces Research, 39*, 10.1029/2002WR001298.

Vanderbilt, K. L., K. Lajtha and F. J. Swanson (2003), Biogeochemistry of unpolluted forested watersheds in the Oregon Cascades: temporal patterns of precipitation and stream nitrogen fluxes, *Biogeochemistry, 62,* 87–117.

Vidon, P. G. F., and A. R. Hill (2004), Landscape controls on nitrate removal in stream riparian zones, *Water Resour. Res., 40*, W03201, doi:10.1029/2003WR002473.

Vitousek, P.M., L. O. Hedin, P. A. Matson, J. H. Fownes and J. Neff (1998), Within-system element cycles, input-output budgets, and nutrient limitation. In: *Successes, Limitations, and Frontiers in Ecosystem Science.* Pace, M. and Groffman, P. (eds). p. 432–451.

Wagener, T., D. P. Boyle, M. J. Lees, H. S. Wheater, H. V. Gupta and S. Sorooshian (2001), A framework for development and application of hydrological models, *Hydrology and Earth System Sciences, 5*(1), 13–26.

Weishaar, J. L., G. R. Aiken, B. A. Bergamaschi, M. S. Fram, R. Fujii and K. Mopper (2003), Evaluation of Specific Ultraviolet Absorbance as an Indicator of the Chemical Composition and Reactivity of Dissolved Organic Carbon, *Environ. Sci. Technol., 37,* 4702-4708.

Woods, R., and L. Rowe (1996), The changing spatial variability of subsurface flow across a hillside, *Journal of hydrology. New Zealand, 35*, 51-86.

Yano, Y., K. Lajtha, P. Sollins and B. A. Caldwell (2004), Chemical and seasonal controls on the dynamics of dissolved organic matter in a coniferous old-growth stand in the Pacific Northwest, USA, *Biogeochemistry, 71,* 197-223.

Yano, Y., K. Lajtha, P. Sollins and B. A. Caldwell (2005), Chemistry and dynamics of dissolved organic matter in a temperate coniferous forest on andic soils: effects of litter quality, *Ecosystems, 8*, 286-300.

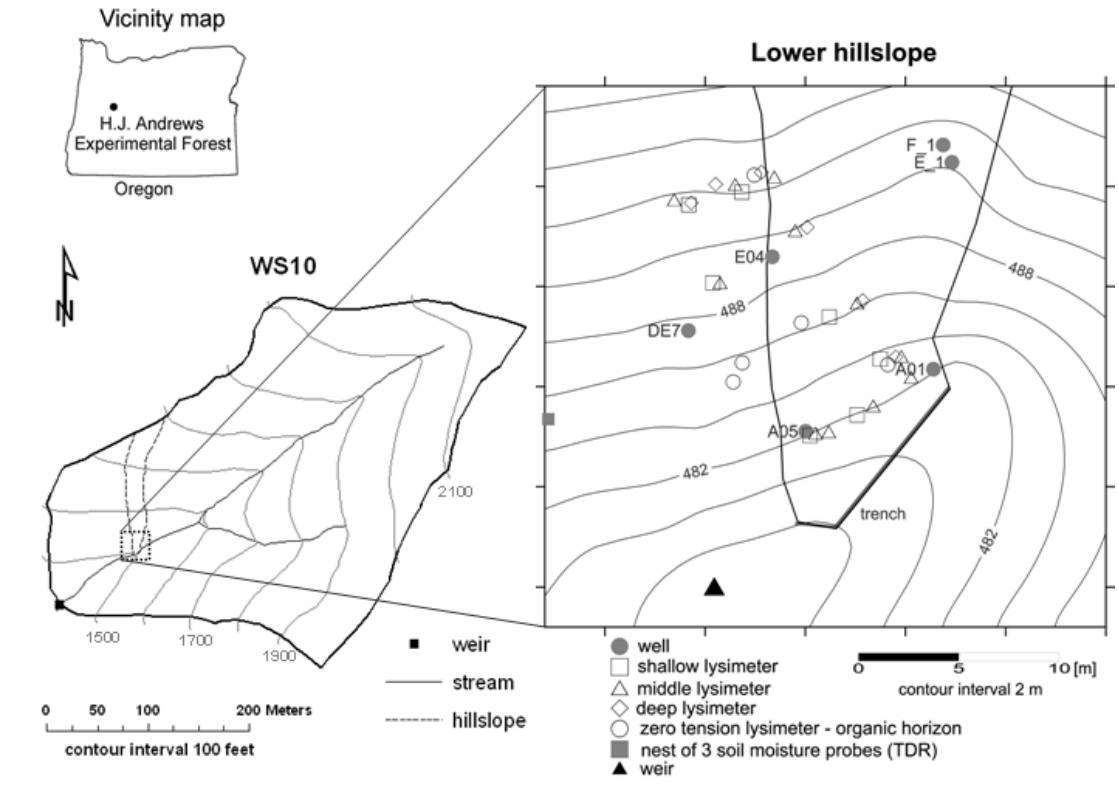

Figure 3.1. Map of WS10 showing the location of the hillslope study area and lower hillslope with the instrumentation.

Table 3.1. Mean (± SD) of DOC, DON, NH_4-N, NO_3-N concentrations and DOC:DON and SUVA.

	DOC [mg l^{-1}]	DON [mg l^{-1}]	NH_4-N [mg l^{-1}]	NO_3-N [mg l^{-1}]	DOC: DON	$SUVA_{254}$ [L mg $C^{-1}m^{-1}$]
Throughfall	1.4 (0.5)	0.07 (0.04)	0.008 (0.008)	0.008 (0.008)	25 (21)	2.8 (0.8)
Organic horizon	12.3 (5.3)	0.45 (0.60)	0.072 (0.970)	0.045 (0.173)	35 (20)	5.3 (1.8)
Shallow lysimeter	9.1 (15.5)*	0.25 (0.29)	0.032 (0.052)	0.029 (0.099)	25 (20)	4.5 (6.4)
Middle lysimeter	4.3 (2.4)	0.15 (0.10)	0.028 (0.022)	0.020 (0.066)	40 (44)	3.5 (2.0)
Deep lysimeter	1.4 (0.6)	0.10 (0.07)	0.035 (0.033)	0.005 (0.017)	21 (23)	1.8 (0.9)
Groundwater seep	4.0 (1.0)	0.07 (0.02)	0.014 (0.009)	0.013 (0.016)	63 (27)	0.9 (0.6)
Transient groundwater	8.5 (6.7)	0.30 (0.30)	0.254 (0.331)	0.311 (0.489)	32 (28)	5.4 (5.2)
Lateral subsurface flow	4.8 (1.3)	0.11 (0.07)	0.005 (0.005)	0.004 (0.005)	64 (279)	0.7 (0.5)
Stream water	5.1 (1.5)	0.14 (0.07)	0.007 (0.010)	0.004 (0.005)	49(76)	1.6 (0.7)

* high SD is caused by one lysimeter that was installed in an area with woody debris with high DOC concentations

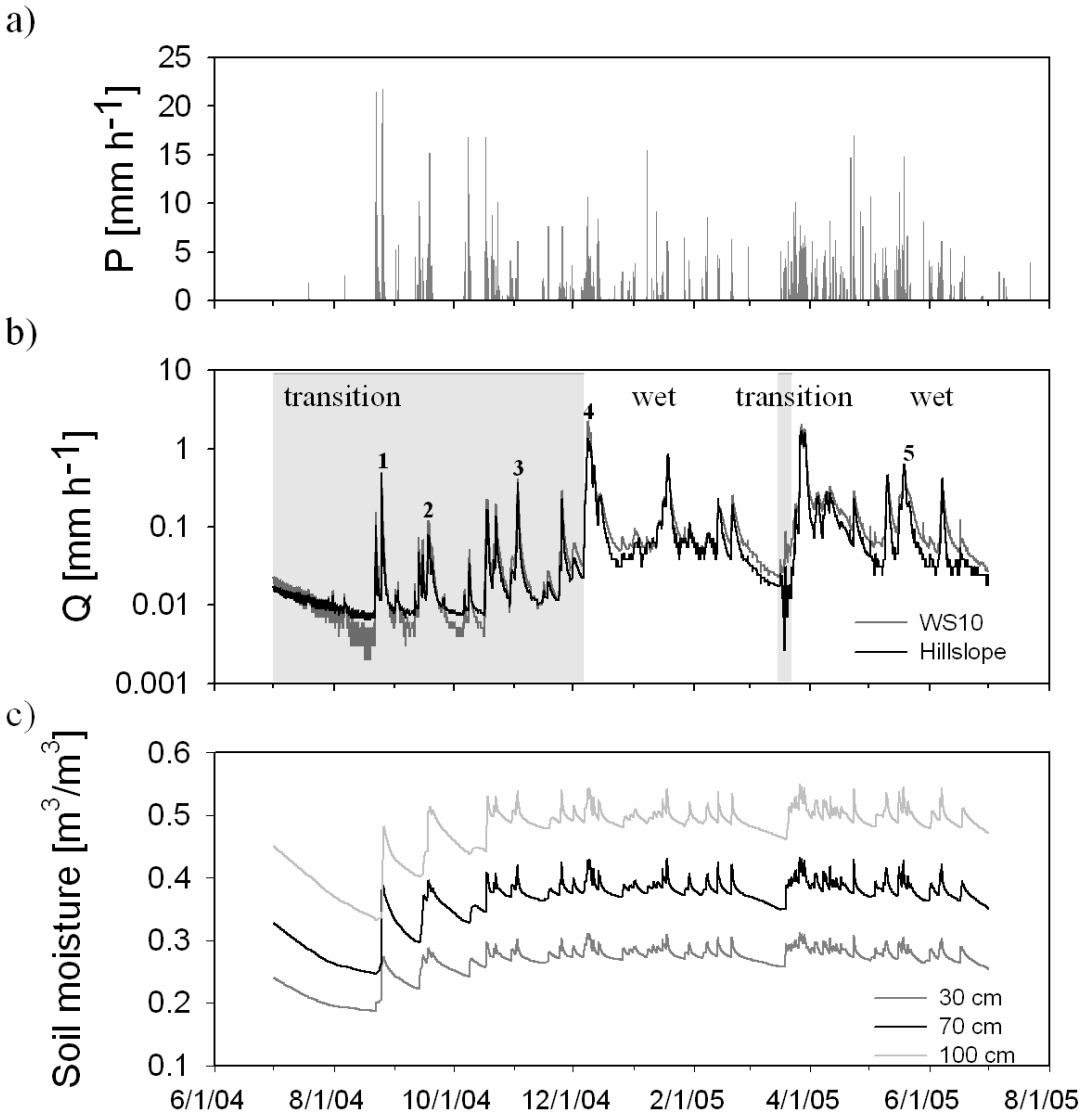

Figure 3.2. Time series of hydrological data during the study period: a) rainfall, b) discharge from the hillslope and watershed with different hydrological conditions during the year: transition periods (light gray background) characterized by an increase in hillslope and watershed baseflow and soil moisture and a wet period (white background) characterized by high 'steady' hillslope and watershed baseflow conditions. The numbers in the graph refer to storms that were sampled, c) soil moisture content (m^3/m^3).

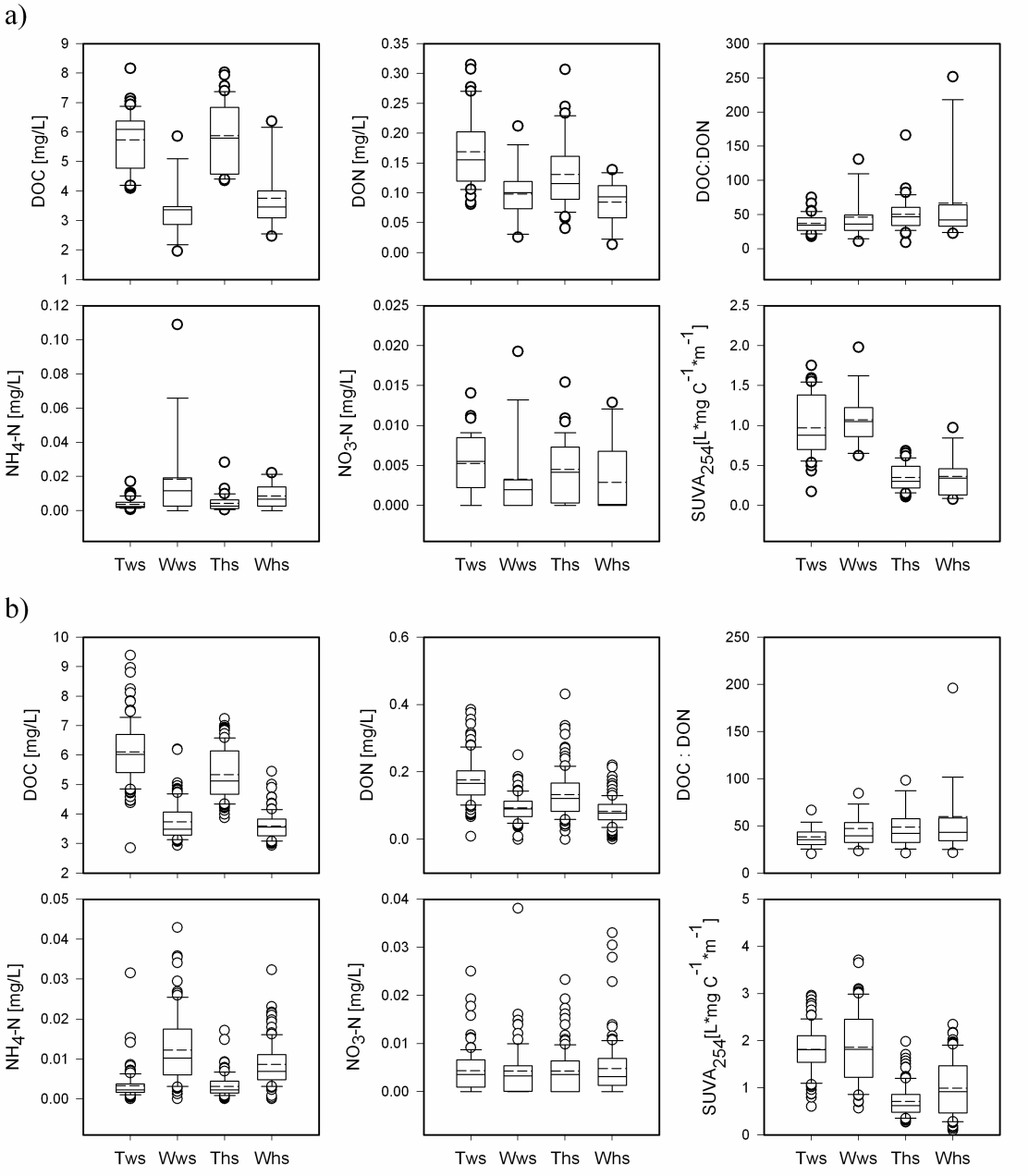

Figure 3.3. Box plots of DOC, DON, NH_4-N, NO_3-N concentrations, DOC:DON and SUVA during a) baseflow conditions and b) stormflow conditions, during different hydrological conditions (T=transition period, W=wet period) for stream water at WS10-oulet (ws) and lateral subsurface flow from the trenched hillslope (hs). The dashed line in the box plot is the average value and the solid line is the median value. The boundary of the box indicates the 75th percentile. The error bars above and below the box indicate respectively the 90th and 10th percentile. Circles are outliers.

Table 3.2. Storm event characteristics and DOC, DON and DIN peak and flow weighted average concentrations for lateral subsurface flow and stream water.

	Storm 1	Storm 2	Storm 3	Storm 4	Storm 5
Start date	08-24-04	09-16-04	11-01-04	12-06-04	05-14-05
End date	08-29-04	09-20-04	11-04-04	12-12-04	05-24-05
Gross precipitation [mm]	71	44	42	200	100
10-min max. rainfall intensity [mm/h]	21.7	15.2	6.1	10.7	14.8
Rainfall duration [h]	39	74	49	132	195
Runoff ratio WS10 [%]	6.3	9.7	20	74.5	36.7
Runoff ratio hillslope [%]	4.2	5.6	15.2	55.6	37
AMI_7 [m^3/m^3]	0.200	0.260	0.279	0.275	0.276
AMI_{14} [m^3/m^3]	0.200	0.257	0.280	0.276	0.276
AMI_{30} [m^3/m^3]	0.199	0.255	0.277	0.275	0.276
Stream water					
DOC peak [mg l^{-1}]	9.4	7.5	6.7	5.1	4.7
DON peak [mg l^{-1}]	0.39	0.25	0.30	0.18	0.25
DIN peak [mg l^{-1}]	0.030	0.022	0.015	0.053	0.039
flow weighted average DOC [mg l^{-1}]	7.6	5.9	5.3	3.6	3.6
flow weighted average DON [mg l^{-1}]	0.24	0.14	0.17	0.09	0.11
flow weighted average DIN [mg l^{-1}]	0.010	0.007	0.009	0.016	0.019
Lateral subsurface flow					
DOC peak [mg l^{-1}]	8.0	6.5	5.8	4.2	5.0
DON peak [mg l^{-1}]	0.73	0.25	0.19	0.21	0.22
DIN peak [mg l^{-1}]	0.033	0.027	0.017	0.036	0.063
flow weighted average DOC [mg l^{-1}]	6.5	5.0	4.6	3.2	3.7
flow weighted average DON [mg l^{-1}]	0.20	0.11	0.12	0.08	0.10
flow weighted average DIN [mg l^{-1}]	0.008	0.007	0.008	0.016	0.011

Table 3.3. Pearson correlation coefficients [r] between DOC, DON and DIN flow weighted average and peak concentrations of WS10 stream water and lateral subsurface flow and AMI_7.

	AMI_7 Pearson correlation coefficient [r]	
	WS10 stream water	Lateral subsurface flow
DOC peak [mg l^{-1}]	-0.94**	-0.97***
DON peak [mg l^{-1}]	-0.79	-0.93**
DIN peak [mg l^{-1}]	0.25	0.26
flow weighted average DOC [mg l^{-1}]	-0.93**	-0.94**
flow weighted average DON [mg l^{-1}]	-0.86*	-0.91**
flow weighted average DIN [mg l^{-1}]	0.55	0.53

* $p < 0.1$
** $p < 0.05$
*** $p < 0.01$

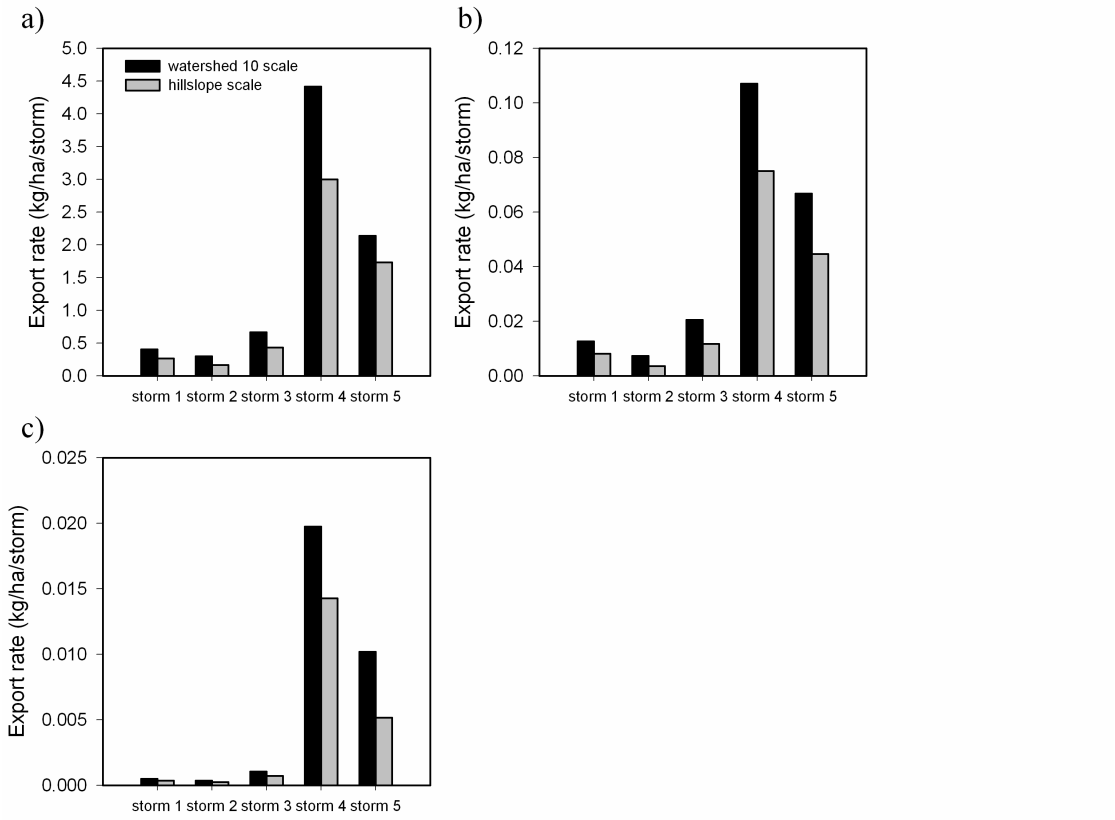

Figure 3.4. Export rates of a) DOC, b) DON, and c) DIN, during sampled storms at the watershed and hillslope scale.

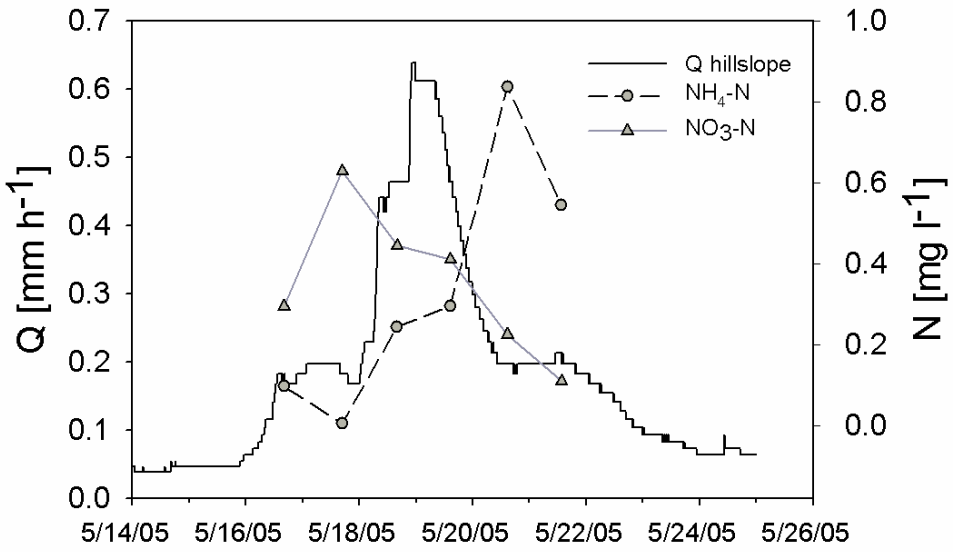

Figure 3.5. Hillslope discharge and NO_3-N and NH_4-N patterns in transient groundwater from well E04, during storm 5.

4 A mechanistic assessment of nutrient flushing at the catchment scale

Van Verseveld, W. J.
McDonnell, J. J.
Lajtha, K.

4.1 Introduction

The hydrological controls on nutrient flushing at the catchment scale are poorly understood (Weiler and McDonnell, 2006). During storm events and snowmelt periods, many studies have reported a significant increase in dissolved organic nitrogen (DON), dissolved organic carbon (DOC) and nitrate (NO_3-N), and attributed this increase to a nutrient flushing mechanism (Creed et al., 1996; Boyer et al., 1997; McHale et al., 2002; Vanderbilt et al., 2003; McGlynn and McDonnell, 2003). Flushing of nutrients has been explained qualitatively by (1) a rising water table that intersects high nutrient concentrations in the upper soil layer, (2) vertical transport of nutrients, by preferential or matrix flow through the (deeper less bio-active) soil to the soil-bedrock interface and then laterally downslope (Hill et al., 1999; Buttle et al., 2001; Creed et al., 1996), and (3) vertical transport of nutrients and then laterally within the soil profile (e.g. Gaskin et al., 1989). In each of these conceptual models an infinite source of nutrients during storms is assumed, no hydro-biogeochemical studies to date have tested this explicitly.

Mechanistic understanding of flushing of nutrients is essential for model development for prediction of land use change and climate change effects on surface water quality. Understanding the flushing mechanism during storm events is important, since stormflow contributes substantially to total DOC and nitrogen (N) export (Hinton et al., 1997; Bernal et al., 2005). Despite the many studies on nutrient flushing, the exact flushing mechanism at most study sites remains qualitative and mechanistically weak. For instance, whilst McGlynn and McDonnell (2003) found

that the relative timing of riparian and hillslope source contributions to stream water explained stream DOC patterns, they could not determine what flushing mechanism at the hillslope occurred (i.e. if is was flushing mechanism 1, 2, or 3).While patterns of DOC in shallow pore waters and in stream water provide evidence that the shallow soil is a primary source of high DOC concentrations to the stream (e.g. Boyer et al., 1997), we frequently don't know how these sources are hydrologically connected to the stream. Bishop et al. (2004) illustrated the importance of assessing hydrological connectedness. They were able to identify the small riparian area as the only contributor to elevated stream DOC concentrations in a Swedish catchment during storm events, through a combination of hydrometric data and soil water DOC concentrations.

So, how might we mechanistically asses flushing of nutrients? We know there are three possible flushing mechanisms with or without an infinite source of nutrients during storms that we can test as hypotheses in line with recommendations of Hooper (2001). Assessing sources of stream water is an initial step to reject one or more of these hypotheses. Bonell (1998) recommended that conclusions regarding the sources of stream water drawn from runoff hydrochemistry data at the hillslope and catchment scale should be supported by independent hydrometric data. End member mixing analysis (EMMA) can be used as a hydro-chemical technique to resolve possible sources of channel stormflow. Numerous studies (Hagedorn et al., 2000; Mulholland et al., 1997; Inamdar and Mitchell, 2006; McHale et al., 2002; Bernal et al., 2006) have used this technique to investigate sources of and even biogeochemical controls

on DOC and N. Only a small number of studies have used EMMA in conjunction with hydrometric data and conservative isotopic tracers (e.g. McGlynn et al., 1999; McHale et al., 2002) to identify sources and flowpaths of stream water. In addition to EMMA and hydrometric techniques, the chemical character of dissolved organic matter (DOM) (DOC:DON, specific UV absorbance (SUVA), fluorescence spectroscopy) can provide information to help elucidate sources of DOM at seasonal scales (Hood et al., 2003; McKnight et al., 1997; Hood et al., 2005) and during storms at the catchment scale (Hagedorn et al., 2000; Hood et al., 2006; Katsuyama and Ohte, 2002).

Measurements of matric potential at different depths in the soil may also provide critical information to to reject one or more of the flushing mechanism hypotheses. In catchments with steep hillslopes, flushing mechanism 3, vertical transport of nutrients and then laterally within the soil profile may occur. Vertical and lateral flow vectors have been studied through detailed field experiments (Harr, 1977; Torres et al., 1998; Retter et al., 2006) and modeling studies (McCord et al., 1991; Jackson, 1992) with often contradicting results about the relative importance of lateral flow within the soil profile of hillslopes.

While several studies have identified the forest floor and upper soil layer as an important source of elevated DOC and N concentrations in stream water during storm events, whether this source is finite or infinite remains poorly understood. The few studies that have focused on DOC concentrations in the upper soil profile during storm events concluded that DOC was an infinite source (McGlynn and McDonnell, 2003;

Jardine et al., 1990). A synthesis of 42 studies that have focused on DOC and DON concentrations in the upper soil layer at coarser time scales in temperate forests (Michalzik et al., 2001) concluded that there was no dilution effect of precipitation for both DOC and DON concentrations, indicating an unlimited supply of DOM from the organic layer. In contrast Boyer et al. (1997) observed that DOC concentrations in shallow lysimeters decreased rapidly during the snowmelt season in an alpine catchment. This suggests that at their site DOC was a finite source at the time scale of about four months. Thus detailed temporal measurements of nutrient concentrations in the organic horizon and shallow soil layer during storm events are essential to quantify whether DOC and N are a finite or infinite source during flushing of these solutes.

This study examines two storm events using a combination of continuous fluorescence measurements at the hillslope and catchment scale, hydrometric data and chemical measurements of soil, groundwater, lateral subsurface flow and stream water to test the three flushing mechanism hypotheses. We address the following questions: (1) What is the DOC and N flushing pattern at the hillslope and catchment scale? (2) What sources of lateral subsurface flow and stream water can we identify with end member mixing analysis? (3) Can hydrometric data be used to validate the end member mixing analysis? (4) What is the lag time between start of rainfall and lateral subsurface flow, stream flow and internal hillslope hydrometric data and how do water and nutrient flow directions in the unsaturated zone shift through an event? (5) What pattern of DOC and N concentrations in the organic horizon, soil and groundwater do we observe?

4.2 Site description

This study was conducted in Watershed 10 (WS10), a 10.2 ha headwater catchment located on the western boundary of the H. J. Andrews Experimental Forest (HJA), in the western-central Cascade Mountains of Oregon, USA (44.2° N, 122.25° W) (Figure 4.1). HJA has a Mediterranean climate, with wet mild winters and dry summers. Average annual rainfall is 2220 mm of which about 80% falls between October and April during storms characterized by long duration and low rainfall intensity. Light snow accumulations in WS10 are common but seldom exceed 30 cm, and generally melt within 2 weeks (Sollins et al., 1981). Elevations range from 470 m at the watershed flume to a maximum watershed elevation of 680 m at the southeastern ridge line. The watershed was harvested during May-June 1975 and is now dominated by a naturally regenerated second growth Douglas-fir (*Pseudotsuga menziesii*) stand. Several seep areas along the stream have been identified (Harr, 1977; Triska, 1984). These seep areas are related to the local topography of bedrock and/ or saprolite, or to the presence of vertical, andesitic dikes approximately 5 meters wide, which are located within the southern aspect hillslope (Swanson and James, 1975; Harr, 1977).

The hillslope study area is located on the south aspect of WS10, 91 m upstream from the stream gauging station (Figure 4.1). The 125 m long stream-to-ridge slope has an average gradient of 37º, ranging from 27º near the ridge to 48º adjacent to the stream (McGuire, 2004). Elevation of the study hillslope ranged from 480 to 565 m. The bedrock is of volcanic origin, including andesitic and dacitic tuff and coarse

breccia (Swanson and James, 1975). The depth to unweathered bedrock ranges from 0.3 to 0.6 m at the stream-hillslope interface and increases gradually toward the ridge to approximately 3 to 8 m. Soils are about 1 m deep, and formed either in residual parent material or in colluvium originating from these deposits. Surface soils are well aggregated, but lower depths (70-110 cm) exhibit more massive blocky structure with less aggregation than surface soils (Harr, 1977). Soil textures change little with depth. Surface soils are gravelly loams, lower soil layers are gravelly silty clay loams or clay loams and subsoils are characterized by gravelly loams or clay loams (Harr, 1977). The soils are highly andic and vary across the landscape as either Typic Hapludands or as Andic Dystrudepts (Yano et al., 2005), and are underlain by 1-8 m relatively low permeability subsoil (saprolite), which formed in the highly weathered coarse breccia (Ranken, 1974; Sollins, 1981).

Benchmark hydrological studies (Harr, 1977; Ranken 1974) were conducted at this site during the 1970s and the site was re-established by McGuire (2004) in 2002. As part of these 1970's studies, a total of 450 soil cores from eleven soil pits were collected at depths of 10, 30, 70, and 110 cm in the soil and 130, 150 and 250 cm in subsoil. These soil cores were analyzed for hydraulic conductivity, porosity, pore-size distribution, bulk density, soil moisture – tension relationships and stone-content (Ranken 1974; Harr, 1977).

4.3 Methods

4.3.1 Instrumentation

To measure lateral subsurface flow at a natural seepage face a 10 m long trench was constructed (McGuire et al., 2007). Intercepted subsurface water was routed to a calibrated 30º V-notch weir that recorded stage at 10-minute time intervals using a 1-mm resolution capacitance water-level recorder (TruTrack, Inc., model WT-HR). Rainfall was measured with a tipping bucket and storage gauge located in a small canopy opening on the hillslope. The drainage area of the hillslope was delineated topographically from a total station survey of the entire hillslope (0.17 ha) and verified by a water balance calculation (McGuire et al., 2007). We used a rounded value of 0.2 ha in all analyses. As part of the long term monitoring at the H.J. Andrews Experimental Forest, watershed discharge of WS10 is measured with a trapezoidal flume since 1973. Since 1997 a V-notch weir is used during the summer. Stage was measured with a Model 2 Stevens Instruments Position Analog Transmitter (PAT) (0.001 ft resolution).

We instrumented the gauged hillslope with four nests of porous cup suction lysimeters (Soil Moisture Equipment Corp., Model 1900, 2 bar) at 30, 70 and 110 cm depths, except for site AL, where the deepest lysimeter was installed at 80 cm depth (depth of bedrock) (Figure 4.1). These suction lysimeters were installed in addition to four nests that were already installed (McGuire, 2004). Six plastic 10 x 10 cm zero tension lysimeters, were installed below the organic layer, three were installed at 20 cm depth, and two with a size of 15 x 15 cm were installed at 40 cm depth (Figure

4.1). Twenty seven prenart superquartz tension lysimeters (Prenart Equipment ApS, 0.5 bar) were installed at 20 cm, 30-40 cm, and 70-110 cm at a 30º angle according to the method described by Lajtha et al. (1999).

Transient saturation was measured with 69 maximum cork rise wells (1.25 inch diameter), and were screened for the lower 25 cm, the maximum water height observed by Harr (1977). We equipped a total of four wells including one well in the seepage area (A01) that showed consistent transient saturation with 1-mm resolution capacitance water level recorders (TruTrack, Inc., model WT-HR). We sampled five groundwater wells (Figure 4.1) at three-weekly intervals, and we sampled wells that showed persistent saturation during storms prior to, during, and after these events. All the wells were installed until refusal by a hand auger.

Soil water content (θ) was measured with water content reflectometers (WCR) (CS615, Campbell Scientific, Inc.). The soil moisture probes were installed horizontally (i.e., with the slope) at 3 depths (30, 70, and 100 cm) in three soil pits in lower portion of the hillslope. The nests were located 15, 20 and 25 m from the slope base (McGuire, 2004).

Soil matric potential was measured by 7 fast responding tensiometers (type: UMS T4, 1 bar porous cups), that were installed vertically in a triangle pattern, three tensiometers at 30 depth, three tensiometers at 70 cm depth, and one tensiometer at 100 cm depth. The tensiometer triangle was located 25 meter upslope from the base of the hillslope. We installed the tensiometers close to each other in a triangle to calculate unsaturated flow directions without bias of an elevation gradient. This enabled us to

investigate the possible occurrence of an unsaturated lateral flow component during storms. Saturation was defined as pore pressure = 0.25 kPa.

4.3.2 Flow direction analysis

A plane was fitted through the total head values for each timestep at tensiometer locations at 30 cm depth and 70 cm depth respectively. The direction of the lateral gradient was defined as the gradient parallel to the soil surface (46°) at the tensiometer triangle. The normal vectors to these planes defined the size of the lateral gradient at each depth. The direction of the vertical gradient was defined as normal to the soil surface. The vertical gradient between planes at 30 and 70 cm depth was calculated as the average of the gradients at the three tensiometer locations. The vertical gradient at 70 cm depth was calculated at the tensiometer location with three tensiometers at depths 30, 70 and 100 cm. The resultant flow direction from the lateral and vertical flow gradient was expressed as the deviation from the true vertical flow direction (Figure 4.2).

4.3.3 Sampling

Throughfall, lateral subsurface flow, seepage and transient groundwater, WS10 stream water and soil water (zero tension and tension) samples were collected between August 2004 and June 2005 at three-weekly intervals, and prior to, during, and after five storm events. Throughfall was captured using the technique of Keim and Skaugset (2004). Tension lysimeters were evacuated to -50 kPa and allowed to collect water for

24 hours. We used samples from porous cup tension lysimeters for the analysis of sulfate (SO_4^{2-}) and chloride (Cl^-), and samples from super quartz tension lysimeter for the analysis of DOC, TDN, NO_3-N, ammonium (NH_4-N) and UV-absorbance. All water samples except porous cup lysimeter samples were analyzed for DOC, TDN, NO_3-N, NH_4-N and UV-absorbance. A subset of all water samples was analyzed for SO_4^{2-} and Cl^-. The gauged hillslope and watershed outlet were both sampled with ISCO samplers between 1 and 4 hour intervals during several storms. Fluorescence in the field at the gauged hillslope and watershed outlet were measured continuously at a 5 sec. interval using a field fluorometer (10-AU, Turner Designs, Inc., Sunnyvale, CA) during the December 2004 and May 2005 storm events.

4.3.4 Chemical analysis

DOC and TDN were measured with Pt-catalyzed high-temperature combustion (Shimadzu TOC-V CSH analyzer with TN unit). Nitrate-N was measured with the hydrazine sulfate reduction method and NH_4^+-N was determined by the Berthelot reaction method with a an Orion Scientific AC 100 continuous flow auto-analyzer (Westco Scientific Instruments, Inc., Danbury, CT). DON was calculated as the difference between TDN and DIN (NO_3-N and NH_4-N). Because DON was calculated by difference, values sometimes fell slightly below 0 mg L^{-1}. Negative DON values were considered to be 0 mg L^{-1}. SO_4^{2-} and Cl^- were measured using a Dionex Model DX 500 Ion Chromatograph. UV absorbance (UVa) was measured at 254 nm with a Hitachi V-2001 spectrophotometer.

4.3.5 End member mixing analysis (EMMA)

We performed EMMA (Christophersen and Hooper, 1992; Burns et al., 2001; McHale et al, 2002; James and Roulet, 2006, Inamdar and Mitchell, 2006) to identify end-members of stream and lateral subsurface water at the annual scale and during two storm events. The following solutes were used in EMMA: DOC, UVa, Cl^- and SO_4^{2-}. EMMA relies on the assumption that mixing of end-members is a linear process, and thus solutes used in EMMA should behave conservatively and end-members should have time invariant compositions. We recognize that DOC and UVa may behave non-conservatively. However several studies have used DOC to identify expression of the O-horizon or shallow soil water in stream water (Brown et al., 1999; Inamdar and Mitchell, 2006; James and Roulet, 2006). In addition, Cl^- and SO_4^{2-} are considered quasi-conservative; Cl^- can sorb onto soils and be stored in plants by plant-uptake and SO_4^{2-} can undergo significant biological transformations (Swank et al., 1984). While Cl^- may behave quasi conservatively, the average Cl^- concentration of precipitation was 1.29 mg l^{-1} during the period 1990-2003 (PRIMET station, HJA), which is in the high range of Cl^- wet deposition in USA (NADP), and probably behaved relatively more conservatively in comparison to sites with lower Cl^- wet deposition values (<0.1 mg l^{-1}). Because the solutes used in EMMA may behave non- to quasi-conservatively, we used EMMA as an investigative tool to identify possible end-members for lateral subsurface flow and stream water.

4.4 Results

4.4.1 DOC and N flushing pattern at the hillslope and catchment scale

DOC concentrations in lateral subsurface flow during the December 2004 storm event showed a dilution pattern, with a maximum concentration of 4.18 mg l^{-1} (Figure 4.3.a). DON showed maximum concentrations on the rising limb of the storm with a 1.8 times increase during the rising limb of the hydrograph. DIN concentrations during the storm did increase with maximum concentrations around the hydrograph peak. SUVA and raw fluorescence increased 2.4 and 1.8 times respectively on the rising limb during the storm event. DOC, SUVA, raw fluorescence and DON all showed a clockwise hysteresis pattern; higher DOC and DON concentrations and SUVA, and raw fluorescence values on the rising limb compared to the falling limb of the hydrograph. The flushing pattern of DON was not clear because of high variability of DON concentrations.

DOC concentrations in stream water increased 1.2 times and DON concentrations increased 1.7 on the rising limb of the December storm event (Figure 4.3.a). Highest DIN concentrations were found during the last hydrograph peak of the storm. SUVA and raw fluorescence increased both 1.5 times, during the rising limb of the storm. DOC, SUVA, raw fluorescence and DON all showed a clockwise hysteresis pattern. For lateral subsurface flow, the flushing pattern of DON was not clear because of high variability of DON concentrations

During the May storm both lateral subsurface flow and stream water showed a DOC, SUVA, raw fluorescence and DON clockwise hysteresis pattern (Figure 4.3.b).

Stream DOC and subsurface flow DOC increased 1.5 and 1.2 times respectively. DON in stream and subsurface flow water did not show a clear flushing pattern because of high variability in DON concentrations during the storm. DON concentrations on the rising limb of the storm hydrograph increased by 11.7 and 25.8 times respectively. DIN concentrations in stream water were highly variable and increased from 0.021 mg l^{-1} to 0.039 mg l^{-1} on the rising limb of the storm. DIN concentrations in lateral subsurface flow, were also highly variable and showed (after the first high DIN (0.0628 mg l^{-1}) sample) an increase from 0.0076 mg l^{-1} to 0.0198 mg l^{-1} on the rising limb. SUVA and raw fluorescence values in stream water increased 2.3 and 2.4 times respectively, on the rising limb of the storm. SUVA and raw fluorescence in lateral subsurface flow increased on the rising limb of the storm 4.4 and 2.8 times respectively.

4.4.2 Runoff sources of lateral subsurface flow and stream water

We used end member mixing analysis (EMMA) to evaluate the contribution of runoff components to lateral subsurface flow and stream water during the December 2004 and May 2005 storm. The principal component analysis we used for EMMA indicated that between 78 and 95% of the variability in lateral subsurface flow and stream water during the December and May storm could be explained by two prinicipal components. This indicates that variation in the lateral subsurface flow and stream water could be accounted for by three end-members. End members were selected based on the following criteria: for all storm events lateral subsurface flow

and stream samples could be explained by more than one combination of three end members; we choose end members combinations that were as similar as possible for stream water and lateral subsurface flow during individual storm events and bounded the solute space most complete.

Lateral subsurface flow water during the December storm event was bounded by the three end-members: baseflow, throughfall and organic horizon water (Figure 4.4.b). The proportion of organic horizon water was higher on the rising limb of the hydrograph compared to the falling limb of the hydrograph, while on the falling limb of the hydrograph the proportion of throughfall water increased (Figure 4.5). Stream water during the December storm event was bounded by three end-members: baseflow, throughfall and organic horizon water (Figure 4.4.a). During the storm the maximum proportion of througfall was 49% during the falling limb of the hydrograph, while the maximum proportion of organic horizon water was 36% during the rising limb of the hydrograph.

Lateral subsurface flow during the May storm was bounded by baseflow, throughfall and transient groundwater end members (Figure 4.4.d). Deep soil water projected close to the end-member throughfall in the lateral subsurface flow U-mixing space. Maximum contribution (54%) to runoff by transient groundwater was found on the rising limb of the hydrograph. Throughfall contribution to runoff increased during the storm with highest values (46%) at the hydrograph peak. Stream water during the May storm was bounded by the end-members throughfall, shallow soil water and transient groundwater (Figure 4.4.c). As in the lateral subsurface flow mixing U-space,

deep soil water and throughfall projected close to each other in the stream water mixing U-space. The end-member organic horizon was projected in the same positive U-mixing space as shallow soil water, however organic horizon did not bound the solutes as completely as shallow soil water. Shallow and throughfall water contributions to runoff varied the most during the storm (compared to transient groundwater contributions), with higher contributions of shallow soil water than throughfall during the rising limb and a reversed pattern during the falling limb of the hydrograph (Figure 4.5.).

4.4.3 Hydrometric data to validate EMMA

To evaluate the EMMA derived contributions of end members for stream and lateral subsurface flow water we compared these contributions to hydrometric measurements (Figure 4.6) at the hillslope study area. We calculated pearson correlation coefficients (r) between hydrometric data and EMMA derived contributions. The pearson correlation coefficient between water height in well A01 and EMMA derived baseflow contribution to subsurface lateral flow was -0.90 (p <0.001) during the December event and –0.92 (p <0.001) during the May event. Furthermore, the timing of EMMA derived baseflow contributions were in close agreement with the measured water height in well A01 (Figure 4.6). The pearson correlation (r = 0.52, p <0.01) for the organic horizon EMMA derived contribution to lateral subsurface flow and soil moisture measured at this soil profile position for the December event was smaller than the pearson correlation for baseflow. The organic

horizon EMMA derived contribution was likely overestimated at the start of the event, since the EMMA derived contribution was much higher than the soil moisture contribution (Figure 4.6).

Soil matric potential at 100 cm depth located 5 m upslope from well E04 was used as a proxy for transient groundwater in well E04 during the May 2005 storm event, because the transient groundwater hydrograph was affected by sampling during this event. The pearson correlation coefficient of EMMA derived baseflow to stream water during the December event was -0.58 ($p < 0.01$) and the timing of EMMA derived baseflow was in general agreement with the water height in well A01 (Figure 4.6). For the May event, the pearson correlation between transient groundwater EMMA derived contribution to lateral subsurface flow and soil matric potential at the deep soil profile position was 0.52 ($p <0.01$). The pearson correlation coefficient of organic horizon was low (r = 0.36) for stream water during the December 2004 event with a $p < 0.1$; during the start of the event, the EMMA organic horizon derived contribution was largely overestimated (Figure 4.6). The pearson correlations for the EMMA derived contribution of transient groundwater and shallow soil water to stream water during the May event were -0.66 ($p <0.001$) and -0.65 ($p <0.001$) respectively, and timing of these contributions and measurements were generally in agreement.

4.4.4 Lag time and flow direction analysis

The physical hydrological dynamics of the December 2004 and May 2005 storm events were evaluated through calculation of time lags of soil moisture, soil

matric potential, seep and transient groundwater, lateral subsurface flow and stream flow to the start of rainfall (Table 4.1. and Figure 4.7). In addition we also present results from the flow direction analysis that was done to test if a lateral flow component within the soil profile is an important part of the flushing mechanism. Responses of shallow soil moisture, shallow soil matric potential and lateral subsurface flow and stream flow to rainfall were similar and lagged rainfall by 8 to 12 hours, except for the 30 cm soil moisture probe at the middle slope location that lagged rainfall by 17.8 hours (Table 4.1.). The soil moisture response at deep soil profile position and 122 cm (well E04) lagged rainfall by 15.7 to 25.7 hours. The 15.7 hour lag time is from the upper soil moisture probe location on the hillslope and precedes the soil moisture probe response at 70 cm by 1.7 hours. While this may indicate preferential flow, the overall soil moisture response at 70 cm preceded the soil moisture response at 100 cm. Transient groundwater response in wells DE7 at 215.5 cm depth and A05 at 40.5 cm depth, lagged rainfall by 48.2 and 51.8 hours respectively.

During the May 2005 event, responses of seep groundwater (A01), shallow soil moisture, shallow soil matric potential and lateral subsurface and stream flow to rainfall were similar and lagged rainfall by 45 to 48 hours, except for the shallow soil moisture probe and tensiometers at the upper slope location that lagged rainfall by 31 to 33 hours (Table 4.1.). Deeper soil moisture and matric potential responded to rainfall by 45 and 63 hours. Transient groundwater height observations were not

available because sampling of wells during the storm affected the groundwater hydrographs to a large extent.

The flow direction analysis based on the tensiometer triangle installed 25 meter upslope showed that the direction of flow was mainly directed vertically during the December and May storm events (Figure 4.8.). Flow direction (r) with a positive deviation (a) from the vertical flow direction (v) is considered a lateral flow component. Flow direction parallel to the slope of the hillslope is characterized by an a of 44°. During the December event the maximum deviation from the vertical flow direction at 30 cm depth was 2.4° and most of the time (77%) smaller than zero and thus directed into the hillslope. During the May event maximum a at 30 cm depth was 10°, and a was 36% of the time <0°. Although the maximum deviation from the vertical flow direction at 70 cm depth was 25° during the December event and coincided with positive pore pressures at 100 cm depth (Figure 4.8), 86% of the time a was < 10°. During the May event maximum a was 19°, however a was 65% of the time < 10°. The negative changes of a (flow direction changes in upslope direction) during both storm events coincide with large positive changes in rainfall intensity (Figure 4.7 and 4.8), indicating that changes in rainfall intensity are the driving force for changes in flow direction at both depths. In general these results show that a significant lateral flow at considerable lengths of time does not exist at 30 cm and 70 cm depth.

4.4.5 DOC and N in organic horizon, soil and groundwater

DOC and N in throughfall, from the organic horizon and in soil water were sampled frequently during the December 2004 and May 2005 storm events to investigate if DOC and N were a limited or unlimited supply during these storm events. Pre-storm mean DOC and DON concentrations in the organic horizon during the December storm, between 12/02 and 12/09, decreased from 11.7 to 7.4 mg l^{-1} and from 0.45 to 0.14 mg l^{-1} respectively (Figure 4.9). Between 12/09 and 12/12 both DOC and DON concentrations in the organic horizon increased slightly. DON increased in throughfall during the storm. In contrast DOC in throughfall showed a dilution pattern. The increase in DIN concentration in the organic horizon during the storm is probably to some extent caused by the increase in DIN concentration in throughfall. DOC concentrations at 20 cm and 30-40 cm depth did not show significant variation during the storm, while at 70-110 cm DOC increased slightly. DON soil solution concentrations did show variation during the storm: (1) at 20 cm depth, DON decreased from 0.2 to 0.1 mg l^{-1} between 12/09 and 12/12, (2) DON showed a overall increase in concentration at 30-40 cm depth compared to pre-storm DON, with a peak at 12/09, and (3) DON increased from 0.04 to 0.1 mg l^{-1} at 70-110 cm depth. DIN at 20 cm depth did not show any variation, while it showed some variation at deeper soil depths.

During the May storm in 2005, DOC and DIN concentrations showed little variation in throughfall, while DON concentrations decreased between 05/19 and 05/22. The decrease in DOC and total nitrogen (TN) during the storm in the organic

horizon indicates a dilution pattern, and a finite source of DOC and N. DIN data was not available for the organic horizon. DOC and DON concentrations increased at 20 cm soil depth during the storm, while DOC and DON concentrations at 30-40 cm depth did not show a large amount of variation. DOC concentrations increased at 70-110 cm soil depth, from 0.9 to 1.6 mg l^{-1}, and in contrast DON concentrations decreased at this soil depth range.

EMMA indicated that organic horizon, seep and transient groundwater were important end members. Furthermore, the flow vector analysis suggested a possible strong connection between the organic horizon and groundwater. To elucidate the connectedness between the organic horizon and transient and seep groundwater we compared organic horizon DOC and N concentrations and SUVA values with transient and seep groundwater DOC and N concentrations and SUVA values during the two storm events. During the December storm event DOC and DON concentrations and SUVA values of the organic horizon and transient groundwater were very similar, while seepage groundwater was characterized by lower values (Table 4.2). This suggests in combination with predominantly vertical flow from the flow vector analysis vertical preferential flow. In addition, during the May storm event and December storm event, DOC concentrations and SUVA values of transient groundwater indicate an organic horizon/ shallow soil signal.

4.5 Discussion

While many studies (e.g. Boyer et al., 1997; Vanderbilt et al., 2003; Hood et al., 2006) described higher stream nutrient concentrations on the rising limb compared to the falling limb of the hydrograph, description of the flushing mechanism has been largely qualitative. In the literature three different flushing hypotheses have been described: (1) a rising water table that intersects high nutrient concentrations in the upper soil layer, (2) vertical transport of nutrients, by preferential or matrix flow through the (deeper less bio-active) soil to the soil-bedrock interface and then laterally downslope, and (3) lateral transient flow within the shallow soil profile. It is difficult to reject one or more of these hypotheses because we need a variety of hydrological and chemical approaches to do so. However, it is important given that a mechanistic understanding of flushing of nutrients is essential for model development for prediction of land use change and climate change effects on surface water quality.

The main objective of our paper was to mechanistically assess nutrient flushing at the catchment scale, through measurements at the point, hillslope and catchment scale. We used hydrometric data (groundwater level observations, soil matric potential and soil moisture measurements) to validate our chemical end-member analysis of different sources of lateral subsurface flow and stream water. Lateral subsurface and stream water both showed highest DOC and DON, and SUVA values during the rising limb of the hydrograph during the December and May storm events. EMMA indicated generally three different sources for lateral subsurface flow and stream water during the December and May storm events: 1) organic horizon water or shallow soil water or

transient groundwater, 2) baseflow and 3) throughfall. EMMA derived baseflow contributions to stream water and lateral subsurface flow were in good agreement with groundwater level variations in seepage well A01. Soil moisture dynamics in the organic horizon were in agreement with the EMMA derived organic horizon water contribution to stream water and lateral subsurface flow, although EMMA likely over-estimated the organic horizon contribution during the rising limb of the hydrograph. Furthermore, deep soil matric potential patterns were in agreement with EMMA derived transient groundwater contributions to stream water and lateral subsurface flow. The flow direction analysis and high DOC and DON concentrations and SUVA values in transient groundwater suggest vertical preferential flow to depth and a strong connection between the organic horizon/ shallow soil and transient groundwater. Groundwater heights above the bedrock were very shallow (about 10-15 cm) and the predominantly vertical flow component in the unsaturated zone during the storm events reject flushing mechanisms (1) and (3). Our results support flushing mechanism 2: vertical transport of nutrients through preferential flow and then laterally downslope at the soil bedrock interface occurred at our site. Furthermore, DOC and DON were a finite source in the organic horizon, while DOC and DON concentrations from shallow and deep lysimeters did not show large temporal variation. This suggests that the DOC and DON flushing pattern observed in lateral subsurface flow and stream flow was caused by organic horizon dynamics. However, the combination of EMMA, SUVA and hydrometric data showed evidence that flushing mechanism 2 including a finite source of DOC and DON is not sufficient to explain our observations. Mixing of

different sources of water both spatially and temporally needs to be included to explain nutrient flushing mechanistically. We will describe this in more detail in the following sections.

4.5.1 Mixing at hillslope and catchment scale

Since the end-members throughfall and deep soil water at the hillslope scale projected close to each other in the U-mixing space we were not able to separate these two end-members. At the hillslope scale we did choose throughfall since it encompassed the variability in samples well, and throughfall was a likely end-member for the following reasons. Hydrograph separation of storm events based on conservative isotopes ($d^{18}O$) at the hillslope and catchment scale (McGuire, 2004) with TRANSEP (Weiler et al., 2003) showed event water contributions of < 30%. When we would have used deep soil water as an end-member instead of throughfall the contribution of event water would have been in disagreement with the hydrograph separation results based on $d^{18}O$ for the May storm event. Baseflow, transient groundwater and soil water may be considered 'old' water, while organic horizon water and throughfall may be considered 'new' water. Using deep soil water instead of throughfall, and organic horizon instead of transient groundwater would have resulted in an underestimation of new water (2.8%). In addition, we used throughfall as an end-member at the catchment scale since we were able to separate throughfall and deep soil water for the December storm. The reason we could not separate throughfall and deep soil water during the May storm was that deep soil water changed on a seasonal

scale to a more throughfall signature because of dilution: average Cl^- concentrations in deep soil water were 2.79 mg l^{-1} in August and diluted to 0.56 mg l^{-1} in April and stayed low throughout the rest of the study period. The EMMA derived new water contributions (throughfall and organic horizon) at the catchment scale and hillslope scale, were higher than the range of $d^{18}O$ -derived new water contributions (McGuire, 2004). EMMA derived new water contributions during the December storm were 43% and 49%, and during the May storm were 34% and 29%, respectively at the catchment and hillslope scale. This over-estimation of the new water contribution may have been caused by the inability to separate the end-members throughfall and deep soil water in the end-member mixing space and high variability in the end members.

4.5.2 Conceptual model of DOC and DON flushing

The clockwise hysteresis patterns of DOC and DON during the December and May storm event at the hillslope and catchment scale has also been observed in other studies at this site (Hood et al., 2006) and at other sites (McGlynn and McDonnell, 2003; Buffam et al., 2001). The response times of soil and groundwater, and lateral subsurface and stream flow to the start of rainfall indicated that the rapid increase in DOC and DON during the early response of the December and May storm, at the hillslope and catchment scale, was mainly derived from a shallow soil water source near the stream. At the hillslope scale depth to bedrock increased upslope from about 0.3-0.6 m at the hillslope stream interface to 3-8 m at the ridge of the hillslope. This increase in depth to bedrock for the lower hillslope above the trench is illustrated in

Figure 4.11. Thus shallow soil depths at the soil stream interface enabled water to move relatively quickly to the soil-bedrock interface resulting in high DOC and DON concentrations during the early response of storms (Figure 4.12.a).

SUVA and raw fluorescence did increase when DOC and DON concentrations did rapidly rise during the early response of the storm events. Several studies have found that SUVA is strongly related to the aromatic content of DOM (Weishaar et al., 2003; Hood et al., 2005). Furthermore, the aromatic content and SUVA values of DOM decrease with soil depth with highest values in the organic horizon and lowest values in deep soil water (Hagedorn et al., 2000; Van Verseveld, 2007). Van Verseveld (2007) showed that at this site SUVA values and DOC and DON concentrations decreased with soil depth, suggesting preferential retention of aromatic DOM in soils. However, transient groundwater showed high DOC, DON concentrations and high SUVA values (Van Verseveld, 2007), indicating that vertical preferential flow occurred. Thus high DOC, DON concentrations and SUVA values during the early response of the storm events at the hillslope and catchment scale were caused by a combination of vertical preferential flow from the organic layer and lateral subsurface flow above the bedrock in the near stream zone. Later in the event, but still on the rising limb more upslope sources became important (Figure 4.12.b). For example during the December event well E04 started responding to rainfall 19 hours after rainfall started. Travel time from this hillslope position is about 24 hours based on a average subsurface flow velocity of 0.5 m h^{-1}, that was calculated from a Br^- tracer injection in this well during a sprinkler experiment (Graham et al., in prep), and

is in agreement with subsurface flow velocity calculations at this hillslope by McGuire (2004). Thus the second peak and subsequent peaks in DOC, SUVA and raw fluorescence during the December storm event were derived from at least the lower 15-20 meter of the hillslope.

The organic and shallow soil horizon were important contributors to high DOC, DON concentrations and SUVA values in lateral subsurface flow and stream water during storm events based on hydrometric data and EMMA. However the question remains what caused the clockwise hysteresis pattern of DOC, DON and SUVA. The organic horizon showed a dilution pattern during the December and May storm events, which indicates that DOC and DON were both a limited source during storm events. Since transient groundwater and the organic horizon were strongly connected the decreasing DOC and DON concentrations at the organic horizon during storm events explain lower DOC and DON concentrations during the falling limb of the lateral subsurface flow and stream water hydrograph. Indeed, DOC and DON concentrations patterns in seepage and transient groundwater during the December and May event support this respectively (Figure 4.10). However, organic horizon SUVA values did not change much during the storm events, and SUVA remained high in transient groundwater during the storm events (Table 4.2). Thus, while the organic horizon dynamics explain the lower DOC and DON concentrations, it does not explain the lower observed SUVA values during the falling limb of the lateral subsurface flow and stream water hydrograph. EMMA showed maximum values of throughfall contribution which was likely a mix between throughfall and deep soil water during

the falling limb of the lateral subsurface flow and stream water hydrograph. Deep soil water, seep groundwater and throughfall to a lesser extent were characterized by low SUVA values. We argue that the seep groundwater/ deep soil water contribution was higher during the falling limb than the rising limb of the storms at the hillslope and watershed scale and caused lower SUVA values and lower DOC and DON concentrations during the falling limb of the hydrograph (Figure 4.12.c). Seep groundwater is fed by mostly slow drainage of deep soil water throughout the year that likely extends much higher upslope where soil depths reach up to 8 m, than the lower 15-20 meter of the hillslope that is characterized by transient groundwater dynamics. Slow drainage results in preferential retention of aromatic carbon which explains the low SUVA values of seep groundwater and lateral subsurface flow. For example during the December and May events average DOC and DON concentrations and SUVA values were lower in seep groundwater (well A01) than in transient groundwater (Table 4.2). In addition, SUVA values decreased in seepage groundwater during the December storm event (Figure 4.10). Furthermore, comparing groundwater height dynamics of seep groundwater (A01) and transient groundwater (E04) suggests that seep groundwater contributed more during the falling limb of the December storm event. Thus the clockwise hysteresis pattern was caused by a combination of a finite source of DOC and DON in the organic horizon and higher contribution of seepage groundwater/ deep soil water on the falling limb of the lateral subsurface flow and stream flow hydrograph. Flushing mechanism 2 alone could not explain our

observations. The change in mixing of water sources during storm events had to be included.

4.6 Concluding remarks

We mechanistically assessed nutrient flushing at the hillslope and catchment scale during a December and May storm event. We posed the three following flushing mechanisms as hypotheses: (1) a rising water table that intersects high nutrient concentrations in the upper soil layer, (2) vertical transport of nutrients, by preferential or matrix flow through the (deeper less bio-active) soil to the soil-bedrock interface and then laterally downslope, and (3) vertical transport of nutrients and then laterally within the soil profile, and tested these hypotheses based on a combination of hydrometric and natural tracer data.

Sources and flowpaths of stream water and lateral subsurface flow were examined at the storm event scale through the use of hydrometric and natural tracer data. End-members from end-member mixing analysis were essentially grouped in the following categories (1) organic horizon water or shallow soil water or transient groundwater, (2) baseflow and (3) throughfall. Detailed measurements of DOC and DON concentrations in the organic horizon showed a dilution pattern. High DOC and DON concentrations and SUVA values in the organic horizon and transient groundwater suggested vertical preferential flow and a strong connection between the organic horizon and transient groundwater. Groundwater was characterized by maximum groundwater levels of 10-15 cm. Furthermore the unsaturated flow vector

analysis showed that flow in the unsaturated zone was predominantly vertical during both storm events. Thus, hydrometric data in combination with natural tracers enabled us to reject flushing mechanism 1 and 3, and to accept flushing mechanism 2 that included a finite source of DOC and DON in the organic horizon.

However DOM quality, expressed as SUVA was needed to further refine our conceptual model based on flushing mechanism 2. During the early response of the December and May storm events DOC and DON were mainly transported from near stream zones, while upslope sources (~20 m upslope) became more important later in the event, but still on the rising limb of the hydrograph. The organic horizon DOC and DON dilution pattern and the strong connection between the organic horizon and transient groundwater during the storms could explain the lower DOC and DON concentrations during the falling limb of the hydrograph, resulting in a clockwise hysteresis pattern. However, SUVA that also showed a clockwise hysteresis pattern did not change significantly in the organic horizon and transient groundwater during storms. We argued based on hydrometric data and SUVA that the contribution of seep groundwater/deep soil water was higher during the falling limb compared to the rising limb of the hydrograph and had a dilution effect of DOC and DON concentrations and SUVA values.

This study showed the importance of combining hydrometric and tracer data that enabled us to mechanistically assess nutrient flushing at our site and to develop a conceptual model of how DOC and DON were transported from the soil to the stream at the hillslope and catchment scale during storm events. In addition it demonstrated

the value of using SUVA as a measure of DOM quality. Without SUVA we would not have been able to refine our accepted flushing mechanism hypothesis of vertical transport of nutrients by preferential flow to the soil-bedrock interface and then laterally downslope.

4.7 Acknowledgements

This work was supported through funding from the National Science Foundation (grant DEB 021-8088 to the Long-Term Ecological Research Program at the H. J. Andrews Experimental Forest) and Department of Forest Engineering at Oregon State University. We thank Marloes Bakker and John Moreau for providing field assistance. We also thank R. D. Harr and D. Ranken for initiating the hillslope studies at WS10, and K. J. McGuire for re-initiating this site.

4.8 References

Bernal, S., A. Butturini and F. Sabater (2005), Seasonal variations of dissolved nitrogen and DOC:DON ratios in an intermittent Mediterranean stream, *Biogeochemistry, 75*, 351–372.

Bernal, S., A. Butturini and F. Sabater (2006), Inferring nitrate sources through end member mixing analysis in an intermittent Mediterranean stream, *Biogeochemistry, 81*, 269–289.

Bishop, K., J. Seibert, S. Kölhler, and H. Laudon (2004), Resolving the double paradox of rapidly old water with variable responses in runoff chemistry, *Hydrol. Processes, 18*, 185-189.

Bonell, M. (1998), Selected challenges in runoff generation research in forests from the hillslope to headwater drainage basin scale, *Journal of the American Water Resources Association, 34*, 765-785.

Boyer, E. W., G. M. Hornberger, K. E. Bencala, and D. M. McKnight (1997), Response characteristics of DOC flushing in an Alpine catchment, *Hydrol. Processes, 11*, 1635-1647.

Brown, V. A., J. J. McDonnell, D. A. Burns, and C. Kendall (1999), The role of event water a rapid shallow flow component and catchment size in summer stormflow, *J. Hydrol., 217*, 171– 190.

Buffam, I., J. N. Galloway, L. K. Blum and K. J. McGlathery (2001), A stormflow/baseflow comparison of dissolved organic matter concentrations and bioavailability in an Appalachian stream, *Biogeochemistry, 53*, 269-306.

Buttle, J. M., S. W. Lister and A. R. Hill (2001), Controls on runoff components on a forested slope and implications for N transport, *Hydrol. Processes, 15,* 1065–1070

Burns, D. A., J. J. McDonnell, R. P. Hooper, N. E. Peters, J. E. Freer, C. Kendall, and K. J. Beven (2001), Quantifying contributions to storm runoff through end-member mixing analysis and hydrologic measurements at the Panola Mountain Research Watershed (Georgia, USA), *Hydrol. Processes, 15*, 1903–1924

Creed, I. F., L. E. Band, N. W. Foster, I. K. Morrison, J. A. Nicolson, R. S. Semkin, and D. S. Jeffries (1996), Regulation of nitrate-N release from temperate forests: A test of the N flushing hypothesis, Water *Resour. Res., 32,* 3337–3354.

Christopherson, N., and R. P. Hooper (1992), Multivariate analysis of stream water chemical data: The use of principal component analysis for the end-member mixing problem, *Water Resour. Res., 28,* 99–107.

Gaskin, J. W., J. W. Dowd, W. L. Nutter and W. T. Swank (1989), Vertical and Lateral Components of Soil Nutrient Flux in a Hillslope, *J. Environ. Qual., 18*: 403-410.

Hagedorn, F., P. Schleppi, P. Waldner, and H. Fluhler (2000), Export of dissolved organic carbon and nitrogen from Gleysol dominated catchments—The significance of water flow paths, *Biogeochemistry, 50,* 137–161.

Harr, R. D., (1977), Water flux in soil and subsoil on a steep forested slope, *J. Hydrol., 33*, 37-58.

Hill, A. R., W. A. Kemp, J. M. Buttle, and D. Goodyear (1999), Nitrogen chemistry of subsurface storm runoff on forested Canadian Shield hillslopes, *Water Resour. Res., 35,* 811 –821.

Hinton M. J., S. L. Schiff and M. C. English (1997), The significance of storms for the concentration and export of dissolved organic carbon from two Precambrian Shield catchments, *Biogeochemistry, 36*: 67–88.

Hood, E., D. M. McKnight and M. W. Williams (2003), Sources and chemical character of dissolved organic carbon across an alpine/subalpine ecotone, Green Lakes Valley, Colorado Front Range, United States, *Water Resour. Res., 39(7),* 1188, doi:10.1029/2002WR001738.

Hood, E., M. W. Williams and D. M. McKnight (2005), Sources of dissolved organic matter (DOM) in a Rocky Mountain stream using chemical fractionation and stable isotopes, *Biogeochemistry, 74,* 231-255.

Hood, E., M. N. Gooseff, and S. L. Johnson (2006), Changes in the character of stream water dissolved organic carbon during flushing in three small

watersheds, Oregon, *J. Geophys. Res., 111,* G01007, doi:10.1029/2005JG000082.

Hooper, R. P., (2001), Applying the scientific method to small catchment studies: a review of the Panola Mountain experience, *Hydrol. Process., 15*, 2039–2050.

Hooper, R. P., (2003), Diagnostic tools for mixing models of stream water chemistry, *Water Resour. Res., 39(3),* 1055, doi:10.1029/2002WR001528.

Inamdar, S. P., and M. J. Mitchell (2006), Hydrological and topographical controls on storm-event exports of dissolved organic carbon (DOC) and nitrate across catchment scales, *Water Resour. Res., 42*, W03421, doi:10.1029/2005WR004212.

Jackson, C. R., (1992), Hillslope infiltration and lateral downslope unsaturated flow, *Water Resour. Res., 28,* 2533-2539.

James, A. L., and N. T. Roulet (2006), Investigating the applicability of end-member mixing analysis (EMMA) across scale: A study of eight small, nested catchments in a temperate forested watershed, *Water Resour. Res., 42,* W08434, doi:10.1029/2005WR004419.

Jardine, P.M., G.V. Wilson, and R.J. Luxmoore (1990), Unsaturated solute transport through a forest soil during rain events, *Geoderma,* 46:103–118.

Katsuyama, M. and N. Ohte (2002), Determining the sources of stormflow from the fluorescence properties of dissolved organic carbon in a forested catchment, *J. of Hydr.*, 268, 192-202.

Keim, R. F., and A. E. Skaugset (2004), A linear system model of dynamic throughfall rates beneath forest canopies, *Water Resour. Res., 40*, W05208 doi:10.1029/2003WR002875

Lajtha, K., W. M. Jarrell, D. W. Johnson and P. Sollins (1999), Collection of Soil Solution. In: Robertson G. P., and others, Eds. Standard Soil Methods for Long-Term Ecological Research. New York: Oxford, University Press, p 166–182.

McCord, J. T., D. B. Stephens, and J. L. Wilson (1991), Hysteresis and state-dependent anisotropy in modeling unsaturated hillslope hydrologic processes, *Water Resour. Res., 27,* 1501–1518.

McGuire, K. J., (2004), Water residence time and runoff generation in the western Cascades of Oregon, Ph.D., Oregon State University, Corvallis.

McGuire, K. J., J. J. McDonnell and M. Weiler (2007), Integrating tracer experiments with modeling to infer water transit times, *Advances in Water Resources, 30,* 824-837.

McGlynn, B. L., and J. J. McDonnell, Role of discrete landscape units in controlling catchment dissolved organic carbon dynamics, *Water Resour. Res., 39(4),* 1090, doi:10.1029/2002WR001525, 2003.

McGlynn, B., J. J. McDonnell, J. Shanley and C. Kendall (1999), Riparian zone flowpath dynamics during snowmelt in a small headwater catchment, *J. Hydr., 222,*75-92.

McHale, M. R., J. J. McDonnell, M. J. Mitchell, and C. P. Cirmo (2002), A field-based study of soil water and groundwater nitrate release in an Adirondack

forested watershed, *Water Resour. Res., 38(4),* 1031,doi:10.1029/2000WR000102.

McKnight, D. M., R. Harnish, R. L. Wershaw, J. S. Baron, and S. Schiff (1997), Chemical characteristics of particulate, colloidal and dissolved organic material in Loch Vale Watershed, Rocky Mountain National Park, *Biogeochemistry, 36,* 99–124.

Michalzik, B., K. Kalbitz, J. H. Park, Solinger, S., and E. Matzner (2001), Fluxes and concentrations of dissolved organic carbon and nitrogen—A synthesis for temperate forests, *Biogeochemistry,* 52, 173–205.

Mulholland, P. J., and W. R. Hill (1997), Seasonal patterns in streamwater nutrient and dissolved organic carbon concentrations: Separating catchment flow path and in-stream effects, *Water Resour. Res., 33(6),* 1297-1306.

Ranken, D. W., (1974), Hydrologic properties of soil and subsoil on a steep, forested slope, M.S., Oregon State University, Corvallis.

Retter, M., P. Kienzler and P. F. Germann (2006), Vectors of subsurface stormflow in a layered hillslope during runoff initiation, *Hydrology and Earth System Sciences, 10,* 309-320.

Sollins, P., K. J. Cromack, F. M. McCorison, R. H. Waring, and R. D. Harr, (1981), Changes in nitrogen cycling at an old-growth Douglas-fir site after disturbance, *J. Enivron. Qual.,, 10,* 37-42.

Swank, W. T., J. W. Fitzgerald and J. T. Ash (1984), Microbial transformation of sulfate in forest soils, *Science, 223,* 182-184.

Swanson, F. J., and M. E. James, (1975), Geology and geomorphology of the H.J. Andrews Experimental Forest, western Cascades, Oregon., Res. Pap. PNW-188, U.S. Department of Agriculture, Forest Service, Pacific Northwest Forest and Range Experiment Station, Portland, OR.

Triska, F. J., J. R. Sedell, K. Cromack, S. V. Gregory, and F. M. McCorison, (1984), Nitrogen budget for a small coniferous forest stream, *Ecological Monographs, 54,* 119-140.

Torres, R., W. E. Dietrich, D. R. Montgomery, S. P. Anderson and K. Loague (1998), Unsaturated zone processes and the hydrologic response of a steep, unchanneled catchment, *Water Resour. Res.,34,*1865-1879.

Vanderbilt, K. L., K. Lajtha and F. J. Swanson (2003), Biogeochemistry of unpolluted forested watersheds in the Oregon Cascades: temporal patterns of precipitation and stream nitrogen fluxes, *Biogeochemistry, 62,* 87–117.

Van Verseveld, W. J. (2007), Hydro-biogeochemical coupling at the hillslope and catchment scale, Ph.D., Oregon State University, Corvallis.

Weiler, M., B. L. McGlynn, K. J. McGuire, and J. J. McDonnell (2003), How does rainfall become runoff? A combined tracer and runoff transfer function approach, *Water Resour. Res., 39,* 1315, doi:10.1029/2003WR002331.

Weiler, M. and J.J. McDonnell (2006), Testing nutrient flushing hypotheses at the hillslope scale: A virtual experiment approach. *Journal of Hydrology*, 319: 339–56.

Weishaar, J. L., G. R. Aiken, B. A. Bergamaschi, M. S. Fram, R. Fujii and K. Mopper (2003), Evaluation of Specific Ultraviolet Absorbance as an Indicator of the Chemical Composition and Reactivity of Dissolved Organic Carbon, *Environ. Sci. Technol., 37,* 4702-4708.

Yano, Y., K. Lajtha, P. Sollins and B. A. Caldwell (2005), Chemistry and Dynamics of Dissolved Organic Matter in a Temperate Coniferous Forest on Andic Soils: Effects of Litter Quality, *Ecosystems, 8,* 286-300.

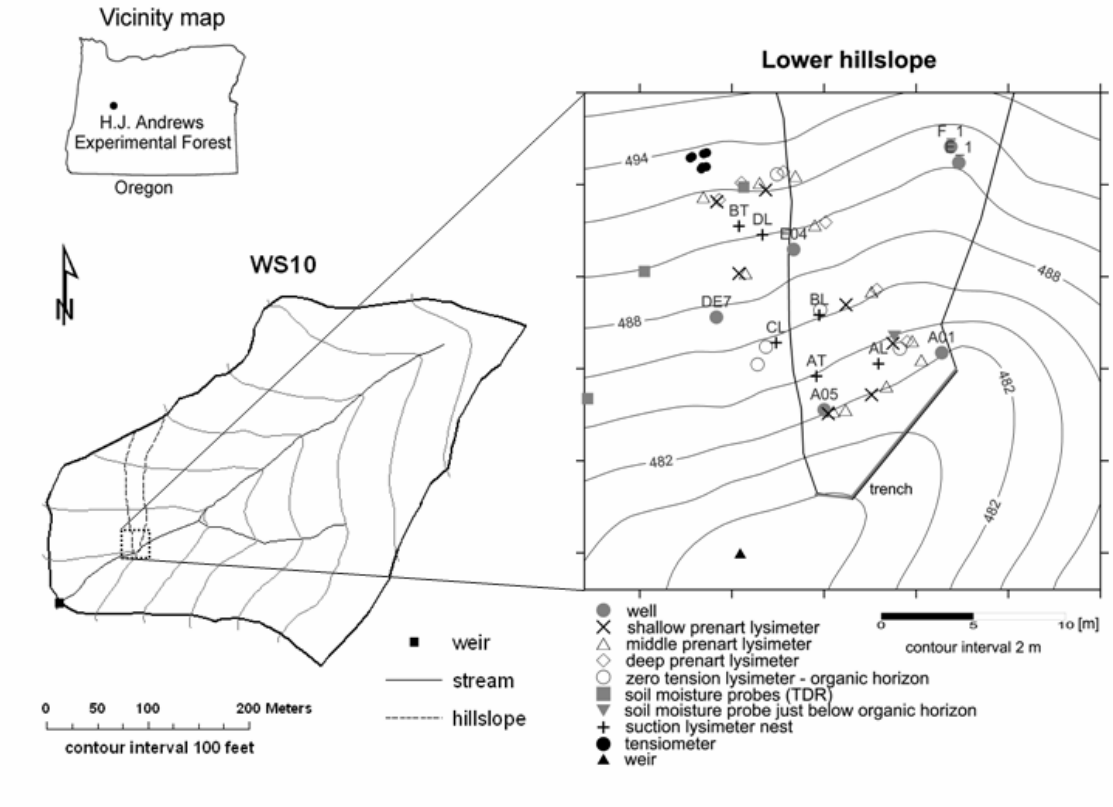

Figure 4.1. Map of WS10 showing the location of the hillslope study area and hillslope with the instrumentation.

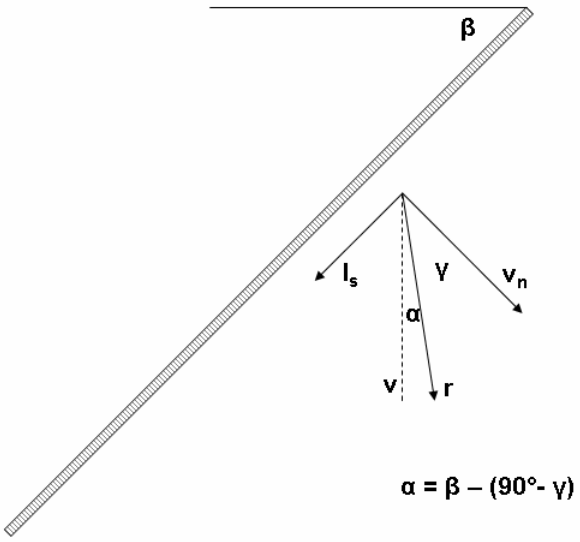

Figure 4.2. Schematic overview of gradients; l_s and v_n are the lateral (parallel to the slope) and vertical gradient (normal to slope) respectively, r is the resultant gradient of l_s and v_n, and v is the vertical. The flow direction deviation from the vertical is a.

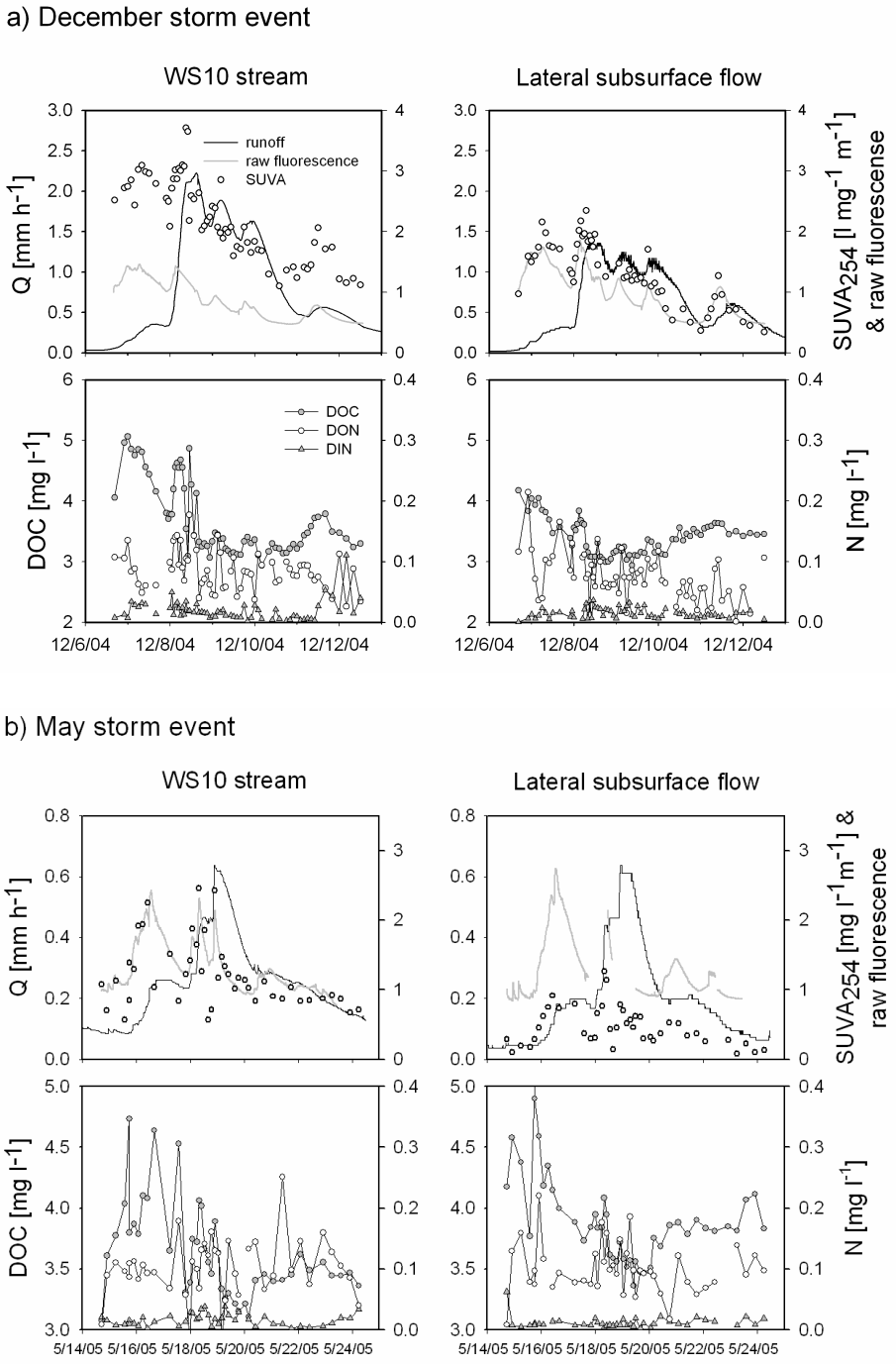

Figure 4.3. SUVA, raw fluorescence, DOC, DON and DIN concentrations in stream water and lateral subsurface flow, during a) the December 2004 and, b) May 2005 storm event.

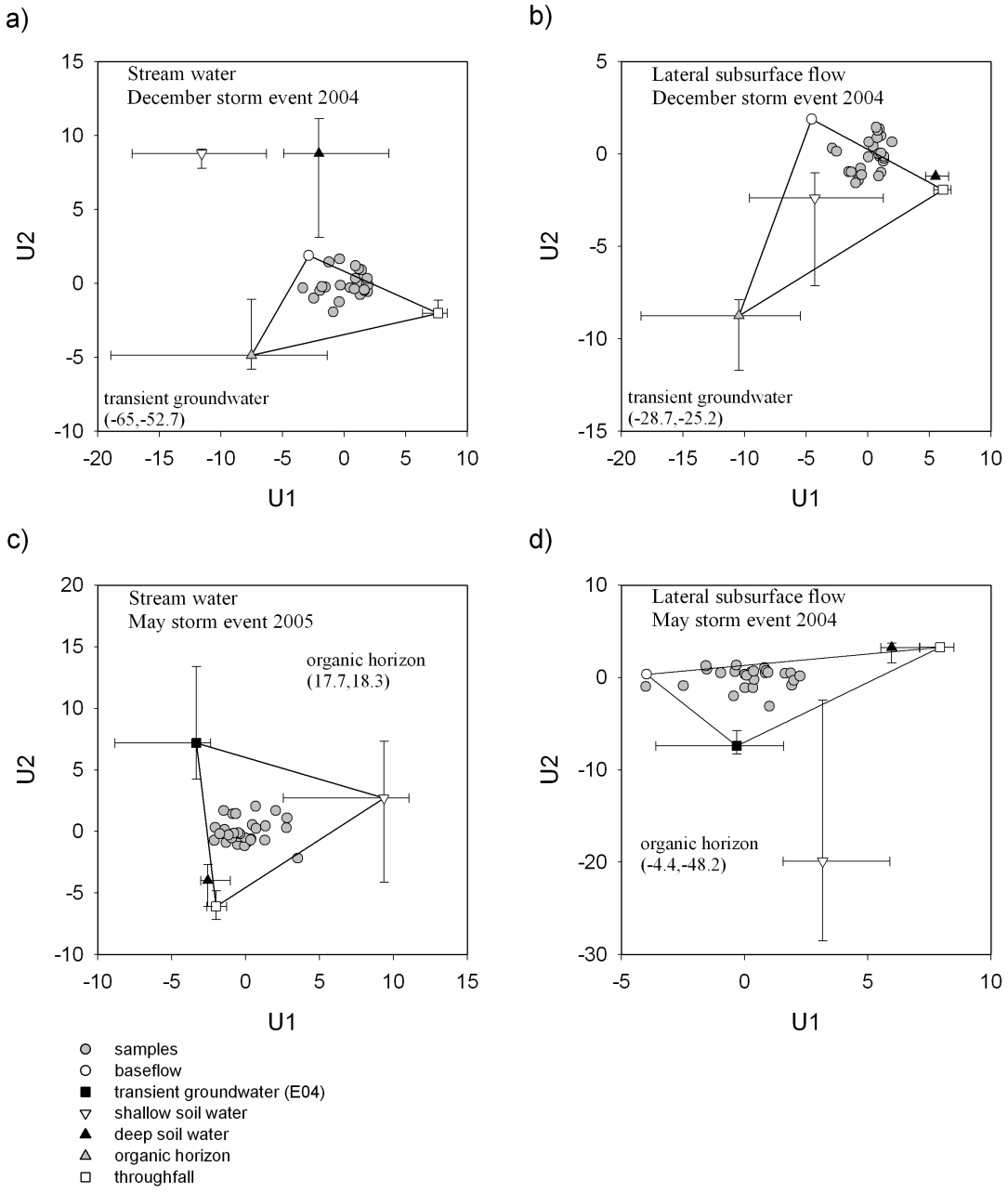

Figure 4.4. EMMA for a) stream water during the December 2004 storm event, b) lateral subsurface flow during the December 2004 storm event, c)stream water during the May 2005 storm event and d) lateral subsurface flow during the May 2005 storm event.. Medians and the 25th and 75th percentiles of each possible end-member are plotted. U1 and U2 median coordinates are given for end-member outside the graph range. Note differences in scale between graphs.

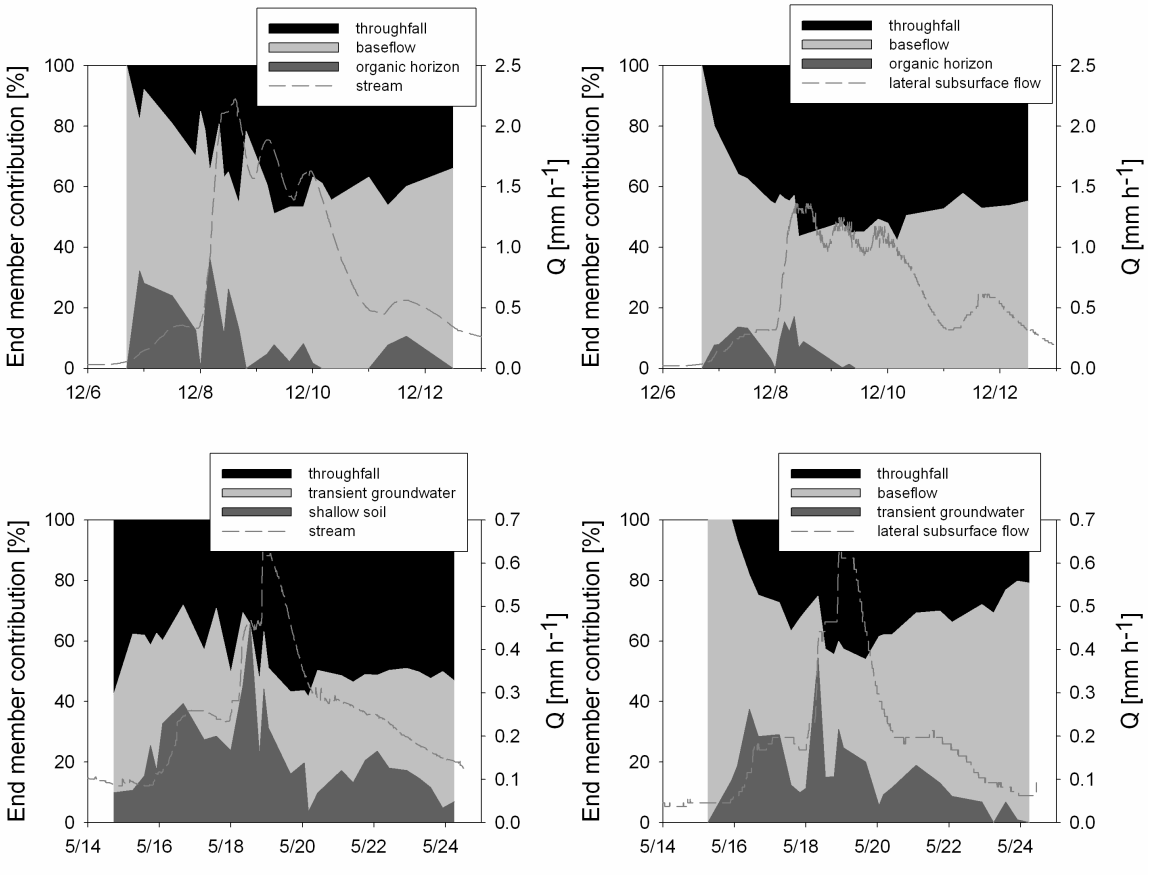

Figure 4.5. End member derived contributions during the December 2004 and May 2005 storm events.

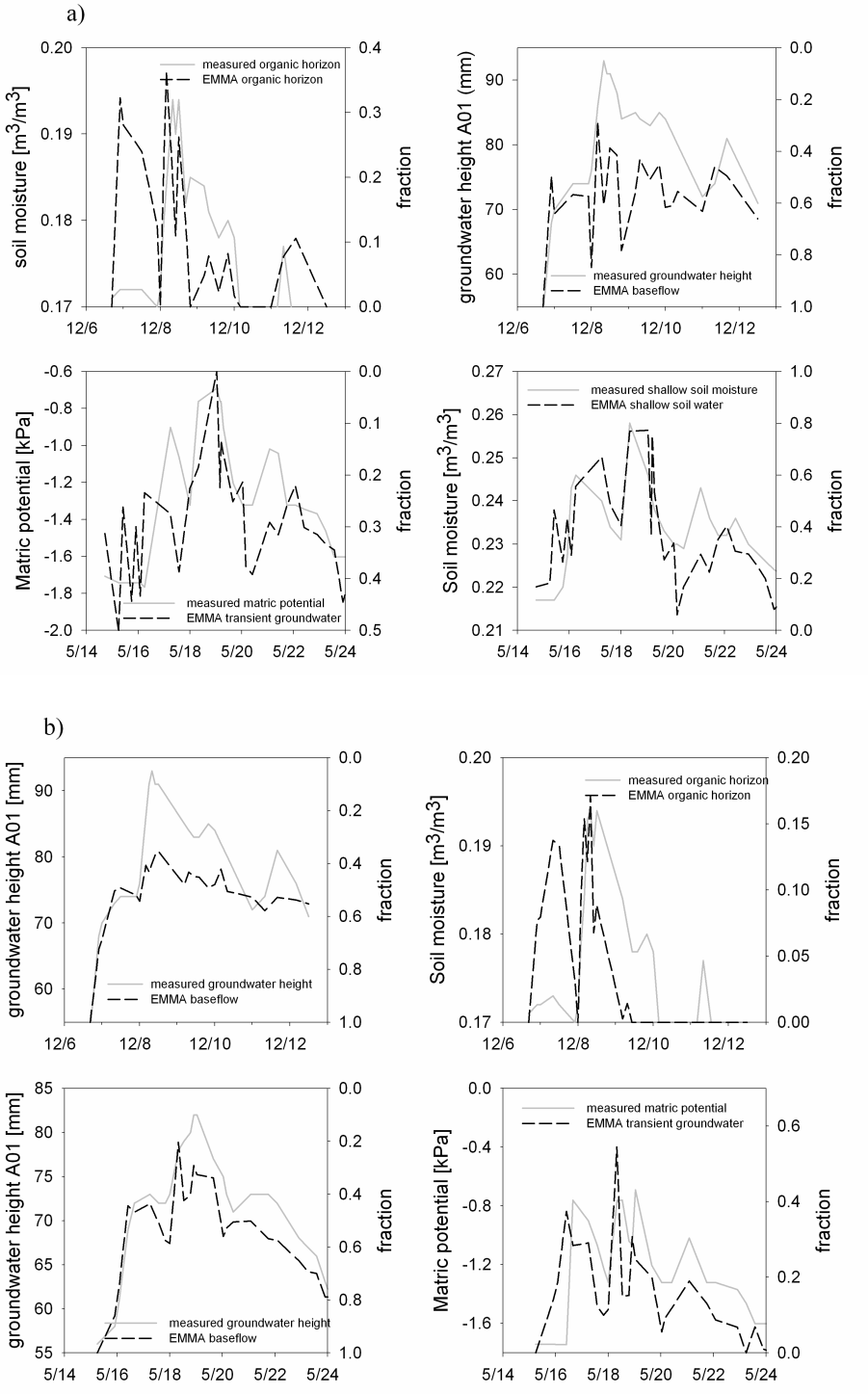

Figure 4.6. Comparison of EMMA derived contributions with hydrometric data for a) stream water and b) lateral subsurface flow

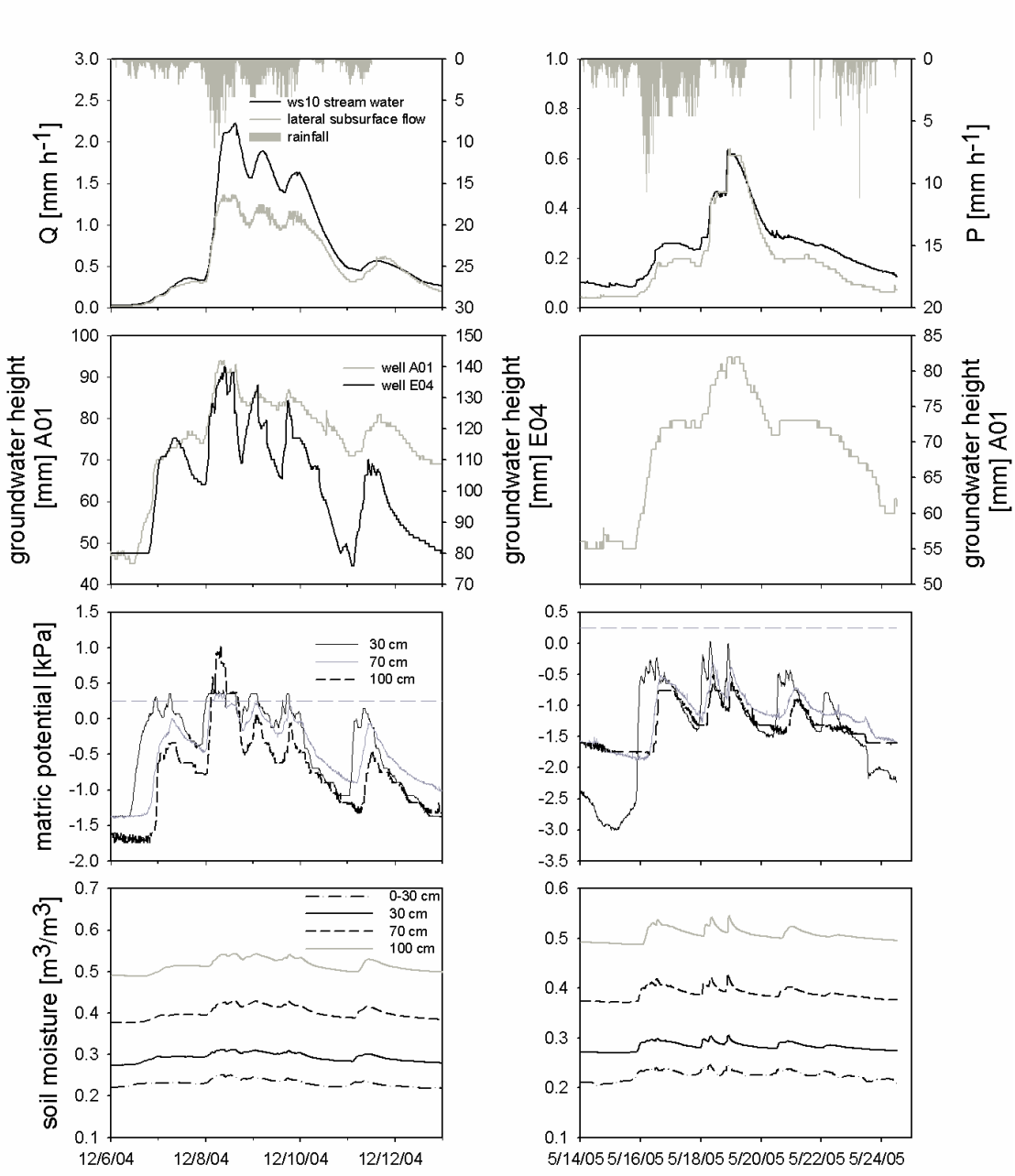

Figure 4.7. Hydrological dynamics during the December 2004 and May 2005 storm event.

Table 4.1. Hydrological response timing to rainfall of December 2004 and May 2005 storms events.

Site	December storm 2004	May storm 2005
	Time lag from start rainfall event (hour)	
Soil moisture lower soil pit (30 cm)	8.33	45.17
Soil moisture lower soil pit (70 cm)	14	45.83
Soil moisture lower soil pit (100 cm)	17.83	49.83
Soil moisture middle soil pit (30 cm)	11.33	33
Soil moisture middle soil pit (70 cm)	17.33	49
Soil moisture midlle soil pit (100 cm)	15.67	52.67
Soil moisture upper soil pit (30 cm)	17.83	47.83
Soil moisture upper soil pit (70 cm)	24.5	58.17
Soil moisture upper soil pit (100 cm)	25.67	62.17
Tensiometer (30 cm)	9.33	31.67
Tensiometer (70 cm)	16.33	52.67
Tensiometer (100 cm)	19.67	58.33
Groundwater (well E04)	19	-
Groundwater (well DE07)	51.83	-
Groundwater (well A05)	48.17	-
Groundwater (well A01)	11.83	44
Lateral subsurface flow	9.67	45.17
WS10 outlet	9.5	44.67

a) December 2004 storm event

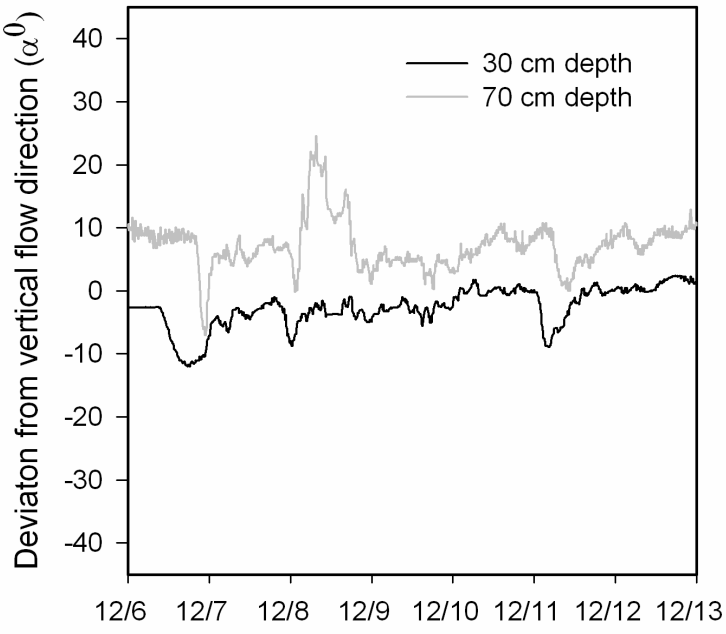

b) May 2005 storm event

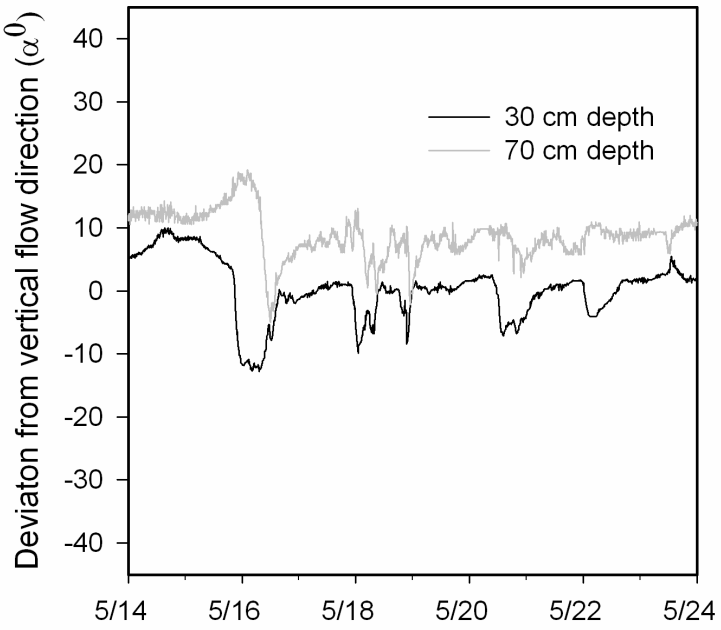

Figure 4.8. Flow direction at 30 cm and 70 cm depth during a) the December storm event and b) during the May storm event.

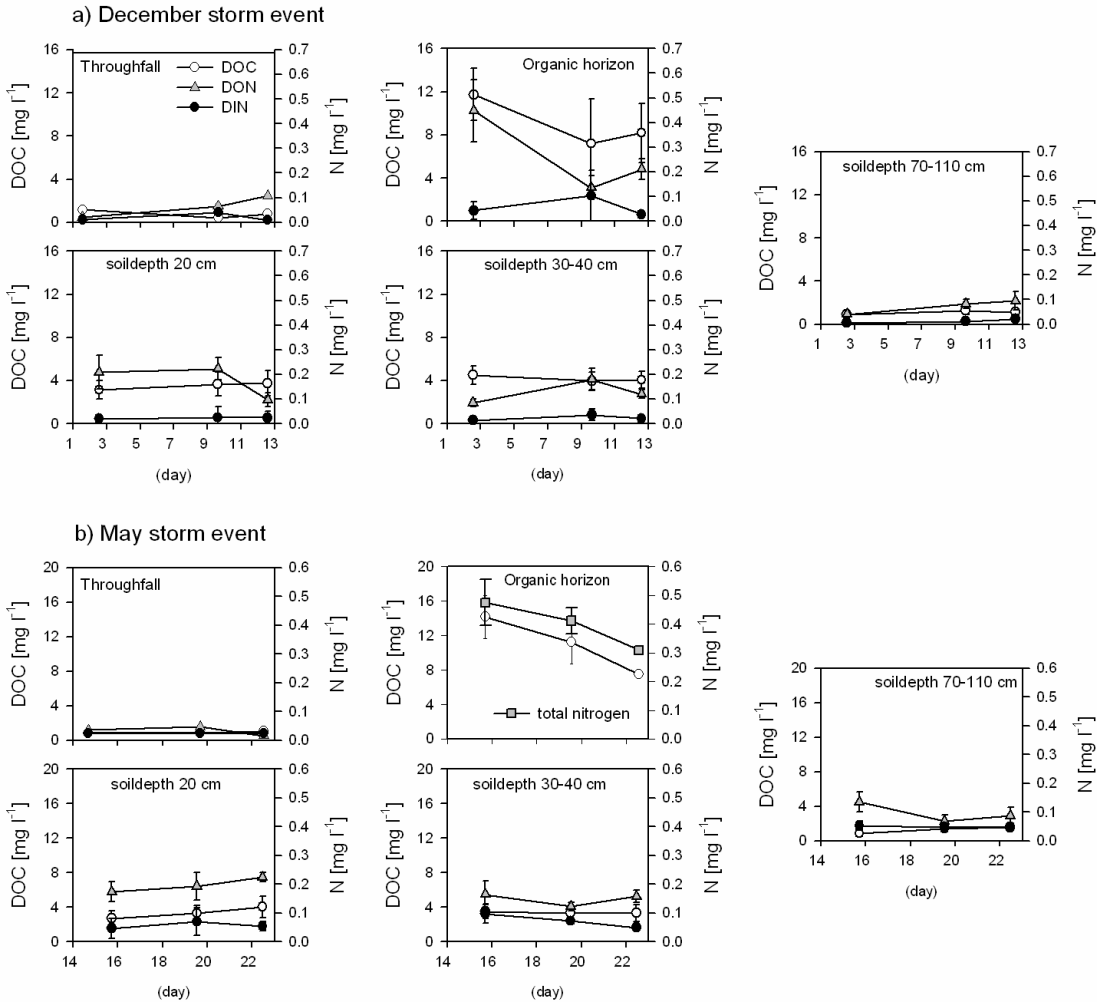

Figure 4.9. Mean (±SE) DOC, DON and DIN concentrations in throughfall, organic horizon water, and soil water at 20, 30-40 and 70-110 cm depth during a) the December 2004 storm event, and b) the May 2005 storm event.

Table 4.2. Mean (SE) of DOC, DON, DIN and SUVA in transient and seep groundwater during December 2004 and May 2005 storm events.

	December 2004 event			May 2005 event		
	Organic horizon	Transient groundwater	Seep groundwater	Organic horizon	Transient groundwater	Seep groundwater
DOC [mg L^{-1}]	9.0 (1.3)	10.8 (2.0)	3.4 (0.07)	12.9 (1.2)	4.7 (0.7)	3.7 (0.2)
DON [mg L^{-1}]	0.27 (0.06)	0.23 (0.11)	0.075 (0.006)	n.a.	0.21 (0.04)	0.049 (0.009)
DIN [mg L^{-1}]	0.049 (0.017)	0.86 (0.51)	0.026 (0.006)	n.a.	0.81 (0.23)	0.028 (0.005)
SUVA [l mg^{-1} m^{-1}]	5.5 (0.5)	4.8 (3.2)	1.3 (0.2)	4.9 (0.4)	2.5 (0.2)	0.6 (0.1)

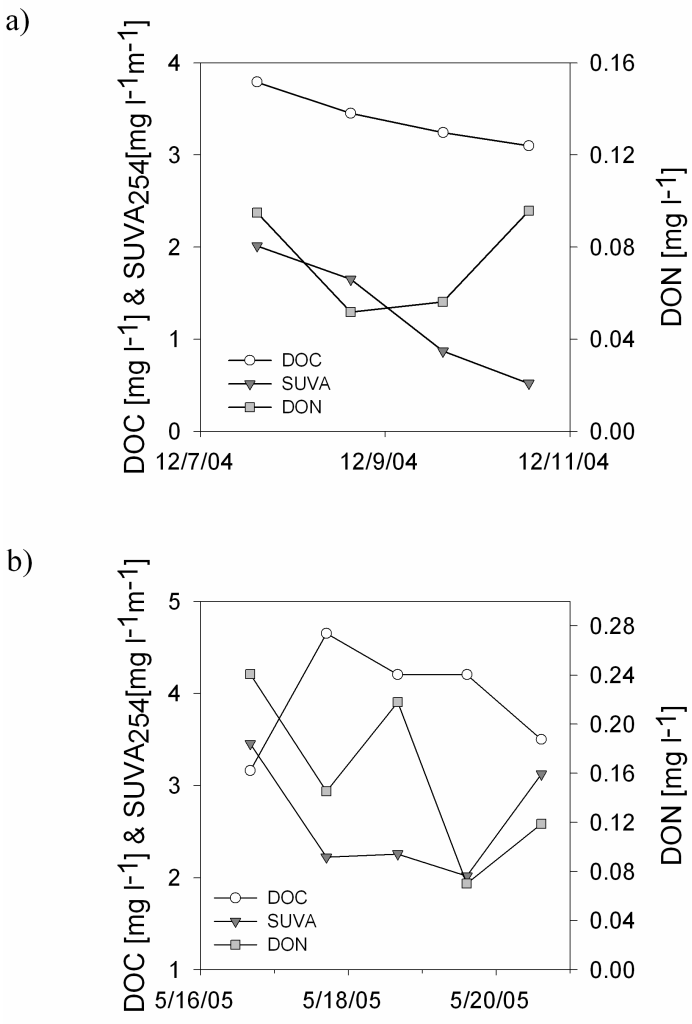

Figure 4.10. DOC, DON concentrations and SUVA values in a) seepage groundwater (well A01) during the December storm event, and b) transient groundwater (well E04) during the May storm event

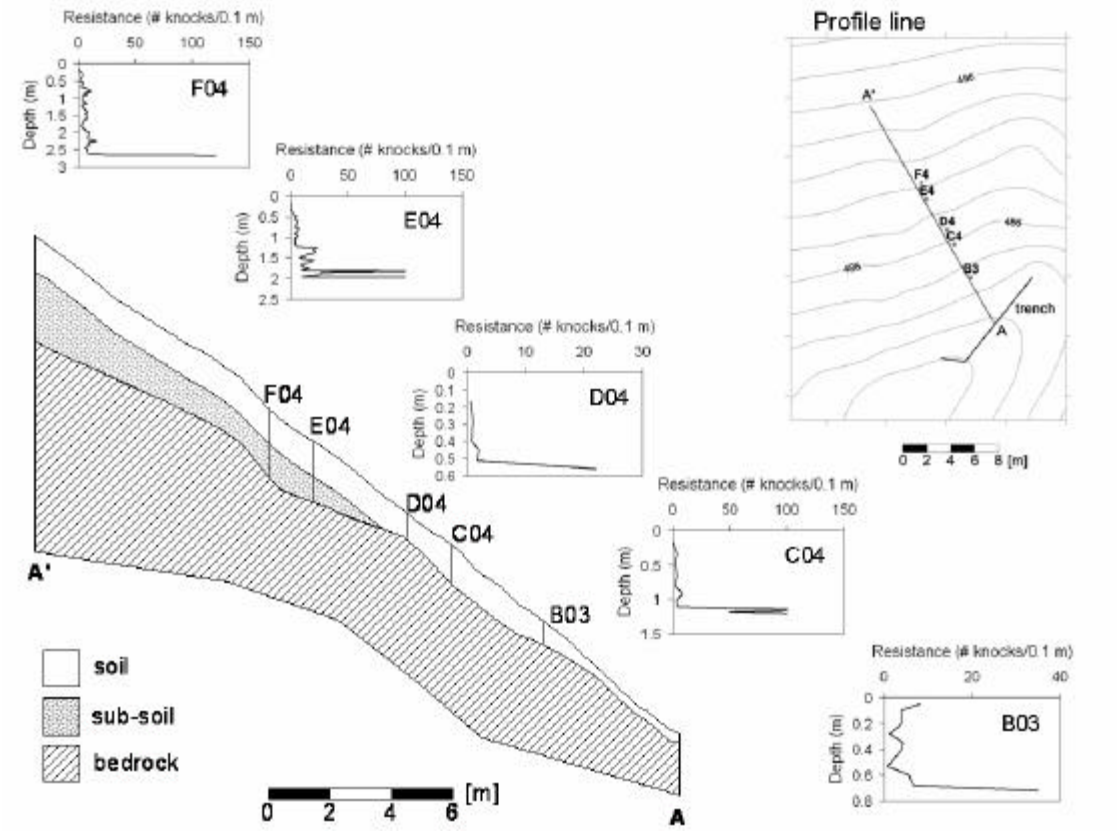

Figure 4.11. Cross-section of the hillslope above the trench along the profile line A-A'. Depth to bedrock and soil resistance was measured with a knocking pole. Maximum soil depth was assumed to be 1.1 m based on Ranken (1974) and Harr (1977). Depth to bedrock was defined as at least 20 knocks per 0.1 m.

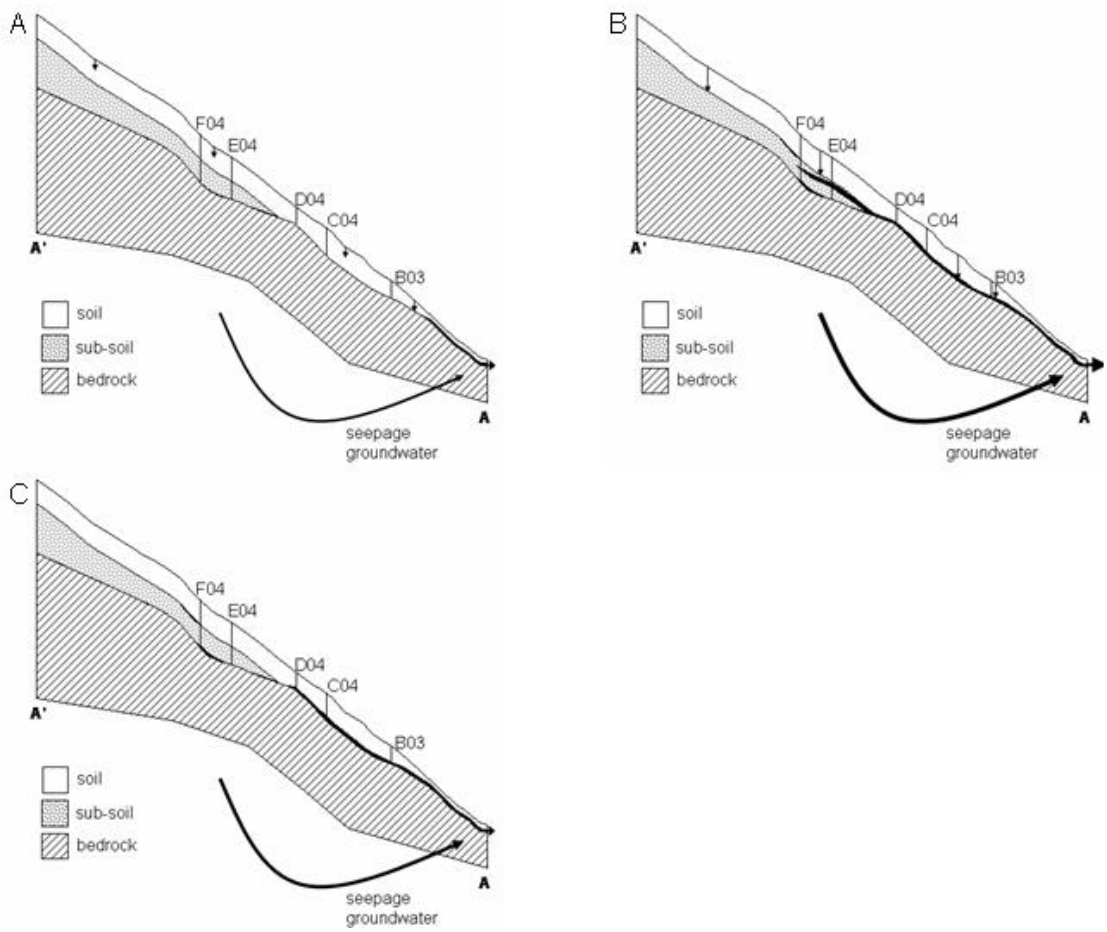

Figure 4.12. Conceptual model of nutrient flushing during A) start of the storm with vertical flow that reaches the soil bedrock interface of the lower hillslope section resulting in transient groundwater at this location, and contribution of seepage groundwater/ deep soil water, resulting in the first rapid increase of DOC, DON, SUVA and raw fluorescence, B) later in the storm event on the rising limb of the hydrograph vertical flow reaches greater depths and more upslope sources of transient groundwater become important, and contribution of seepage groundwater/ deep soil water increases, causing DOC, DON, SUVA and fluorescence to remain high, C) during the falling limb of the hydrograph, transient groundwater contribution moves downslope and decreases while seepage groundwater/ deep soil water contribution remains high compared to the start of the storm, resulting in a dilution pattern of DOC, DON, SUVA and raw fluorescence. Furthermore, the finite source of DOC and DON in the organic horizon during the storm event contributes to decreasing concentrations of these solutes during the storm.

5 Mechanistic assessment of the double paradox in hydrology and biogeochemistry: A hillslope sprinkling experiment

Van Verseveld, W. J.

Barnard, H. R.

Graham, C. B.

McDonnell, J. J.

Lajtha, K.

Brooks, R. J.

5.1 Introduction

The double paradox in catchment hydrology and (bio)-geochemistry (Kirchner, 2003) is a source of major debate and discussion in hydrology at present (Bishop et al, 2004; Jones et al., 2006; Kienzler and Naef, 2007). A simple definition of the double paradox is the rapid mobilization of stored, pre-event water to the stream during storm events but variable runoff chemistry. Taken individually, the individual elements of the double paradox have been described for many years. For instance, Martinec (1975, p.496) noted the rapid delivery of "old water" where he stated that "by the concept, the quick reaction of outflow to a massive groundwater recharge is brought to agreement with the long residence time of the infiltrated water". Since then, many studies have attempted to mechanistically assess how stored water is rapidly effused to the stream via macropore flow (McDonnell, 1990), transmissivity feedback (Kendall et al., 1999; Bishop et al, 2004), hydrodynamic mixing (Jones et al., 2006), and pressure wave propagation (Torres, 1998; Williams et al., 2002). In terms of variable runoff chemistry, these patterns have been noted since 1964 (e.g. Hendrickson and Kreiger, 1964; Miller and Drever, 1977), where during events, some constituents become dilute, others more concentrated and some remain unchanged through the event (Walling and Foster, 1975). Since then, several studied have attempted to explain these different geochemical behaviors with end member mixing approaches (Swistock et al., 1989; Hooper et al., 1990), hysteresis pattern analysis (Evans and Davies, 1998) and reaction path modeling (Plummer et al., 1990; Appelo et al., 1987).

Resolving the double paradox is essential to improve our understanding of flowpaths and predicting transport of contaminants and natural (bio)-geochemical solutes at the hillslope and catchment scale. One very recent study has begun to tackle the two elements of the double paradox together. Bishop et al. (2004) described in a recent commentary how to resolve the double paradox for spring flood events in the Nyänget catchment in Sweden. The rapid mobilization of old water was explained by the transmissivity feedback, where the addition of relatively little water caused the groundwater level to rise and mix with 'old' water held in the unsaturated zone. The resolution of variable runoff chemistry of old water was explained by lateral flow rates that intersected distinct vertical soil solution chemistry profiles of dissolved organic carbon (DOC), calcium (Ca^{2+}) and chloride (Cl^{-1}) in the riparian area. Another study, before the double paradox was presented by Kirchner (2003), demonstrated in two papers (Anderson et al., 1997a; Anderson et al., 1997b) an explanation for the double paradox. They conducted a sprinkler experiment in a 860-m^2 catchment in the Oregon Coast Range and added deuterium as a tracer to the sprinkler water. Rapid mobilization of old water was attributed to displacement of old water (plug flow) in the unsaturated zone that mixed with lateral saturated flow paths emerging from the bedrock (Anderson et al., 1997a). Through the application of both high and low ionic strength sprinkler water of >200 mm, variation in runoff chemistry of a variety of solutes was explained by (1) buffering of the sprinkler water signal in soil water, (2) mixing of soil water with water exfiltrating from the bedrock, (3) water contact time with bedrock depending on flow conditions, and (4) exchange of water and solutes

between small and large pores in bedrock during start of sprinkler application (Anderson et al., 1997b). These explanations were in agreement with the rapid mobilization of old water.

Both studies (Bishop et al., 2004; Anderson et al., 1997a, 1997b) have improved our understanding of the double paradox. However, the study of Bishop et al. (2004) was conducted under natural conditions and thus relied on passive and variable isotope inputs to determine the contribution of old water during storm events. Characterization of the isotope input under natural conditions is difficult because of spatial and temporal variation in inputs (rainfall and snowmelt) at the catchment scale. Often we sample the isotope input at one location which can result in considerable uncertainty in hydrograph separation and residence time modeling (McGuire and McDonnell, 2006). Furthermore, identifying flowpaths contributing to runoff under natural conditions is complex. Bishop et al. (2004) showed in a plausible way that lateral flowpaths that intersected distinct vertical soil solution chemistry profiles controlled variable runoff chemistry. However, vertical preferential unsaturated flowpaths may have supplied solutes from the upper soil profile. DOC was used as a tracer to explain sources of stream water and thus variable runoff chemistry in their study. Several other studies have used variation of DOC concentrations in the soil profile as a natural tracer (e.g. Brown et al., 1999; Inamdar et al., 2006), to explain sources of stream water. However, whether this source is supply limited (e.g. DOC in the organic horizon shows a dilution pattern during a rainfall event) or unlimited (e.g. DOC in the organic horizon is an infinite source and not affected by rainfall events) at

the time-scales of individual storm events remains poorly understood and makes a mechanistic assessment of variable runoff chemistry and thus the double paradox problematic. The study of Anderson et al. (1997a, 1997b) was conducted under controlled sprinkler conditions and thus avoided issues with input characterization (McGuire and McDonnell, 2006) and identifying flowpaths contributing to runoff under natural conditions. Their sprinkler experiment was of such duration that deuterium only peaked significantly in shallow soil lysimeters and breakthrough curves in soil water were incomplete. This made it difficult to determine if vertical flow in the unsaturated zone followed a plug flow model or an advection-dispersion model. The distinction between these two models is important since the advection-dispersion model allows for mixing of old and new water in the unsaturated zone, and the plug flow model does not.

Most field based studies of conservative tracer movement at the hillslope scale have focused on qualitative and or conceptual descriptions of observed transit times, velocities and dispersion of solutes (e.g. Anderson et al., 1997a; Nyberg et al., 2003). The advection dispersion equation (ADE) with or without (first order) mass transfer has been used to quantitatively describe solute movement through soil columns (e.g. Van Genuchten and Wierenga, 1977; Brusseau, 1992) and soil pedons (e.g. Tsuboyama et al., 1994) but not at the hillslope scale to address the double paradox. One approach to address the double paradox in a mechanistic and quantitative plausible way (Kirchner, 2003) is to model conservative solute breakthrough curves with the advection dispersion equation (ADE) with mass transfer. Mass transfer is the

movement of solutes between mobile and immobile domains (Coats and Smith, 1964; Van Genuchten and Wierenga, 1976) of the subsurface or soil column. In unsaturated soils, immobile zones may develop when soil water is only connected through preferential mobile flow paths (Kim et al., 2005; Maraga et al., 1997). In saturated soils, immobile zones are characterized by zones with low hydraulic conductivities including the size of individual mineral grains (Haggerty et al., 2004). Simulating the observed breakthrough curve (BTC) from an applied conservative tracer at the hillslope scale with the advection-dispersion-mass transfer (ADMT) equation (first order mass transfer) provides parameters as velocity, dispersion, ratio mobile immobile domain, and mass transfer rate between the immobile and mobile domain. These parameters help to form a mechanistic plausible model of the double paradox at the hillslope scale.

This paper reports on a 24-day sprinkler experiment at the hillslope scale that applied a conservative tracer (deuterium (dD)) at the start of the sprinkler experiment. Because of controlled conditions we avoided the input characterization issue occurring under natural conditions. Steady sprinkler rates and long duration of the sprinkler experiment allowed us to identify flowpaths that control variable runoff chemistry of lateral subsurface flow from the hillslope, and to investigate whether nutrients were supply limited or unlimited. Lastly, the duration of the sprinkler experiment enabled us to explore complete breakthrough curves of dD in soil water, groundwater and lateral subsurface flow. We investigated variable runoff chemistry, sources of DOC, nitrogen (N) and electrical conductivity (EC) of lateral subsurface flow, in relation to

old water mobilization and parameters from the modeled dD BTC in lateral subsurface flow to mechanistically assess the double paradox. We address the following questions: (1) Is the supply of nitrogen and carbon from soils limited or unlimited during the sprinkler experiment? (2) What flow paths control variable runoff chemistry of DOC and N during the sprinkler experiment? (3) Is old water rapidly mobilized during the sprinkler experiment? (4) Does modeling the dD BTC in lateral subsurface flow with the ADMT-equation aid to form a mechanistic plausible model of the double paradox at the hillslope scale?

5.2 Site description

This study was conducted in Watershed 10 (WS10), a 10.2 ha headwater catchment located on the western boundary of the H. J. Andrews Experimental Forest (HJA), in the western-central Cascade Mountains of Oregon, USA (44.2° N, 122.25° W) (Figure 5.1). The HJA has a Mediterranean climate, with wet mild winters and dry summers. Average annual rainfall is 2220 mm of which about 80% falls between October and April during storms characterized by long duration and low rainfall intensity. Snow accumulations in WS10 are common but seldom exceed 30 cm, and generally melt within 2 weeks (Sollins et al., 1981). Elevations range from 470 m at the watershed flume to a maximum watershed elevation of 680 m at the southeastern ridge line. The watershed was harvested during May-June 1975 and is now dominated by a naturally regenerated second growth Douglas-fir (*Pseudotsuga menziesii*) stand. Several seep areas along the stream have been identified (Harr, 1977; Triska, 1984).

These seep areas are related to the local topography of bedrock and/ or saprolite, or to the presence of vertical, andesitic dikes approximately 5 meters wide, which are located within the southern aspect hillslope (Swanson and James, 1975; Harr, 1977).

The study hillslope is located on the south aspect of WS10, 91 m upstream from the stream gauging station (Figure 4.1). The 125 m long stream-to-ridge slope has an average gradient of 37º, ranging from 27º near the ridge to 48º adjacent to the stream (McGuire, 2004). The elevation range of this site is between 480 and 565 m. The bedrock is of volcanic origin, including andesitic and dacitic tuff and coarse breccia (Swanson and James, 1975). The depth to unweathered bedrock ranges from 0.3 to 0.6 m at the stream-hillslope interface and increases gradually toward the ridge to approximately 3 to 8 m. Soils are about 1 m deep, and formed either in residual parent material or in colluvium originating from these deposits. Surface soils are well aggregated, but lower depths (70-110 cm) exhibit more massive blocky structure with less aggregation than surface soils (Harr, 1977). Soil textures change little with depth. Surface soils are gravelly loams, lower soil layers are gravelly silty clay loams or clay loams and subsoils are characterized by gravelly loams or clay loams (Harr, 1977). . The soils are highly andic and vary across the landscape as either Typic Hapludands or as Andic Dystrudepts (Yano et al., 2005), and are underlain by 1-8 m relatively low permeability subsoil (saprolite), formed from the highly weathered coarse breccia (Ranken, 1974; Sollins, 1981).

5.3 Methods

5.3.1 Sprinkler experiment and instrumentation

A 10 m long trench was constructed (McGuire et al., 2007) to measure lateral subsurface flow at a natural seepage face. Intercepted subsurface water was routed to a calibrated 30º V-notch weir that recorded stage at 10-minute time intervals using a 1-mm resolution capacitance water-level recorder (TruTrack, Inc., model WT-HR). We conducted the sprinkling experiment for 24 days beginning on Julian day 208 (July 27), 2005 on an approximately 8 m by 20 m section of the study hillslope directly upslope from the trench (Figure 5.1.). We applied a total of 2107 mm of water at an average rate (±SD) of 3.6 (0.5) mm h^{-1} continuously (except for 9 hours with no application of water due to sprinkler malfunction). A pulse of deuterated water was applied to the study area via the sprinkling system for 24.5 hours beginning on Julian day 208. The source of the deuterated water was a 20,000 L reservoir having a natural isotopic signature in which we mixed approximately one liter of 99.8 % of D_2O. For detailed information about the sprinkler experiment design we refer the reader to Graham et al. (2007).

We instrumented the gauged hillslope with four nests of porous cup suction lysimeters (Soil Moisture Equipment Corp., Model 1900, 2 bar) at 0.3, 0.7 and 1.10 m depths, except for site AL, where the deepest lysimeter was installed at 0.8 m depth (soil bedrock interface) (Figure 5.1.). Three plastic zero tension lysimeters of 0.15 x 0.15 m were used; two collected water from the organic horizon, and one collected water at 0.2 m depth. Twenty five superquartz (Prenart Equipment ApS) tension (0.5

bar) lysimeters installed at a 30º angle (Lajtha et al., 1999), were located in an upslope transect at shallow (0.2 m), middle (0.3-0.4 m), and deep (0.7-0.8 m) soil profile positions. Soil matric potential was measured by 7 fast responding tensiometers (type: UMS T4, 1 bar porous cups), installed vertically in an upslope transect, two nests of tensiometers at 0.3 and 0.7 m depth, and one nest of tensiometers at 0.3, 0.7 and 1 m depth. All instrument locations are shown in Figure 5.1.

5.3.2 Sampling

Lateral subsurface flow was sampled with an ISCO sampler every 2 to 4 hours. Fluorescence of lateral subsurface flow was measured continuously at a 5 sec. interval using a field portable fluorometer (10-AU, Turner Designs, Inc., Sunnyvale, CA) equipped with a CDOM Optical Kit (P/N 10-303). For the first 12 days zero tension and tension lysimeters were sampled daily and from Julian day 219 until Julian day 235 were sampled every other day. Tension lysimeters were evacuated to -50 kPa and were allowed to collect water for 24 hours. Groundwater was sampled daily from two wells (A05 and E04, installed at depths 0.45 and 1.25 m respectively) (Figure 5.1) that showed consistent transient groundwater and one well (A01, installed at depth 0.35 m) located in a groundwater seep (Figure 5.1). Well A01 was the only well located at the "soil-bedrock interface". A knocking pole survey before well installation showed that depth of bedrock at well E04 and well A01 was at least 2 and 0.8 m respectively. Wells were augered with a hand auger until refusal.

Soil samples were taken for extraction and incubation from the upper 0.1 m mineral soil one week before, and four times during the sprinkler experiment (at weekly intervals at the sprinkler plot and an adjacent dry control plot) in order to assess potential supply of nutrients. The sprinkler and dry plot were divided in 5 blocks of similar size and two composite samples were used from each two adjacent blocks, resulting in 10 samples from each plot.

5.3.3 Extraction and incubations

Soil samples were sieved through a 1 mm sieve. Two 10 g subsamples of sieved soil were extracted with 100 ml 0.01 M KCl and 100 ml 1 M KCl within 24 hours, shaken for two hours, and filtered with a Whatman no. 40 ashless filter paper, for DOC-TDN and inorganic N analysis, respectively. To determine potential nitrogen mineralization, approximately 10 g of sieved soil was incubated at 70% water-filled pore space and 20 ºC for 28 days in small plastic cups. The lids of the plastic cups contained small openings with plastic wrap between the lid and cup to prevent loss of H_2O (g) and to allow exchange of O_2 and CO_2. After 28 days incubated soil samples were extracted with 100 ml 1 M KCL for inorganic N analysis. Mineral production of N was calculated as $(NO_3^-+NH_4^+)_{final}-(NO_3^-+NH_4^+)_{initial}$.

5.3.4 Chemical analysis

Water samples were analyzed within 24 hours for pH and EC (TDSTestr40, OAKTON). Samples were filtered through combusted Whatman GF/F glass fiber

filters (nominal pore size = 0.7 µm) and stored frozen until analysis for dissolved organic carbon (DOC), total dissolved nitrogen (TDN) and inorganic nitrogen (nitrate (NO_3-N) + ammonium (NH_4-N)). Prenart tension lysimeter samples were not filtered because initial experiments with filtered soil solutions demonstrated that tension lysimeter samples did not need to be filtered (Lajtha et al., 1999). DOC and TDN were measured with Pt-catalyzed high-temperature combustion (Shimadzu TOC-V CSH analyzer with TN unit). NO_3-N was measured with the hydrazine sulfate reduction method and NH_4-N was determined by the Berthelot reaction method with an Orion Scientific AC 100 continuous flow auto-analyzer (Westco Scientific Instruments, Inc., Danbury, CT). DON was calculated as the difference between TDN and DIN (NO_3-N and NH_4-N). Because DON was calculated by difference, values sometimes fell slightly below 0 mg $^{L-1}$. Negative DON values were considered to be 0 mg L^{-1}. UV-absorbance was measured at 254 nm with a Hitachi V-2001 spectrophotometer.

Water samples were analyzed for hydrogen isotope ratios on (1) an isotope ratio mass spectrometer (Delta plus, ThermoQuest Finnigan, Bremen Germany) interfaced with a high temperature conversion/elemental analyzer (TC/EA, ThermoQuest Finnigan) and (2) a liquid water isotope analyzer (Los Gatos Research, Inc). All hydrogen isotope ratios are expressed as dD values relative to Vienna-standard mean ocean water (V-SMOW) in ‰:

$$dD = \left(\frac{R_{sample}}{R_{standard}} - 1 \right) \times 1000‰ \quad (1)$$

where R is the ratio of deuterium to hydrogen atoms of the sample and the standard V-SMOW. Measurement precision was 2‰.

5.3.5 Data analysis

We applied a two-component mixing model to dD breakthrough in lateral subsurface flow:

$$Q_t C_t = Q_p C_p + Q_e C_e, \qquad (2)$$

where Q is runoff, C is concentration, and the subscripts t, p and e stand for total subsurface flow, pre-event and event water, respectively. We used the deuterium concentration in subsurface flow (C_p) before the start of adding labeled water to the sprinkler plot as pre-event water. New water was defined as the average deuterium concentration of the labeled water (C_e). We were able to apply a two-component mixing model because the average dD signal in sprinkler water without labeled water was the same as pre-event water (-75‰).

The breakthrough curve of deuterium in lateral subsurface flow was modeled with the advection-dispersion-first order mass transfer equation:

$$\frac{\partial c_m}{\partial t} + b_{tot}\frac{\partial c_{im}}{\partial t} = \frac{D}{R_m}\frac{\partial^2 c}{\partial x^2} - \frac{v}{R_m}\frac{\partial c_m}{\partial x} \qquad (3a)$$

$$\frac{\partial c_{im}}{\partial t} = a\left(c_m - c_{im}\right) \qquad (3b)$$

where, c_m and c_{im} are the mobile and immobile concentration [ML^{-3}] respectively; b_{tot} [] is the capacity coefficient (ratio of q_{im} (immobile water content) to q_m (mobile water content)); D [$L^2 T^{-1}$] is the dispersion coefficient; R_m [] is the retardation factor in the mobile zone (which for deuterium was assumed to be 1); v [$L T^{-1}$) is the average pore-water velocity; a [T^{-1}] is the first order rate coefficient, x [L] is the space coordinate (1-dimension) and t [T] is time. The following initial and boundary conditions (semi-infinite boundary) were considered:

$$c_m(x,t=0) = c_{im}(x,t=0) = 0 \tag{4a}$$

$$c_m(x \to \infty, t) = c_{im}(x \to \infty, t) = 0 \tag{4b}$$

$$c_m(x=0,t) = c_0\left(u_{c1}(t) - u_{c2}(t)\right) \tag{4c}$$

$$u_c(t) = \begin{cases} 0, & t < c \\ 1, & t \geq c \end{cases} \qquad c \geq 0$$

where $u_c(t)$ is a unit step function, and c_0 is the strength of the step function. The advection-dispersion-mass transfer equation with first order mass transfer with initial and boundary conditions was transformed to the Laplace domain, which resulted in the following equation in the Laplace domain:

$$\hat{c}(x=L,s) = \hat{c}_{input} \exp\left(\frac{vL}{2D}\right) \cdot \exp\left\{-\frac{R_m L}{2D}\sqrt{\left(\left(\frac{v}{R_m}\right)^2 + \frac{4D}{R_m}p[1+\bar{g}]\right)}\right\} \tag{5a}$$

$$\hat{c}_{input} = \frac{\left(e^{(-c_1 s)} - e^{(-c_2 s)}\right)}{s} \tag{5b}$$

$$\bar{g} = \frac{\left(a b_{tot}\right)}{\left(s + a\right)} \tag{5c}$$

where, $\hat{c}$ is flux averaged concentration (Kreft and Zuber, 1978; Parker and Van Genuchten, 1984), s is the Laplace variable, L is the length of the problem, and $\hat{c}_{input}$ is the step input. The Laplace transform was numerically inverted in MATLAB with a modified De Hoog algorithm (De Hoog et al., 1982; Hollenbeck, 1998). We modeled the lateral subsurface dD BTC as a 1-dimensional problem. Equation 5a was numerically integrated (function quadv in MATLAB) in the Laplace domain between $L_{\min}$ and $L_{\max}$, where $L_{\min}$ and $L_{\max}$ are the minimum and maximum upslope distance from the trench to the sprinkler plot. The BTC was modeled with a step input that equaled the 0^{th} moment of the BTC.

The model parameters were determined by performing a Monte Carlo simulation (25000 runs) over expected parameter ranges for the BTC. To evaluate model performance we used the Nash-Sutcliffe efficiency (E) (Nash and Sutcliffe, 1970). We defined uncertainty of each parameter as the range of parameter values with an E value of at least or equal to the maximum E value minus 0.1 The parameter a [h^{-1}] range was fixed to the range $1x10^{-6}$ to 1, based on literature values (e.g. Maraqa et al., 1997, Griffioen et al., 1998). The parameter b_{tot} [] range was fixed to 0.3-3. This range was approximately equal to a range of immobile water content between 0.15 and 0.45, if we assume a total porosity of 0.6 based on soil characteristics from this site reported by Ranken (1974) and earlier modeling work of McGuire et al. (2007). The lower limit of the range for dispersion [m^2 h^{-1}] and pore-water velocity [m h^{-1}] were both fixed at $1x10^{-6}$. These values were based on minimum dispersion values of field and soil column studies (order of 10^{-5} m^2 h^{-1}) (Nielsen et al.,

1976; Kirda et al., 1973; Bejat et al., 2000) and minimum unsaturated fluxes (order of 10^{-4} m h^{-1}, with Darcy velocity of 0.5 mm h^{-1} and porosity of 0.6) calculated by Harr (1977). Maximum pore water velocity was set to 1 m h^{-1} for lateral subsurface flow. This value was based on an estimated pore water velocity of 0.42 m h^{-1} for the subsoil where K_{sat} equals ~0.5 m h^{-1}, gradient and porosity values were assumed 0.5 and 0.6 respectively. Dispersion was modeled for a tracer well injection at the hillslope with an advection-dispersion equation (Victory, 2007), which was 1.7 m^2 h^{-1}, and an upper limit of 10 m^2 h^{-1} was assumed to cover possible values of dispersion.

The dD tracer was applied under transient flow conditions (i.e. lateral subsurface flow increasing to steady state flow conditions). From the start of dD application (Julian day 208) until Julian day 212 lateral subsurface flow increased from 0.012 L s^{-1} to 0.049 L s^{-1}. After Julian day 212 lateral subsurface flow increased slowly until semi-steady state flow conditions were achieved and lateral subsurface flow was varying between approximately 0.055 and 0.065 L s^{-1}. Consequently, significant transient flow conditions occurred during about 17% of the total duration of the sprinkler experiment (24 days). The advection-dispersion-first order mass transfer equation assumes steady state flow conditions with a constant pore water velocity and constant soil moisture content. These assumptions were violated during part (17%) of the sprinkler experiment. However, Porro and Wierenga (1993) found similar transport parameters by modeling solute transport in an unsaturated soil column during water infiltration under steady-state and transient flow experiments. During these experiments the solute pulses lagged behind the wetting front, and thus

'experienced' small variations in soil moisture content. Furthermore, Wierenga (1977) modeled solute concentration profiles and breakthrough curves with transient and steady state models, and found that solute transport during transient conditions was well approximated with a steady state model when concentrations were expressed as a function of cumulative drainage instead of time. In contrast, Ruso et al. (1989) concluded that applying a steady state model may considerably overestimate the effective vertical solute velocity. Meyer-Windel et al. (1999) found that a steady state model with cumulative drainage as a time coordinate predicted transport of reactive and non-reactive tracers well in homogeneous soils without preferential flow features during transient flow conditions. From these studies it appears that the application of a steady state model is justified, especially when the solute pulse lags behind the wetting front. Furthermore the number of irrigation cycles used in these studies to create transient flow conditions was much larger with likely more flow and soil water content variations than during our experiment. We believe based on findings from these studies, in combination with the relative short duration of significant transient flow conditions during our sprinkler experiment without many irrigation cycles that the approximation of transport parameters with a steady state model is valid.

5.4 Results

5.4.1 DOC and N dynamics in soil extracts and incubations

Soil extracted DOC, DON and DIN [mg kg^{-1}] were high before the start of the sprinkler experiment (day 203) at the both the sprinkler plot and non-sprinkled dry

plot. We found no significant difference in soil extracted DOC, DON and DIN between the dry and sprinkler plot (Table 5.1). When we compare soil extracted DOC, DON and DIN throughout the sprinkler experiment (Julian day 208-236) between the dry and sprinkler plot at individual sample days, DOC was significantly lower at the sprinkler plot on one sample day, DON was significantly lower at the sprinkler plot on two sample days and DIN was significantly higher at the sprinkler plot on three sample days. Differences between soil extracted DOC, DON and DIN averaged over all sample days throughout the sprinkler experiment between the dry and sprinkler plot were significant (see *p* values in Table 5.1).

Soil extracted DIN from incubated soils from the dry and sprinkler plot showed high values before the start of the sprinkler experiment compared to values during the sprinkler experiment (Table 5.2). Differences between soil extracted DIN from incubated soils at individual sample days and for all sample days throughout the sprinkler experiment between the dry and sprinkler plot were not significant.

5.4.2 DOC and N dynamics in sprinkler, soil, ground and lateral subsurface water

During the sprinkler experiment, mean DOC, DON and NH_4-N concentrations in sprinkler water were higher than under natural conditions in throughfall measured at the site (Table 5.3). Both DOC and DON decreased from highest values immediately below the organic horizon, to “deep soil lysimeters” most likely due to sorption of DOC and DON to soil mineral surfaces. Transient groundwater DOC, DON and DIN

concentrations in two wells (A05 and E04) were high compared to seepage groundwater (from well A01) (Table 5.3) implying vertical preferential flow.

DOC in water collected from the organic horizon, at 0.2 m depth in a zero tension lysimeter and from tension lysimeters at 0.2 m and 0.3-0.4 m depths showed a dilution pattern. DOC from tension lysimeters at 0.7-0.8 m depth remained constant during the sprinkler experiment with a mean value of 2.4 mg l^{-1} (Figure 5.2). Organic horizon DON and DON at 0.2 m depth in a zero tension lysimeter showed a dilution pattern, except at Julian day 224 for the zero tension lysimeter at 0.2 m when DON reached a high concentration (0.63 mg l^{-1}). DON in tension lysimeters at 0.2 m depth did show a dilution pattern, while DON in tension lysimeters at 0.3-0.4 m depth reached a maximum concentration and started to decrease at day 218. DIN concentrations in zero- and tension lysimeters were low and did not show any pattern (flushing or dilution).

Lateral subsurface flow DOC and DON concentrations increased rapidly at the start of the sprinkler experiment (Figure 5.3.a and Figure 5.3.c), DOC and DON peaked within 15 and 11 hours respectively. DOC decreased to a relatively constant concentration after day 210, while DON showed variable concentrations after the DON peak (Figure 5.3.c). Raw fluorescence measurements were linearly related to UV-absorbance (254 nm) ($r^2 = 0.59$, $p<0.0001$), a more standard measurement of DOC quality. Fluorescence and SUVA patterns during the sprinkler experiment showed that the DOC-quality changed rapidly to a more aromatic character until discharge decreased after the sprinklers were shut off (Figure 5.3.b). Fluorescence showed a

diurnal pattern, with highest values when lateral subsurface flow reached a daily minimum and lowest values when lateral subsurface flow reached a daily maximum. Similar to the fluorescence diurnal pattern, DOC concentrations showed a weak diurnal pattern, and both EC and pH showed a strong diurnal pattern, suggesting that these patterns were caused by a concentration effect.

5.4.3 Deuterium breakthrough in soil, ground and lateral subsurface water

Water enriched in dD was observed in lateral subsurface flow within 4 hours of application and dD peaked after approximately 21 hours (Figure 5.4). Total mass recovery of dD (over the period Julian day 208-Julian day 236) in lateral subsurface flow was 38%. Water balance calculations showed deep seepage was insignificant because almost all sprinkler water showed up at the WS10 catchment outlet. This suggests flowpaths with dD bypassed the trench, in agreement with water balance calculations (Graham et al., in prep). Seep groundwater did not show significantly elevated levels of dD during the entire sprinkler experiment and was thus not a significant contributor to elevated dD in lateral subsurface flow (Figure 5.5). In contrast, dD in transient groundwater increased rapidly (Table 5.4). All lysimeters showed significant increases in dD. The shallow lysimeters at 0.3 m responded most rapidly to the dD input and dD peaks in lysimeters at 0.7 and 1.1 m followed the dD peak at 0.3 m (Table 5.4 and Figure 5.5). We calculated the average vertical velocity of labeled water by assuming that the dD peak in lysimeters and wells marked the

passage of the dD peak in sprinkled water (consistent with the method of Anderson et al. (1997a)).

$$v = \frac{d}{\Delta t} \qquad (6)$$

where d is depth of lysimeter or well, and Δt is the travel time between start of dD peak in sprinkler water and dD peak in soil- or groundwater. At all locations the dD peak arrival time was on the order of 5.7-16.4 mm h^{-1} and was sequential with depth. One exception was well E04 where the average vertical velocity was about 2-3 times higher than the average vertical velocity of the deep lysimeters (Table 5.4).

5.4.4 Mixing at the hillslope scale

The dD-based two component mixing model showed that the peak of event water fraction was 26% and occurred at day 209, 20 hours after the initial dD application. After day 209, the fraction of event water gradually decreased to ~1% on Julian day 234 (Figure 5.6).

A bivariate mixing plot of dD against EC for lateral subsurface flow samples, revealed possible sources of lateral subsurface flow during the sprinkler experiment (Figure 5.7). Baseflow, defined as lateral subsurface flow prior sprinkling with dD labeled water, was characterized by low dD values (~-75 ‰) and high EC values (~ 166 µS). During the sprinkler experiment, lateral subsurface flow shifted rapidly to a mix of baseflow and dD labeled water, with a maximum fraction of dD labeled water in lateral subsurface flow on Julian day 209. Soil water dD peaked on Julian day 209 at 0.3 m depth. We compared this soil water dD peak at 0.3 m with the arrival time of

nearly saturated conditions at the lower and middle slope position tensiometers at 0.3 m depth. The arrival time of nearly saturated conditions was defined as the first three consecutive measurements with ? < 0.1 kPa. The arrival time of nearly saturated conditions at the lower and middle slope position tensiometers at 0.3 m depth was on day 209.41 and 208.76 respectively. This indicates that the observed dD and DOC peak (day 209) in lateral subsurface flow was derived mainly from shallow soil water. After Julian day 212, nearly saturated conditions were observed at 0.7 m depth on Julian day 212.18 and 211.86 at the lower and middle slope position respectively. The dD peak at deeper tension lysimeters and well E04 occurred at Julian day 212-213 and Julian day 211.74 respectively. Thus deeper flowpaths became important after Julian day 212.

5.4.5 Mass transfer at the hillslope scale

The dD BTC in lateral subsurface flow was well represented by the ADMT equation with first order mass transfer. Table 5.5 shows the best fit parameter sets based on the Monte Carlo simulations. The model efficiency (E) for the BTC was 0.97. Uncertainty ranges were high for parameters b_{tot} and a , and covered the entire parameters range used in the Monte Carlo analysis. The parameters v and D were more identifiable with the Monte Carlo simulation (Figure 5.8). The modeled pore-water velocity and dispersion coefficient of lateral subsurface flow was 0.19 m h^{-1} and 2.4 m^2 h^{-1} respectively. The residence time of pore water in the mobile zone (t_{adv}) was described by:

$$t_{adv} = \frac{LR_m}{v} \quad (7)$$

where L [L] is the average length of the hillslope, R_m [] the retardation factor in the mobile zone and v [L T^{-1}] the average pore water velocity. The residence time of pore water in the mobile zone was 63 hours. We used the Dahmkohler number [] to evaluate the importance of first order mass transfer at our site:

$$Da_1 = \frac{t_{adv}(1 + b_{tot})}{t_a} \quad (8a)$$

$$t_a = \frac{1}{a} \quad (8b)$$

where the pore water residence time is scaled by $(1 + b_{tot})$ and represents the mean solute residence time (Harvey and Gorelick, 1995; Haggerty et al., 2004), and t_a is the mass transfer time (Haggerty et al., 2000). When $Da_1 >> 1$, mass transfer time can be considered too fast to influence the problem significantly. For lateral subsurface flow, Da_1 was 18, which suggests that mass transfer was important and influenced the mass transport significantly. From B_{tot} (ratio of immobile zone divided by mobile zone) we can calculate the percentage of water participating in the flow (mobile water). For lateral subsurface flow the percentage of mobile water was 29%. This indicates a relatively high proportion of water at the hillslope scale was immobile.

5.5 Discussion

The double paradox in catchment hydrology and (bio)-geochemistry is a source of major debate and discussion in hydrology despite work aimed at resolving it

(Bishop et al, 2004; Jones et al., 2006; Anderson et al., 1997a, 1997b). The rapid mobilization of stored, pre-event water to the stream during storm events but with variable runoff chemistry still challenges our mechanistic understanding of flowpaths and transport of (bio)-geochemical solutes. Bishop et al. (2004) showed that the transmissivity feedback and lateral flowpaths intersecting distinct vertical soil solution chemistry profiles of DOC, Ca^{2+} and Cl^- in the riparian zone resolved the double paradox. Anderson et al. (1997a, 1997b) showed during sprinkler experiments that vertical unsaturated flow followed the plug flow model and displaced old water in the unsaturated zone that mixed with lateral saturated flow paths emerging from the bedrock, while dilution of solutes in runoff were caused by low-solute soil water that mixed with bedrock water in agreement with the observation that old water dominated runoff. However, we frequently do not know (1) the importance of vertical (preferential) flow at sites where groundwater dynamics seem to dominate (Bishop et al., 2004), (2) if nutrients like DOC are supply limited or unlimited during storm events, both outstanding issues that make it difficult to assess variable runoff chemistry and thus ultimately the double paradox mechanistically, and (3) what type of mixing (e.g. plug flow model or advection dispersion model) takes place and described quantitatively.

Our work reported here used a sprinkler experiment approach to define boundary conditions and combine isotopic, biogeochemical and internal physical measurements to assess the double paradox at our site mechanistically. We found that DOC (and to a lesser extent DON) were supply limited in the organic and upper soil

layer. The two component mixing model based on dD showed a small contribution of new water (maximum of 26%) to lateral subsurface flow. We identified two flow paths at our site; vertical flow paths through the unsaturated zone and rapid lateral subsurface flow. Modeling the dD breakthrough in lateral subsurface flow as a 1-dimensional problem with the advection-dispersion-first order mass transfer model showed a fast 'preferential' mobile flow path of 'new' water that was attenuated because of dispersive mixing and significant exchange of deuterium between the mobile and immobile domain, consistent with the rapid mobilization of old water. We argue that the early flushing peak of nutrients as DOC (and DON) in lateral subsurface flow was caused by mobile flowpaths; first vertical and then lateral along the soil-bedrock interface, with a strong vertical connection between the organic horizon/ shallow soil and transient groundwater based on nutrient and isotopic data. Later in the event, lateral subsurface flow DOC concentrations decreased because of dilution in the organic horizon.

We are aware that modeling the dD BTC in lateral subsurface flow with the advection-dispersion-first order mass transfer model based on steady state flow conditions, during transient conditions (17% of sprinkler experiment period), may have resulted in non-realistic transport parameters. We consider this issue below.

5.5.1 How realistic are the modeled transport parameter values?

Our analysis showed that the dD breakthrough curve in lateral subsurface flow was well described with the advection-dispersion-first order mass transfer equation.

We are aware that the transport parameters derived from modeling the dD BTC are a first approximation. This is a consequence of transient flow conditions and the assumption that the advection-dispersion-first order mass transfer equation in a 1-D form is an approximation for the hillslope scale flow and transport complexity. So how realistic are the modeled transport parameter values? From B_{tot} we calculated a mobile water percentage of 29%. Pore size distributions from soil pit data (Ranken, 1974) show that pores fall into two quite divergent size classes: pore sizes > 0.294 mm or pore sizes < 0.029 mm. Furthermore, the fraction of the pore size class with pore sizes < 0.029 mm of total porosity increased with soil depth. The pore size class > 0.294 mm represented likely the mobile water domain. We calculated from soil pit 3 (closest to the sprinkler plot) a depth weighted average percentage of total porosity of pore sizes > 0.294 mm of 36%. The modeled B_{tot} was in agreement with the soil pore size distribution of our site. A steady state tracer well (C1) injection was conducted at the hillslope and modeled with the advection dispersion equation (Dunn, 2007) to determine dispersion coefficients and velocities of lateral flowpaths along the soil bedrock interface. The modeled dispersion coefficient was 1.7 $m^2\ h^{-1}$ and the average velocity was 0.78 m h^{-1}. Our modeled dispersion coefficient and pore water velocity were 2.4 $m^2\ h^{-1}$ and 0.19 m h^{-1} respectively, and thus similar to values of Victory (2007). Our transport parameters are effective values of vertical and lateral flowpaths and our lower pore water velocity may have been caused by smaller vertical flow velocities compared to lateral subsurface flow.

The Peclet number $Pe = vL/2D$ is the ratio of advective transport to dispersive transport, and was 0.9 for lateral subsurface flow during the sprinkler experiment. The dispersivity $a_L = D/v$ was 13 m for lateral subsurface flow, roughly equaling the average travel distance (11.65 m). These Peclet and dispersivity values are similar to values found by Kirchner et al. (2001) by applying the advection dispersion equation at the catchment scale. This implies that the subsurface system was heterogeneous up to at least the spatial scale of the sprinkler plot on the hillslope. Our calculated dispersivity value falls in the center of the range of dispersivities observed at 10-20 meter field scale from different studies (Gelhar et al, 1992).

5.5.2 The double paradox and organic horizon and shallow soil DOC and N dynamics

Extracted DIN [mg kg^{-1}] was significantly higher on the sprinkler plot compared to the adjacent dry plot during the sprinkler experiment. Before and after sprinkling, extracted DIN at the sprinkler and dry plot were not significantly different. We know from the incubation study that potential N mineralization was the same for the sprinkler and dry plot on each sample day. This implies that differences in extracted DIN between the sprinkler and dry plot were not caused by differences in potential N mineralization. Higher extracted DIN at the sprinkler plot may have been caused by a flush of NH_4^+ during sprinkling (Cabrera, 1993). Indeed, NH_4-N was significantly higher at the sprinkler plot during sprinkling ($p < 0.05$), and not significantly different prior and after sprinkling based on a Wilcoxon ranksum test. An N flush generally occurs for a few days after rewetting of a dry soil (Birch, 1958; Cabrera,

1993), and elevated NH_4-N [mg kg^{-1}] lasted for at least 14 days was supply unlimited. Continuous sprinkling may have physically disrupted soil aggregates resulting in the release of protected organic matter or de-sorption of organic matter that was mineralized quickly (Miller et al., 2005).

The average extracted DOC and DON were significantly lower at the sprinkler plot compared to the dry plot during the sprinkler experiment when (Julian day 215-235 combined). This suggests that DOC and DON were diluted during the sprinkler experiment and thus largely supply limited. In addition DOC and DON concentrations in the organic horizon and mobile water at 0.2 m depth, and DOC concentrations at 0.2 and 0.3-0.4 m depth showed evidence of a dilution pattern. The result of limited supply of DOC and DON in the organic horizon and shallow layer is significant for understanding the variable runoff chemistry part of the double paradox. At our site we cannot simply perceive the organic horizon and shallow soil layer as a time-invariant geographic source (intersected by vertical flowpaths) to lateral subsurface flow as was the case in the study of Bishop et al. (2004). DON was highly variable in lateral subsurface flow and soil water. This may have been caused by relatively large variation of DON concentrations in sprinkler water or a higher average soiltemperature amplitude during the sprinkler experiment in comparison to before the sprinkler experiment. At 20 cm depth the temperature varied between 18 and 20ºC before the sprinkler experiment, and varied between 18 and 22ºC during the sprinkler experiment, while there was an increase in temperature from 15 to 18ºC at 70 cm depth as a result of the sprinkler experiment. Because of the high variability in DON

concentrations we only consider variable runoff chemistry of DOC in the following sections.

5.5.3 Mechanistic assessment of the double paradox

We identified two main flowpaths at the hillslope scale: vertical flow through the unsaturated zone and lateral subsurface flow at the hillslope scale. Vertical flow moved depth sequential based on ? patterns from tensiometers and dD peaks in soil water and groundwater. The one exception was well E04 that showed an earlier arrival time than deep soil lysimeters based on the dD peak, indicating preferential flow at this location.

From the modeled average pore water velocity of lateral subsurface flow compared to vertical flow velocities based on dD peak arrival times in the unsaturated zone we infer that lateral flow paths at the hillslope scale were faster than vertical flow paths. Even when 29% was mobile in the unsaturated zone (with a total porosity of 0.6) vertical flow pore water velocities would be smaller than the modeled pore water velocity of lateral subsurface flow. The dD breakthrough curve for lateral subsurface flow showed an early breakthrough and long tailing. This would suggest a subsurface system with fast preferential flow paths (mobile zone) followed by slow flowpaths (an immobile zone). The percentage of mobile water at the hillslope scale calculated from the modeled b_{tot} was 29%. Thus, mobile water flows through a small part of the soil domain while the immobile zone provides a large mixing reservoir. The peak dD value in lateral subsurface flow was about +19 ‰, while the labeled sprinkler water had an

average signal of +285 ‰. Our results indicate the mechanism responsible for this large reduction in the dD signal was dispersion and mass transfer between the mobile and immobile zone. Both processes attenuated the observed dD spike in lateral subsurface flow and produced a small new water contribution calculated with the two component mixing model and thus explain the rapid mobilization of stored, pre-event water. These findings are in contrast with results of Anderson et al. (1997a) that attributed rapid mobilization of old water to displacement of old water (plug flow) in the unsaturated zone that mixes with lateral saturated flow paths emerging from the bedrock. Our results are more in line with findings of Collins et al. (2000) who did not observe evidence of complete displacement of old water by new water. In addition, Kienzler and Naef (in press) found by inter-comparison of sprinkler experiments at different sites that sites with large fractions of pre-event water were characterized by indirect feeding of subsurface flow; preferential flow paths were fed indirectly via saturated parts of the soil in contrast to direct feeding by precipitation. Also, they did not see evidence for complete instantaneous mixing of pre-event and event water. Rather, saturation of the soil matrix caused the continuous release of pre-event water from small pores to larger pores. By modeling the dD BTC in lateral subsurface flow we found a similar mechanism (besides dispersive mixing) at our site; event water transferred to the immobile domain (i.e. small pores) during the beginning of the sprinkler experiment and was slowly released during the remainder of the sprinkler experiment. Although we defined the labeled sprinkler water as new water, the slow

release of this ‘new’ water could be perceived as ‘old’ water during the end of the sprinkler experiment.

From the bivariate mixing plot of dD against EC in combination with tensiometer data we were able to show that the dD peak and DOC peak in lateral subsurface flow was derived mainly from a shallow soil depth source. The soil depth at this site increases from 0.1-0.3 m at the bottom at the hillslope to about 3 meter at the upper end of the sprinkler plot, and is consistent with the two main flowpaths at this site and a shallow soil depth source. Since the dD signal in well E04 showed evidence of preferential flow we cannot completely rule out that water was not coming from higher upslope with soildepths > 0.3 m. The DOC breakthrough in lateral subsurface flow was similar to the dD breakthrough; both had an early rapid breakthrough, indicating the same mobile flow paths were responsible for these patterns. The observation that sources of high DOC were from the organic horizon/ shallow soil layer and transient groundwater is in agreement with the two main flowpaths at our site. The tailing of the DOC breakthrough curve was not as pronounced as the tailing of the dD breakthrough. This was likely caused by two or a combination of two mechanisms. Either mass transfer of DOC between the mobile and immobile domain was small, resulting in less pronounced tailing compared to dD. Or DOC that transferred from the mobile to the immobile zone was adsorbed to soil surfaces and became unavailable for transport. Furthermore, the dilution of DOC (and to a lesser extent DON) in the organic horizon and shallow soil layer, and the strong connection of the organic horizon/shallow soil layer with transient groundwater

through mobile flow paths controlled the breakthrough of DOC in lateral subsurface flow. DOC in wells A05 and E04 showed decreasing concentrations over time and these patterns are in agreement with the strong connection between the organic layer/shallow soil layer and transient groundwater. In addition, seepage water had a dilution effect on DOC and dD. Contribution of seepage water during the sprinkler experiment did likely not change much and probably decreased slightly during the sprinkler experiment.

5.6 Conclusions

The combination of isotopic, biogeochemical and internal physical measurements during a long duration sprinkler experiment, with steady sprinkler rates, controlled conditions that avoided the issue of input characterization and 1-D modeling of the dD BTC in lateral subsurface flow resulted in a mechanistically plausible conceptual model that resolved the double paradox at our site. Seepage groundwater was stable throughout the sprinkler experiment and did not show elevated dD as a result from sprinkling with dD labeled water. Flowpaths consisted of vertical flow through the unsaturated zone without significant preferential flow, and rapid lateral subsurface flow. The 1-D modeling of the dD BTC in lateral subsurface flow showed a small mobile water fraction (mobile water flowpath) of 29% and thus a large immobile reservoir. The fast initial breakthrough of dD in lateral subsurface flow was caused by mobile flowpaths, mass transfer to the immobile domain and dispersive mixing. These three processes resulted in rapid mobilization of old water in lateral

subsurface flow, and explain this part of the double paradox in a plausible mechanistic way. Hydrometric data and a bivariate plot of dD against EC showed that the fast initial dD breakthrough was mainly derived from a shallow soil source (~30 cm). Later during the sprinkler experiment more deep flowpaths became important. We inferred from the similarity in the dD and DOC breakthrough in lateral subsurface flow that both were caused by the same mobile flowpaths. Furthermore, relatively high dD and DOC concentrations in transient groundwater showed a strong connection between the organic horizon/shallow soil layer and transient groundwater. We observed that DOC in the organic horizon was supply limited and this controlled in combination with the vertical and lateral flowpaths variable DOC chemistry in lateral subsurface flow.

.

5.7 Acknowledgements

This work was supported through funding from the National Science Foundation (grant DEB 021-8088 to the Long-Term Ecological Research Program at the H. J. Andrews Experimental Forest) and Department of Forest Engineering at Oregon State University. We thank Marloes Bakker, Matthew Bergen and John Moreau for providing field assistance, Sherri Johnson for loan of temperature probes and Roy Haggerty for help with the modeling part. We especially thank the McKenzie River Ranger District for providing sprinkler water during the experiment, and Kari O'Connell and Cheryl Friesen for coordinating logistics. We also thank R. D. Harr and D. Ranken for initiating the hillslope studies at WS10, and K. J. McGuire for re-initiating this site.

5.8 References

Anderson, S. P., W. E. Dietrich, D. R. Montgomery, M. E. Conrad, and K. Loague (1997a), Subsurface flow paths in a steep, unchanneled catchment., *Water Resour. Res., 33*, 2637-2653.

Anderson, S. P., W. E. Dietrich, R. Torres, D. R. Montgomery and K. Loague (1997b), Concentration-discharge relationships in runoff from a steep, unchanneled catchment, flow, *Water Resour. Res., 33*, 211-225.

Appelo, C. A. J., and A. Willemsen (1987), Geochemical Calculations and Observations on Salt Water Intrusions, I.A. Combined Geochemical/Mixing Cell Model, *J. of Hydr., 94*, 313-330.

Bejat, L., E. Perfect, V. L. Quisenberry, M. S. Coyne and G. R. Haszler (2000), Solute Transport as Related to Soil Structure in Unsaturated Intact Soil Blocks, *Soil Sci. Soc. Am. J., 64*, 818–826.

Biggar, J.W., and D.R. Nielsen (1976), Spatial variability of the leaching characteristics of a field soil. *Water Resour. Res. 12*, 78–84.

Birch, H. F. (1958), The effect of soil drying on humus decomposition and nitrogen availability, *Plant and soil, 10*, 9-31.

Bishop, K., J. Seibert, S. Kölhler, and H. Laudon (2004), Resolving the double paradox of rapidly old water with variable responses in runoff chemistry, *Hydrol. Processes, 18*,185-189.

Brown, V. A., J. J. McDonnell, D. A. Burns, and C. Kendall (1999), The role of event water a rapid shallow flow component and catchment size in summer stormflow, *J. Hydrol., 217*, 171– 190.

Brusseau, M. L. (1992), Nonequilibrium transport of organic chemicals: The impact of pore water-velocity, *J. Contam. Hydrol.*, 24, 185-204.

Cabrera, M. L. (1993), Modeling the Flush of Nitrogen Mineralization Caused by Drying and Rewetting Soils, *Soil Sci. Soc. Am. J., 57*, 63-66.

Coats, K. H., and B. D. Smith (1964), Dead end pore volume and dispersion in porous media, *Soc. Pet. Eng. J., 4*, 73-84.

Collins, R., A. Jenkins and M. Harrow (2000), The contribution of old and new water to a storm hydrograph determined by tracer addition to a whole catchment, *Hydr. Processes, 14*, 701-711.

De Hoog, F. R., Knight, J. H., and Stokes, A. N. (1982). An improved method for numerical inversion of Laplace transforms. *S.I.A.M. J. Sci. and Stat. Comput., 3*, 357-366.

Evans, C., and T. D. Davies (1998), Causes of concentration/discharge hysteresis and its potential as a tool for analysis of episode hydrochemistry, *Water Resour. Res., 34*, 129-137.

Gelhar, L. W., C. Welty and K. R. Rehfeldt (1992), A critical review of data on field-scale dispersion in aquifers, *Water Resour. Res., 28*, 1955-1974.

Graham, C. B., W. J. van Verseveld, H. B. Barnard and J. J. McDonnell (in prep), Experimental Closing of the Water Balance.

Griffioen, J. W., D. A. Barry, and J.-Y. Parlange (1998), Interpretation of two-region model parameters, *Water Resour. Res., 34*, 373-384.

Haggerty, R., A. McKenna, and L. C. Meigs (2000), On the late-time behavior of tracer test breakthrough curves, *Water Resour. Res., 36*, 3467-3479.

Haggerty, R., C. F. Harvey, C. Freiherr von Schwerin, and L. C. Meigs (2004), What controls the apparent timescale of solute mass transfer in aquifers and soils? A comparison of experimental results, *Water. Resour. Res., 40,* W01510, doi:10.1029/2002WR001715.

Harr, R. D., (1977), Water flux in soil and subsoil on a steep forested slope, *J. Hydrol., 33*, 37-58.

Harvey, C. F., and S. M. Gorelick (1995), Temporal moment-generating equations: Modeling transport and mass transfer in heterogeneous aquifers, *Water Resour. Res., 37*, 1129-1142.

Hendrickson, G. E., and R. A. Kreiger (1964), Geochemistry of natural waters of the Blue Grass region, Kentucky, *U.S. Geol. Surv. Water Supply Pap. 1700.*

Hollenbeck, K. J. (1998) INVLAP.M: A matlab function for numerical inversion of Laplace transforms by the de Hoog algorithm, http://www.isva.dtu.dk/staff/karl/invlap.htm

Hooper R. P, N. Christophersen and N. E. Peters (1990), Modelling streamwater chemistry as a mixture of soilwater endmembers—an application to the Panola Mountain catchment, Georgia, U.S.A., *J. Hydr., 116*, 321–343.

Inamdar, S. P., and M. J. Mitchell (2006), Hydrological and topographical controls on storm-event exports of dissolved organic carbon (DOC) and nitrate across catchment scales, *Water Resour. Res., 42*, W03421, doi:10.1029/2005WR004212

Jones, J. P., E. A. Sudicky, A. E. Brookfield, and Y.-J. Park (2006), An assessment of the tracer-based approach to quantifying groundwater contributions to streamflow, *Water Resour. Res., 42*, W02407, doi:10.1029/2005WR004130.

Kienzler, P. M., and F. Naef (2007), Subsurface storm flow formation at different hillslopes and implications for the ‘old water paradox’, *Hydrol. Processes*, (in press).

Kim, Y., Darnault, C. J. G., Bailey, N. O., Parlange, J. Y., and T. S. Steenhuis (2005), Equation for describing solute transport in field soils with preferential flow paths, *Soil Sci. Soc. Am. J., 69*, 291-300.

Kirchner, J. W., X. Feng and C. Neal (2001), Catchment-scale advection and dispersion as a mechism for fractal scaling in stream tracer concentrations, *J. Hydr., 254*, 82-101.

Kirchner, J. W., (2003), A double paradox in catchment hydrology and geochemistry, *Hydrol. Processes, 17*, 871-874.

Kirda, C., D. R. Nielsen and J. W. Biggar (1973), Simulateneous transport of chloide and water during water infiltration, Soil Sci. Soc. Amer. Proc., 37, 339-345.

Kreft, A., and A. Zuber, (1978), On the physical meaning if the dispersion equation and its solutions for different initial and boundary conditions, *Chem. Eng. Sci., 33*, 1471-1480.

Lajtha, K., Jarrell, W. M., Johnson, D. W., and P. Sollins (1999), Collection of Soil Solution. In: Robertson G. P., and others, Eds. Standard Soil Methods for Long-Term Ecological Research. New York: Oxford, University Press, p 166–182.

Maraqa, M.A., Wallace, R.B., and T.C. Voice (1997), Effects of degree of water saturation on dispersivity and immobile water in sandy soil columns, *Journal of Contaminant Hydrol. 25*, 199–218.

Martinec, J. (1975), Subsurface flow from snowmelt traced by tritium, *Water Resour. Res., 11*, 496-498.

McGuire, K. J., (2004), Water residence time and runoff generation in the western Cascades of Oregon, Ph.D., Oregon State University, Corvallis.

McGuire, K. J., McDonnell, J. J., and M. Weiler (2007), Integrating tracer experiments with modeling to infer water transit times, *Advances in Water Resources, 30*, 824-837.

McGuire, K. J., and J. J. McDonnell (2006), A review and evaluation of catchment transit time modeling, *J. Hydr., 330*, 543-563.

McDonnell, J. J., (1990), A rationale for old water discharge through macropores in a steep, humid catchment., *Water Resour. Res., 26*, 2821-2832.

Kendall, K. A., J. B. Shanley and J. J. McDonnell (1999), A hydrometric and geochemical approach to test the transmissivity feedback hypothesis during snowmelt, *J. Hydr. 219*, 188–205.

Meyer-Windel, S., B. Lennartz and P. Widmoser (1999), Bromide and herbicide transport under steady state and transient flow conditions, *European Journal of Soil Science, 50*, 23-33.

Miller, W. R., and J. I. Drever (1977), Water chemistry of a stream following a storm, Absaroka Mountains, Wyoming, *Geol. Soc. Am. Bull., 88*, 286–290.

Miller, A. E., Schimel, J. P., Meixner, T., Sickman, J. O. And J. M. Melack (2005), Episodic rewetting enhances carbon and nitrogen release from chaparral soils, *Soil Biology & Biochemistry, 37*, 2195-2204.

Nash, J. E., and J. V. Sutcliffe (1970), River flow forecasting through conceptual models, I, A discussion of principles, *J. Hydrol., 10*, 282-290.

Nyberg, L., A. Rodhe and K. Bishop (1999) Water transit times and flow paths from two line injections of 3H and 36Cl in a microcatchment at Gårdsjön, Sweden. *Hydrol. Processes, 13*, 1557-1575.

Parker, J. C., and M. T. van Genuchten, Flux-averaged and volume averaged concentrations in continuum approaches to solute transport, *Water Resour. Res., 20*, 866–872, 1984.

Plummer, N., J. F. Busby, R. W. Lee and B. B. Hanshaw (1990), Geochemical modeling of the Madison aquifer in parts of Montana, Wyoming, and South Dakota, *Water Resour. Res., 26*, 1981-2014.

Porro, I., and P. J. Wierenga (1993), Transient and steady-state solute transport through a large undisturbed unsaturated column, *Groundwater, 31*, 193-200.

Ranken, D. W., (1974), Hydrologic properties of soil and subsoil on a steep, forested slope, M.S., Oregon State University, Corvallis.

Russo, D., W. A. Jury, and G. L. Butters (1989), Numerical of solute transport during transient irrigation. 1., *Water Resour. Res. 25*, 2109–2118.

Sollins, P., K. J. Cromack, F. M. McCorison, R. H. Waring, and R. D. Harr, (1981), Changes in nitrogen cycling at an old-growth Douglas-fir site after disturbance, *J. Enivron. Qual.,, 10*, 37-42.

Swanson, F. J., and M. E. James, (1975), Geology and geomorphology of the H.J. Andrews Experimental Forest, western Cascades, Oregon., Res. Pap. PNW-188, U.S. Department of Agriculture, Forest Service, Pacific Northwest Forest and Range Experiment Station, Portland, OR.

Swistock, B. R., D. R. DeWalle, and W. E. Sharpe (1989), Sources of acidic storm flow in an Appalachian headwater stream, *Water Resour. Res., 25*, 2139–2147.

Torres, R., W. E. Dietrich, D. R. Montgomery, S. P. Anderson, and K. Loague, (1998), Unsaturated zone processes and the hydrologic response of a steep, unchanneled catchment, *Water Resour. Res., 34*, 1865-1879.

Tsuboyama, Y., R. C. Sidle, S. Noguchi, and I. Hosoda, (1994), Flow and solute transport through the soil matrix and macropores of a hillslope segment, *Water Resour. Res., 30*, 879-890.

Triska, F. J., J. R. Sedell, K. Cromack, S. V. Gregory, and F. M. McCorison, (1984), Nitrogen budget for a small coniferous forest stream, *Ecological Monographs, 54*, 119-140.

Van Genuchten, M. T., and P. J. Wierenga (1977), Mass transfer studies in sorbing porous media II, Experimental evaluation with tritium (^3H_2O), *Soil Sci. Soc. Am. J., 41*, 278-285.

Van Genuchten, M. T., and P. J. Wierenga (1976), Mass transfer studies in sorbing porous media I, Analytical solutions, *Soil Sci. Soc. Am. J., 410*, 473-480.

Victory, N. I. (2007), Quantification of Advection and Dispersion in Lateral Subsurface Flowpaths at the Hillslope-scale, M.S.., Oregon State University, Corvallis.

Walling, D. E., and I. D. L. Foster (1975), Variations in natural chemical concentration of river water during flood flows, and the lag effect: Some further comments, *J. Hydrol., 26*, 237–244.

Wierenga, P. J. (1977), Solute distribution profiles computed with steady-state and transient water movement models, *Soil Sci. Soc. Am. J. 41*, 1050–1055.

Williams, A. G., J. F. Dowd and E. W. Meyles (2002), A new interpretation of kinematic stormflow generation, *Hydrol. Process.,16*, 2791–2803.

Yano, Y., K. Lajtha, P. Sollins and B. A. Caldwell (2005), Chemistry and Dynamics of Dissolved Organic Matter in a Temperate Coniferous Forest on Andic Soils: Effects of Litter Quality, *Ecosystems, 8,* 286-300.

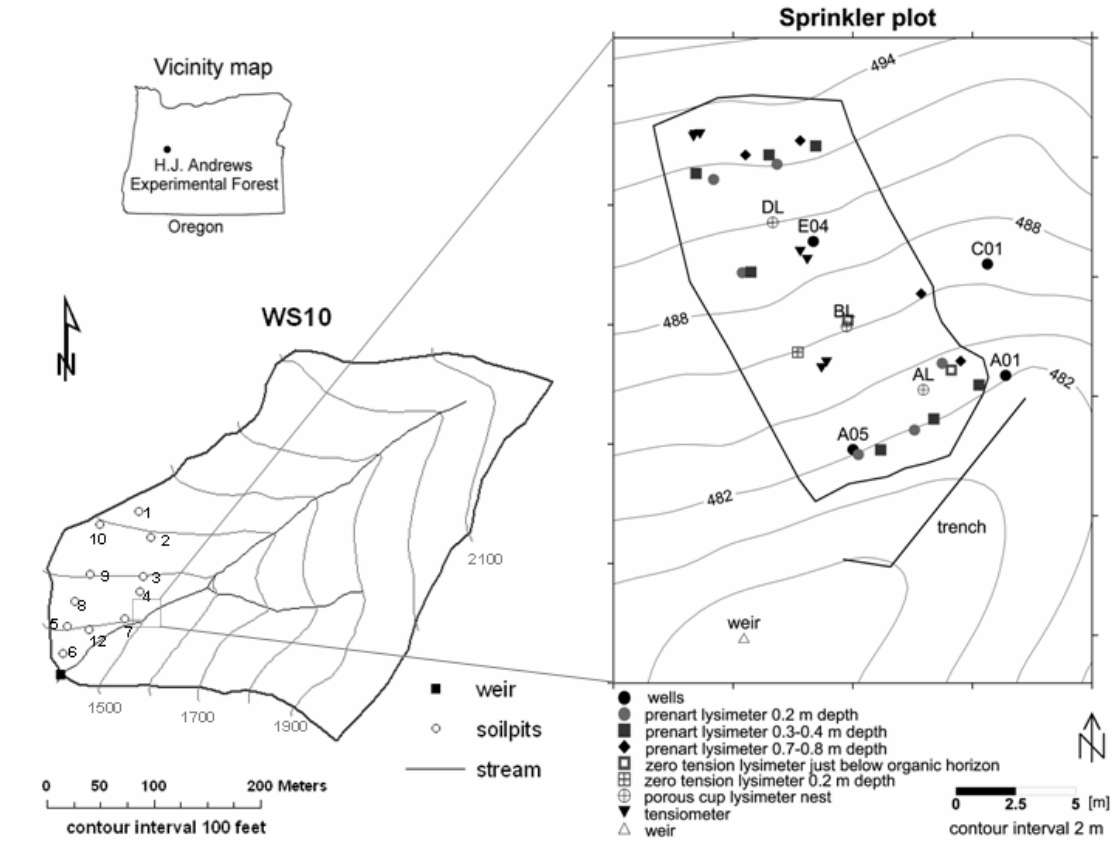

Figure 5.1. Map of WS10 with soilpits and sprinkler area, and sprinkler area with instrumentation.

Table 5.1. Mean (±SE) of soil extracted DOC, DON and DIN at the dry and sprinkler plot before the sprinkler experiment (day 203), at individual and for total sample days throughout the sprinkler experiment (day 215-236). Significant differences (Wilcoxon ranksum test) in soil extracted DOC, DON and DIN between the sprinkler and dry plot are marked with an asterisk.

Julian day	*Dry plot*			*Sprinkler plot*		
	DOC-[C] [mg kg^{-1})	DON-[N] [mg kg^{-1})	DIN-[N] [mg kg^{-1})	DOC-[C] [mg kg^{-1})	DON-[N] [mg kg^{-1})	DIN-[N] [mg kg^{-1})
203	238.8 (60.5)	4.4 (0.7)	5.0 (0.4)	364.1 (75.2)	5.3 (0.7)	7.9 (1.7)
215	135.8 (16.3)	2.3 (0.3)**	1.3 (0.1)**	81.4 (18.4)	1.1 (0.2)	2.2 (0.3)
222	116.5 (15.7)	3.3 (0.6)	1.8 (0.5)*	86.9 (8.2)	2.1 (0.4)	3.2 (0.6)
229	64.2 (8.8)	1.7 (0.2)	1.1 (0.2)***	70.8 (11.4)	1.8 (0.2)	3.9 (0.4)
236	119.7 (37.8)*	3.1 (1.0)**	2.1 (0.7)	63.5 (4.1)	1.2 (0.4)	2.4 (0.4)
215-236	109 (8.6)**	2.6 (0.2)***	1.6 (0.2)***	75.6 (5.8)	1.6 (0.2)	3.0 (0.2)

* $p < 0.05$
** $p < 0.01$
*** $p < 0.001$
*** $p < 0.0001$

Table 5.2. Mean (±SE) of soil extracted DIN from incubated soil from the dry and sprinkler plot before the sprinkler experiment (day 203), at individual and for total sample days throughout the sprinkler experiment (day 215-236).

Julian day	*Dry plot*	*Sprinkler plot*
	DIN-[N] [mg kg^{-1})	DIN-[N] [mg kg^{-1})
203	56.6 (7.8)	51.9 (10.3)
215	5.9 (2.0)	6.3 (2.3)
222	8.9 (1.8)	8.9 (2.4)
229	6.6 (2.3)	7.6 (3.6)
236	7.1 (2.3)	9.7 (2.0)
215-236	7.1 (1.0)	8.1 (1.3)

Table 5.3. Mean (± SD) of DOC, DON, NH_4-N, NO_3-N concentrations and DOC:DON during the sprinkler experiment.

	DOC [mg l^{-1}]	DON [mg l^{-1}]	NH_4-N [mg l^{-1}]	NO_3-N [mg l^{-1}]	DON:TDN	DOC: DON
Irrigation water	4.4 (0.6)	0.14 (0.07)	0.018 (0.016)	0.006 (0.003)	0.85 (0.07)	38 (16)
Througfall*	1.4 (0.5)	0.07 (0.04)	0.008 (0.008)	0.008 (0.008)	0.75 (0.21)	25 (21)
Organic horizon	7.2 (5.4)	0.30 (0.17)	0.052 (0.068)	0.034 (0.057)	0.78 (0.25)	25 (11)
Shallow lysimeter	5.9 (5.3)	0.22 (0.13)	0.027 (0.029)	0.014 (0.014)	0.85 (0.10)	28 (24)
Middle lysimeter	6.3 (4.2)	0.21 (0.23)	0.029 (0.038)	0.014 (0.012)	0.78 (0.22)	44 (36)
Deep lysimeter	2.4 (1.2)	0.13 (0.13)	0.030 (0.033)	0.011 (0.008)	0.75 (0.21)	32 (36)
Groundwater seep	5.3 (1.0)	0.09 (0.04)	0.021 (0.017)	0.011 (0.008)	0.75 (0.13)	59 (17)
Transient groundwater	6.8 (1.8)	0.45 (0.29)	0.319 (0.400)	0.373 (0.420)	0.47 (0.22)	23 (18)
Lateral subsurface flow	4.6 (0.9)	0.11 (0.05)	0.014 (0.012)	0.006 (0.004)	0.83 (0.13)	54 (49)

* Throughfall of this site during Fall 2004 - Summer 2005 as a comparison to irrigation water of sprinkler experiment

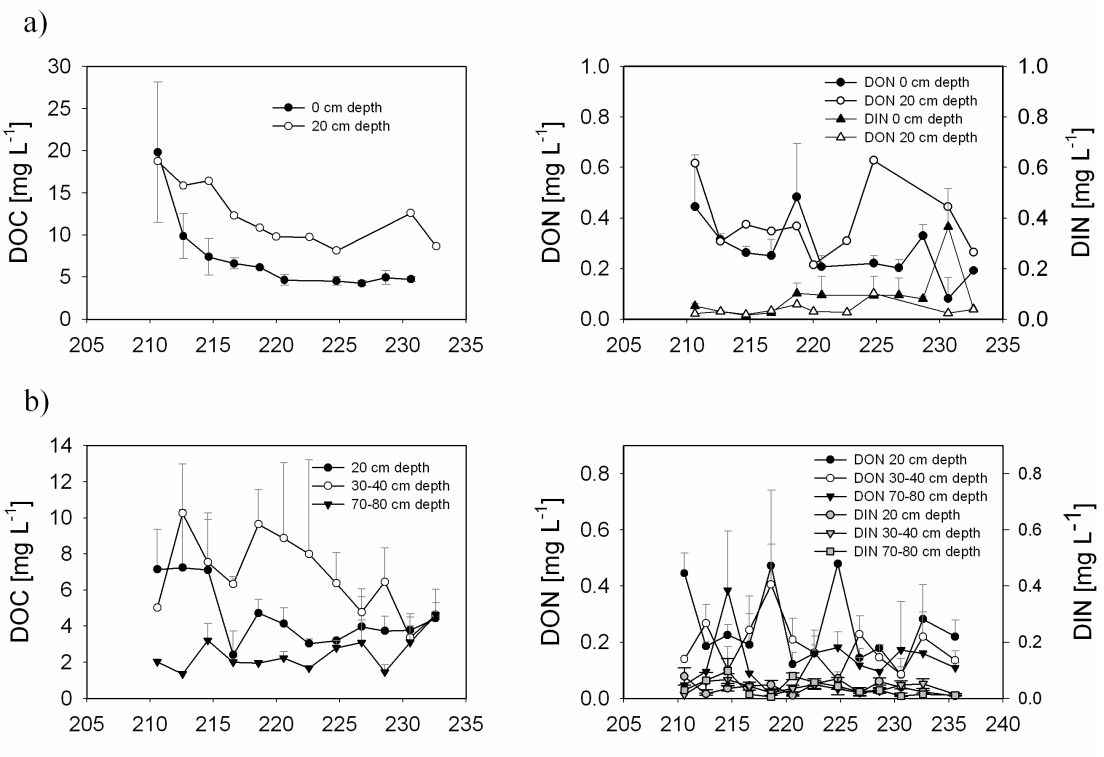

Figure 5.2. Solute concentrations during the sprinkler experiment of a) DOC in the organic horizon and zero tension lysimeter at 20 cm depth, b) DON and DIN in the organic horizon and zero tension lysimeter at 20 cm depth, c) DOC in tension lysimeters, and d) DON and DIN in tension lysimeters.

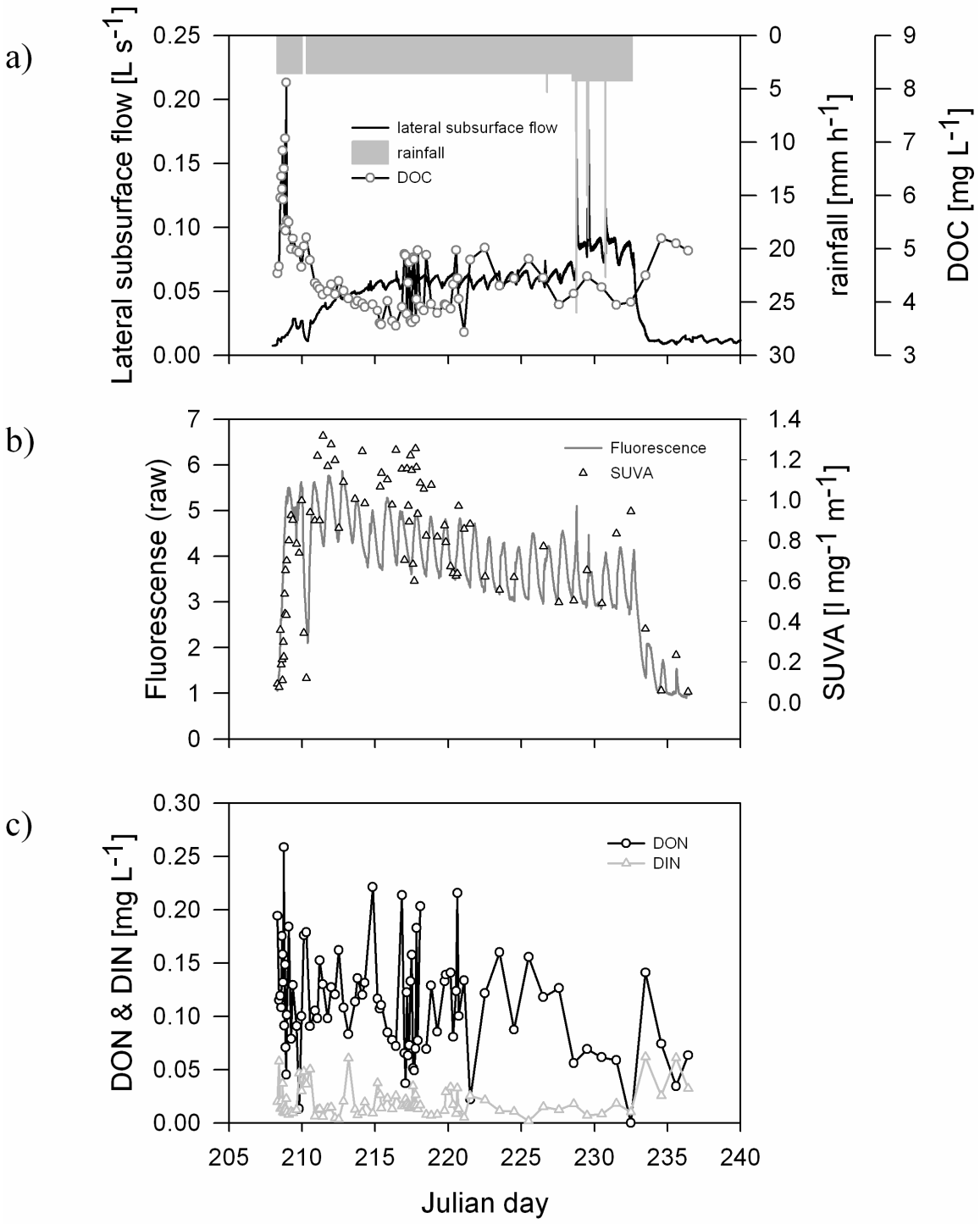

Figure 5.3. Patterns during the sprinkler experiment of a) Rainfall, lateral subsurface flow, DOC concentrations, b) fluorescence, and c) DON and DIN concentrations.

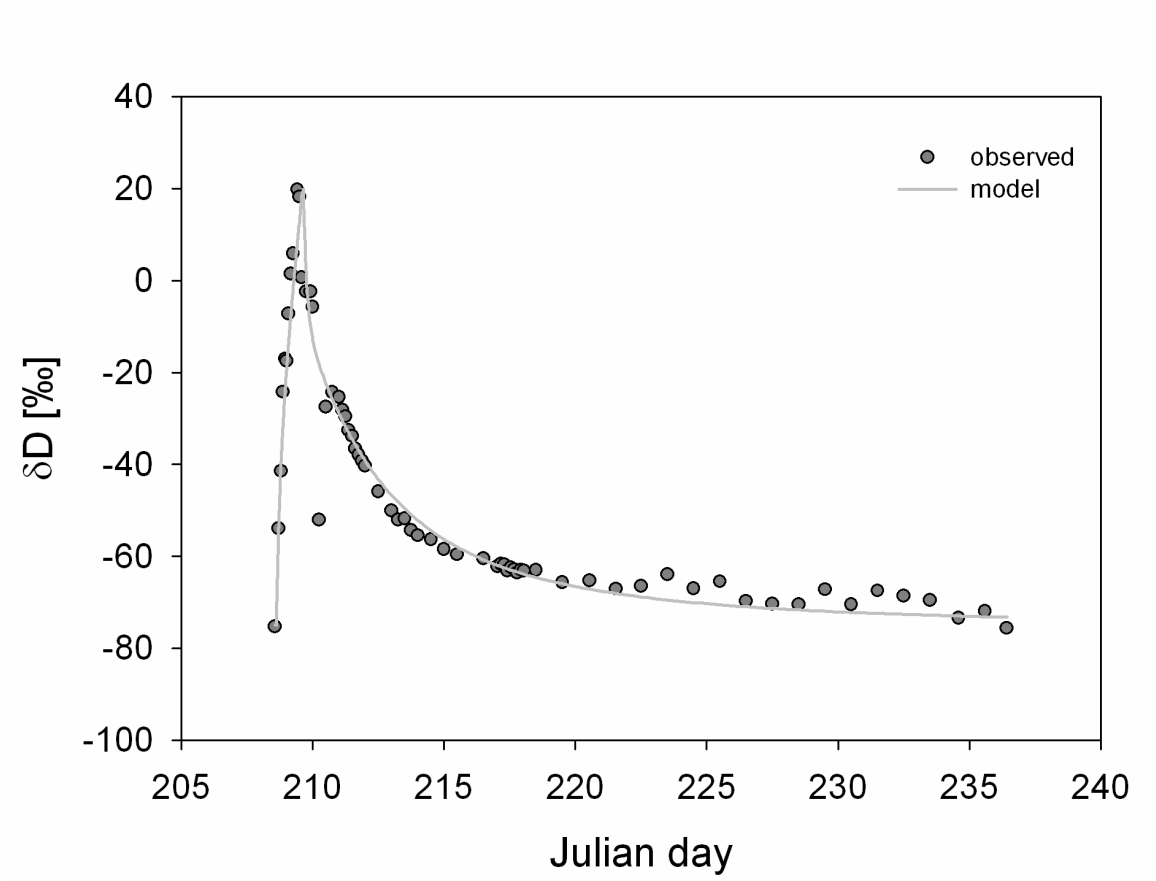

Figure 5.4. dD breakthrough in lateral subsurface flow and modeled dD.

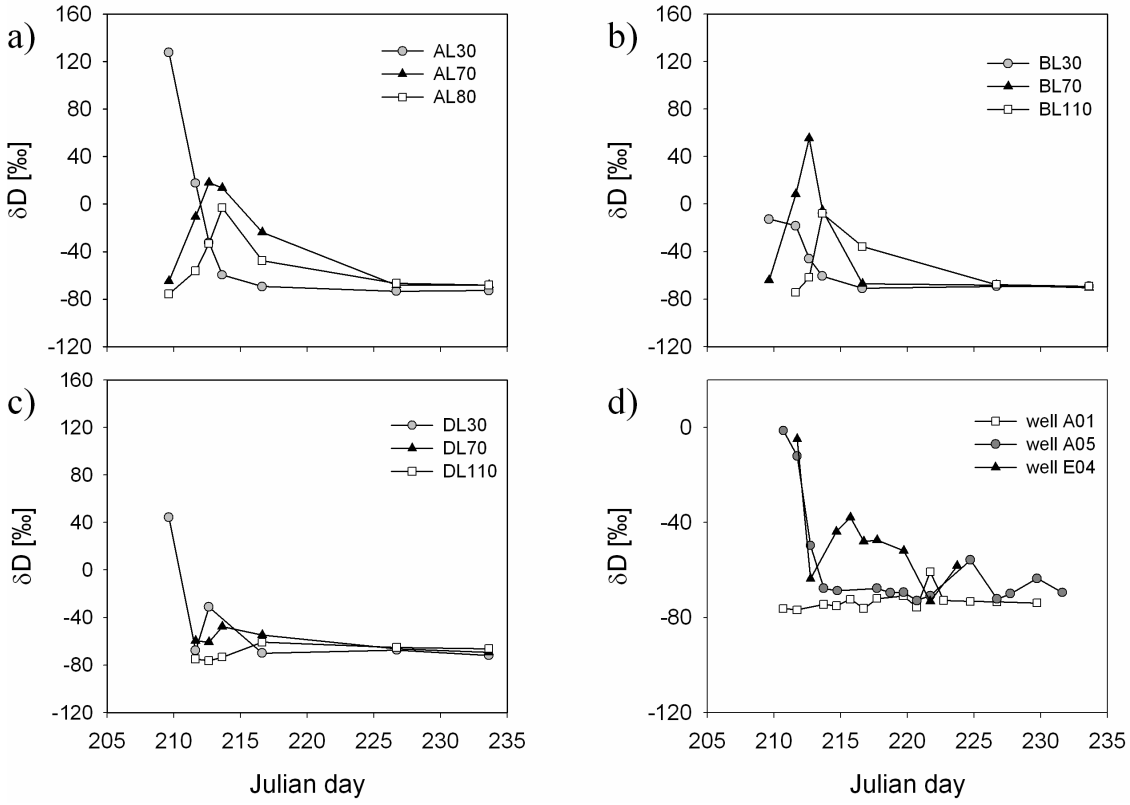

Figure 5.5. Soil water dD breakthrough curves at a) tension lysimeter nest AL, b) tension lysimeter nest BL, c) tension lysimeter nest DL, and d) wells A01, A05 and E04

Table 5.4. Calculated velocities based on timing of dD peak.

Location	Peak dD	Response time [h] to dD input	Depth [m]	Velocity [mm h^{-1}] based on dD peak
A05	-1.3	50.8	0.44	8.7
E04	-4.8	75.8	1.24	16.4
AL30	127.6	25.0	0.3	12.0
BL30	-12.7	25.0	0.3	12.0
DL30	44.3	25.0	0.3	12.0
AL70	17.9	97.0	0.7	7.2
BL70	55.3	97.0	0.7	7.2
DL70	-47.7	121.0	0.7	5.8
AL80	-3.0	121.0	0.8	6.6
BL110	-7.9	121.0	1.1	9.1
DL110	-60.8	193.0	1.1	5.7
ZTL20_1	16.2	25.0	0.2	8.0

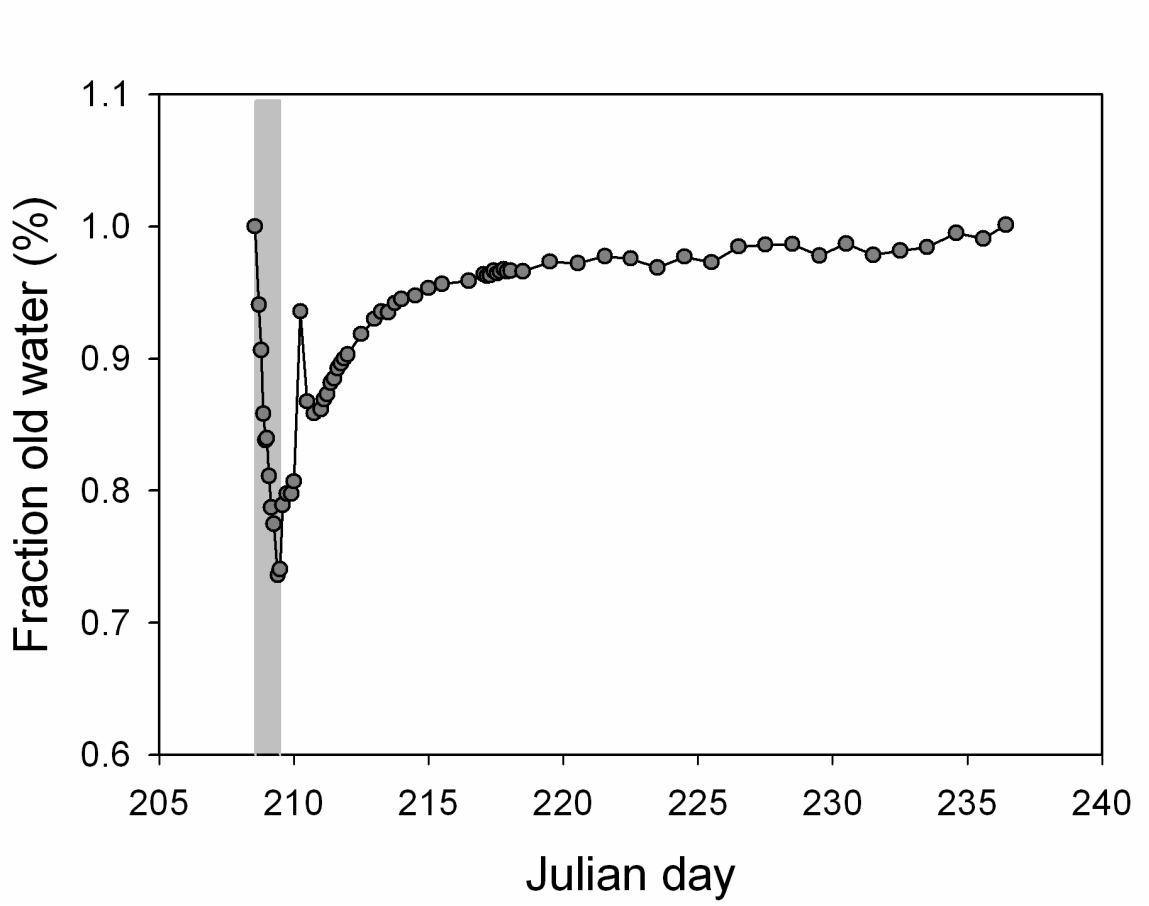

Figure 5.6. Fraction of old water during the sprinkler experiment based on a 2-component mixing model. Gray area represents application of labeled sprinkler water.

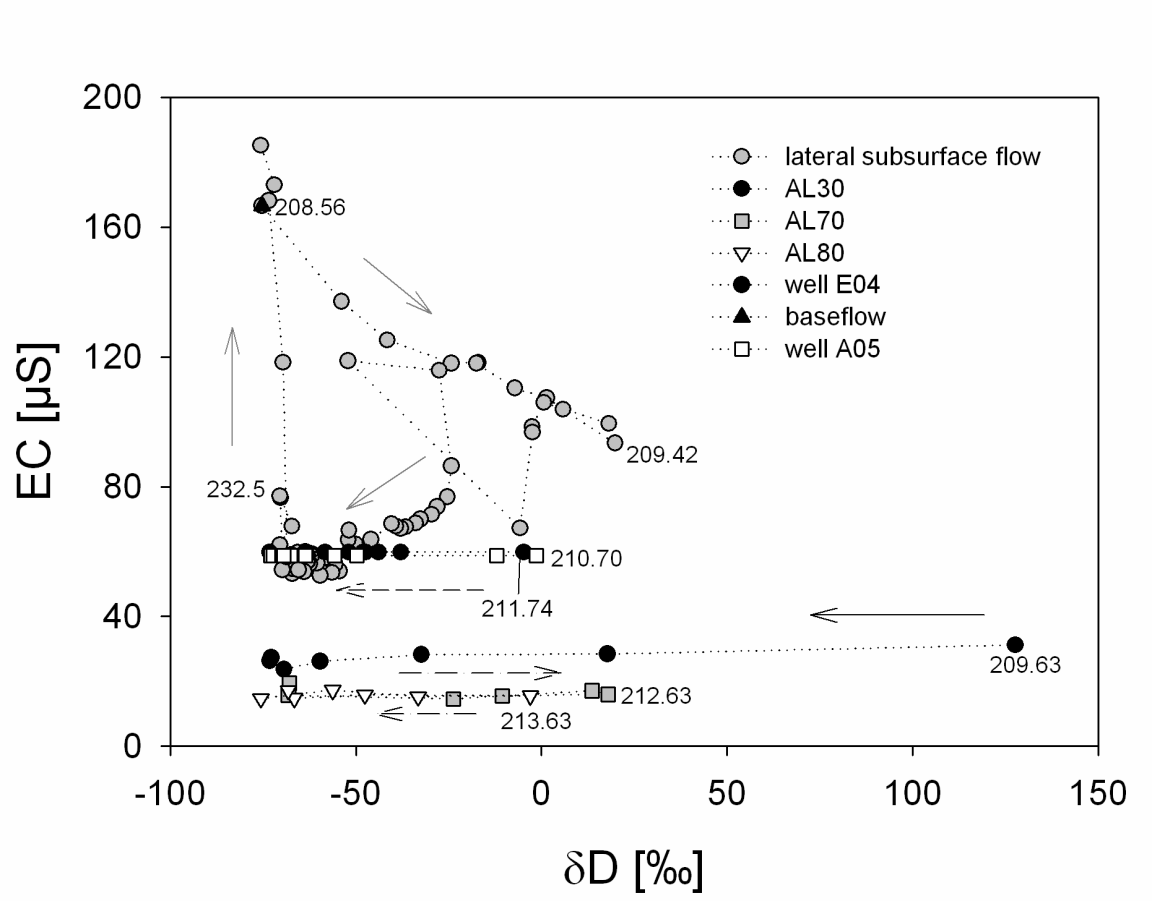

Figure 5.7. Bivariate mixing plot of dD against EC of lateral subsurface flow and possible sources of lateral subsurface flow. Arrows indicate direction of time.

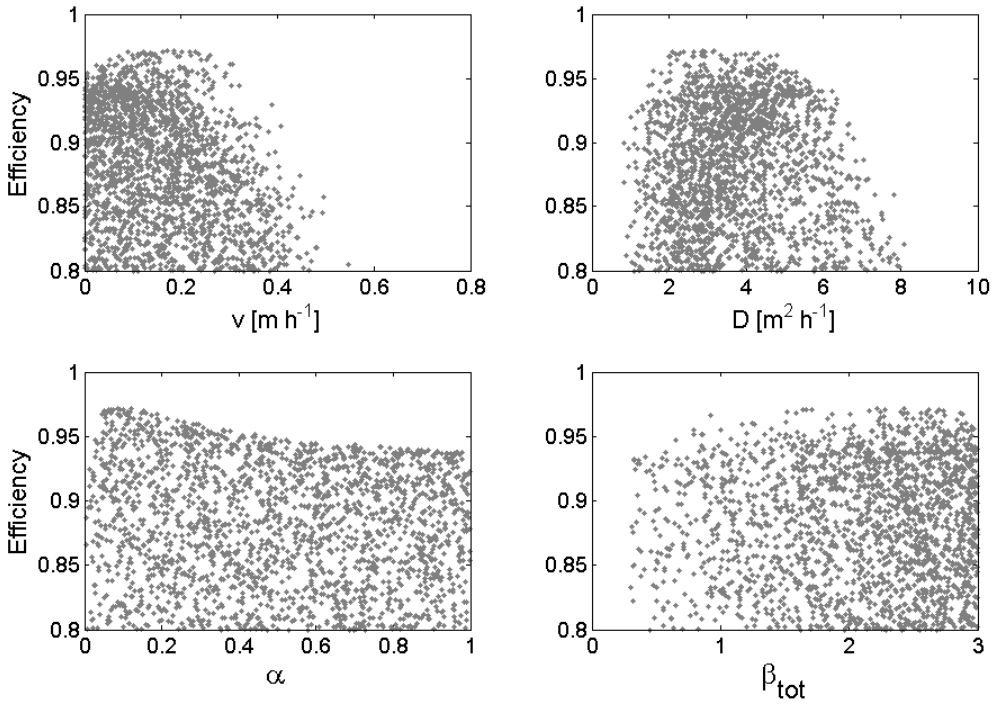

Figure 5.8. Results of Monte Carlo simulations of modeling dD breakthrough of lateral subsurface flow.

Table 5.5. Modeled parameters for the BTC in lateral subsurface flow.

Parameter	Best fit	Uncertainty range
v [m h^{-1}]	0.19	0.003-0.45
D [m^2 h^{-1}]	2.43	0.8-7.2
b_{tot} [ ]	2.43	0.31-3.00
a [h^{-1}]	8.48 10^{-2}	3.89 10^{-3}-1.00
L [m]	11.65	
t_{adv} [h]	63.0	
t_a [h]	11.8	
Da_1 [ ]	18	
E	0.97	
number of behavioral models	1014	

6 Conclusions

6.1 Conclusions

This thesis is a direct response to recent discussion in the hydrological literature that has called for the need for process understanding through field observations (Sidle, 2006), getting the right answers for the right reasons by combining field observations and theory that lead to mechanistically plausible and quantitatively realistic conceptual models (Kirchner, 2006; Sidle, 2006). It responds to specific calls by Burns (2005) to improve our understanding of nutrient flushing by considering both biogeochemical and hydrological controls in our conceptualizations. This study has improved our process understanding of the dominant controls on nutrient flushing at the hillslope and catchment scale by combining hydrometric, natural and isotopic tracer approaches and detailed measurements of soluble nutrients in soil water, groundwater, subsurface flow and streamwater.

Chapter 2 demonstrated using tree regression analysis that there were three dominant subsurface flow behaviors: (1) a disconnection between rainfall and subsurface flow, characterized by soil moisture deficits and filling of storage, (2) a transitional phase, where the unsaturated zone damped the rainfall signal and (3) a wet phase, where groundwater and matric potential were in a semi-steady-state condition, and subsurface flow responded immediately to rainfall. Matric potential values during subsurface flow behavior 3 were mostly in the highly non-linear portion of the unsaturated hydraulic function zone—where the unsaturated hydraulic conductivity increased greatly with small decreases in soil matric potential. This was not the case for subsurface flow behavior 2. This suggested that the different response of

subsurface flow between behavior 2 and 3 was largely controlled by unsaturated zone dynamics. Wetting front velocities were significantly correlated to mean rainfall intensity, and were explained by Darcy-Richard's equation. These observations resulted in a detailed conceptual model of subsurface flow behavior.

Chapter 3 showed that DON was the dominant form of total dissolved organic nitrogen (TDN) in all sampled solutions, except for transient groundwater where dissolved inorganic nitrogen (DIN) was the dominant form. Both the organic horizon/shallow soil water and transient groundwater were characterized by high DOC and N concentrations and SUVA values, indicating a strong connection between the organic horizon and transient groundwater without significant soil matrix interaction. This result was supported by an unsaturated flow vector analysis in chapter 4 that showed predominantly vertical unsaturated flow during the December 2004 and May 2005 storm events. This interpretation was also supported by the sprinkler experiment findings where relatively fast breakthrough of deuterium occurred in transient groundwater. Dry antecedent moisture (lack of prior flushing) and wet antecedent precipitation conditions (rewetting of the organic horizon) resulted in high flow weighted and peak DOC and DON concentrations in lateral subsurface flow and stream water during storm events. DOC and DON concentrations in stream water and lateral subsurface flow were significantly lower during the wet period compared to the transition period during rain driven conditions. This implies a supply-limited source at the seasonal time scale. Supply-limited DOC and DON in the organic horizon was also found during the December and May storm events in chapter 4. SUVA was

always lower in subsurface flow compared to stream water. This suggested that transient groundwater (with high SUVA) mixed differently with seepage groundwater (with low SUVA) at the hillslope and catchment scale, even when subsurface flow and stream water were 'in sync' with respect to DOC and N during the wet period. During the transition period, higher DOC and DON concentrations were observed in stream water compared to lateral subsurface flow during rain-driven conditions. This was mainly attributed to in-stream processes based on low runoff ratios of lateral subsurface flow and stream water. This notwithstanding, a difference in mixing of seepage groundwater and transient groundwater based on SUVA measurements could not be ruled out as a secondary control.

Hydrometric data, natural tracers and biogeochemical solutes measured in organic horizon, shallow and deep soilwater, groundwater (seepage and transient) and lateral subsurface flow and stream water during the December 2004 and May 2005 storm event allowed a mechanistic assessment of the flushing mechanism at the catchment scale. Based on these data, end-member mixing analysis and an unsaturated flow vector analysis, two out of three possible flushing mechanisms were rejected and vertical transport of nutrients, by 'preferential' flow to the soil-bedrock interface and then laterally downslope with a limited supply of DOC and DON in the organic horizon was accepted. Furthermore, SUVA measurements revealed that the contribution of seep groundwater/deep soilwater was higher on the falling limb compared to the rising limb of the hydrograph.

In chapter 5, the combination of isotopic, biogeochemical and internal physical measurements during a long duration steady state sprinkler experiment, enabled a mechanistically assessment of the double paradox at the hillslope scale. The experiment revealed two dominant flowpaths: vertical flow through the unsaturated zone, and rapid lateral subsurface flow. 1-D transport modeling of the deuterium (dD) breakthrough in lateral subsurface flow showed a small mobile water zone and a large immobile zone, mass transfer between these two zones and dispersive mixing. These three processes resulted in rapid mobilization of old water in lateral subsurface flow. Hydrometric data and a bivariate plot of dD against EC showed that the fast initial dD breakthrough was derived mainly from a shallow soil source (~30 cm). Later during the sprinkler experiment, deeper flowpaths were invoked. DOC in the organic horizon was supply limited and this controlled, in combination with vertical and lateral mobile flowpaths, the observed variable DOC chemistry in lateral subsurface flow. These findings supported a new conceptual model that explains rapid mobilization of old water but variable runoff chemistry at the hillslope scale.

The overall thesis findings resulted in a conceptual model of subsurface flow behavior and a mechanistic assessment of DOC and N flushing at the hillslope and catchment scale. This research clearly demonstrated through measuring hydrometric variables and (natural) tracers during natural storm events and a controlled hillslope scale sprinkler experiment that simple 2-D representations of flushing is inadequate; where water flowpaths intersect the distinct vertical soil solution chemistry profiles to explain DOC and N stream patterns. Natural storm events revealed the mixing of

different water sources during storm events. This result was mainly based on SUVA used as a tracer to “fingerprint” sources. In addition, SUVA indicated differences in mixing of transient and seepage groundwater at the hillslope and catchment scale. Furthermore, this study challenges the assumption of unlimited supply of DOC and DON during storm events, an important feature of the flushing mechanism proposed elsewhere. This research also suggested limited supply of DOC and DON at seasonal scales controlled by antecedent wetness conditions and re-wetting of the organic horizon. In a quantitative way, the dominant flowpaths and mobile vs. immobile flowpaths were identified during a sprinkler experiment that supported findings of natural storm events (i.e. mainly vertical ‘preferential’ flow based on an unsaturated flow direction analysis and high DOC and N concentrations and SUVA values in transient groundwater). Lastly, transport modeling of the deuterium breakthrough curve during the sprinkler experiment with the advection-dispersion first order mass-transfer equation showed mass transfer between a small mobile zone and a large immobile zone. Dispersive mixing was also high. These processes resulted in the rapid mobilization of old water. In addition, the two dominant flowpaths in combination with supply-limited DOC in the organic horizon/shallow layer explained variable runoff chemistry of subsurface flow. These results help resolved the double paradox of rapid mobilization of old water but variable runoff chemistry at the study site.

6.2 References

Burns, D., (2005),What do hydrologists mean when they use the term flushing?, *Hydr. Processes, 19,* 1325–1327.

Sidle, S. (2006), Field observations and process understanding in hydrology: essential components in scaling, *Hydrol. Processes, 20*, 1439–1445.

Kirchner, J. W. (2003), A double paradox in catchment hydrology and geochemistry, *Hydrol. Processes, 17*, 871-874.

Kirchner, J. W. (2006), Getting the right answers for the right reasons: Linking measurements, analyses, and models to advance the science of hydrology, *Water Resour. Res., 42*, W03S04, doi:10.1029/2005WR004362.

Kirchner, J. W., X. Feng and C. Neal (2001), Catchment-scale advection and dispersion as a mechism for fractal scaling in stream tracer concentrations, *J. Hydr., 254*, 82-101.

7 Bibliography

Anderson, S. P., W. E. Dietrich, D. R. Montgomery, M. E. Conrad, and K. Loague (1997a), Subsurface flow paths in a steep, unchanneled catchment., *Water Resour. Res., 33*, 2637-2653.

Anderson, S. P., W. E. Dietrich, R. Torres, D. R. Montgomery and K. Loague (1997b), Concentration-discharge relationships in runoff from a steep, unchanneled catchment, flow, *Water Resour. Res., 33*, 211-225.

Appelo, C. A. J., and A. Willemsen (1987), Geochemical Calculations and Observations on Salt Water Intrusions, I.A. Combined Geochemical/Mixing Cell Model, *J. of Hydr., 94*, 313-330.

Bejat, L., E. Perfect, V. L. Quisenberry, M. S. Coyne and G. R. Haszler (2000), Solute Transport as Related to Soil Structure in Unsaturated Intact Soil Blocks, *Soil Sci. Soc. Am. J., 64*, 818–826.

Bernal, S., A. Butturini and F. Sabater (2006), Inferring nitrate sources through end member mixing analysis in an intermittent Mediterranean stream, *Biogeochemistry, 81*, 269–289.

Bernal, S., Butturini, A. and F. Sabater (2005), Seasonal variations of dissolved nitrogen and DOC:DON ratios in an intermittent Mediterranean stream, *Biogeochemistry, 75*, 351–372.

Beven,, K. J. (2006), Benchmark Papers in Hydrology, Streamflow generation processes, Selection, Introduction and Commentary by Keith J. Beven, IAHS Benchmark Papers in Hydrology Series, Editor: J. J. McDonnell.

Biggar, J.W., and D.R. Nielsen (1976), Spatial variability of the leaching characteristics of a field soil. *Water Resour. Res. 12*, 78–84.

Birch, H. F. (1958), The effect of soil drying on humus decomposition and nitrogen availability, *Plant and soil, 10*, 9-31.

Bishop, K., J. Seibert, S. Kölhler, and H. Laudon (2004), Resolving the double paradox of rapidly old water with variable responses in runoff chemistry, *Hydrol. Processes, 18*,185-189.

Bonell, M. (1998), Selected challenges in runoff generation research in forests from the hillslope to headwater drainage basin scale, *Journal of the American Water Resources Association, 34*, 765-785.

Boyer, E. W., G. M. Hornberger, K. E. Bencala, and D. M. McKnight (1997), Response characteristics of DOC flushing in an Alpine catchment, *Hydrol. Processes, 11*, 1635-1647.

Breiman, L., J. Friedman, R. Olshen and C. Stone (1984), *Classification and Regression Trees*, Wadsworth, Belmont, Calif. Richland, Wash.

Brown, V. A., J. J. McDonnell, D. A. Burns, and C. Kendall (1999), The role of event water a rapid shallow flow component and catchment size in summer stormflow, *J. Hydrol., 217*, 171– 190.

Brusseau, M. L. (1992), Nonequilibrium transport of organic chemicals: The impact of pore water-velocity, *J. Contam. Hydrol.*, 24, 185-204.

Buffam, I., J. N. Galloway, L. K. Blum and K. J. McGlathery (2001), A stormflow/baseflow comparison of dissolved organic matter concentrations and bioavailability in an Appalachian stream, *Biogeochemistry, 53*, 269-306.

Buresh, R. J. and W. H. Jr. Patrick (1978), Nitrate reduction to ammonium in anaerobic soil, *Soil Sci. Soc. Am. J., 42*, 913–918.

Burns, D. A., J. J. McDonnell, R. P. Hooper, N. E. Peters, J. E. Freer, C. Kendall, and K. J. Beven (2001), Quantifying contributions to storm runoff through end-member mixing analysis and hydrologic measurements at the Panola Mountain Research Watershed (Georgia, USA), *Hydrol. Processes, 15*, 1903–1924

Burns, D., (2005),What do hydrologists mean when they use the term flushing?, *Hydr. Processes, 19*, 1325–1327.

Buttle, J. M., S. W. Lister and A. R. Hill (2001), Controls on runoff components on a forested slope and implications for N transport, *Hydrol. Processes, 15*, 1065–1070.

Cabrera, M. L. (1993), Modeling the Flush of Nitrogen Mineralization Caused by Drying and Rewetting Soils, *Soil Sci. Soc. Am. J., 57*, 63-66.

Cairns, M.A. and K. Lajtha (2005), Effects of Succession on Nitrogen Export in the West-Central Cascades, Oregon, *Ecosystems, 8*, 583-601.

Campbell, G.S., (1974), A simple method for determining unsaturated conductivity from moisture retention data, *Soil Science, 117*, 311-314.

Chin Y. P., G. R. Aiken and E. O'Loughlin (1994), Molecular weight, polydispersivity, and spectroscopic properties of aquatic humic substances, *Environ. Sci. Technol. 28*, 1853–1858.

Christopherson, N., and R. P. Hooper (1992), Multivariate analysis of stream water chemical data: The use of principal component analysis for the end-member mixing problem, *Water Resour. Res., 28*, 99–107.

Cirmo, C. P., and J. J. McDonnell, (1997), Linking the hydrologic and biochemical controls of nitrogen transport in near-stream zones of temperate-forested catchments: A review, *J. Hydrol., 199*, 88-120.

Coats, K. H., and B. D. Smith (1964), Dead end pore volume and dispersion in porous media, *Soc. Pet. Eng. J., 4*, 73-84.

Collins, R., A. Jenkins and M. Harrow (2000), The contribution of old and new water to a storm hydrograph determined by tracer addition to a whole catchment, *Hydr. Processes, 14*, 701-711.

Compton, J. E., R. M. Church, S. T. Larned and W. E. Hogsett (2003), Nitrogen export from forested watersheds in the Oregon coast range: The role of N_2-fixing Red Alder, *Ecosystems, 6*, 773-785.

Cooper, R., V. Thoss and H. Watson (2007), Factors influencing the release of dissolved organic carbon and dissolved forms of nitrogen from a small upland headwater during autumn runoff events, *Hydrol. Processes, 21*, 622–633

Creed, I. F., L. E. Band, N. W. Foster, I. K. Morrison, J. A. Nicolson, R. S. Semkin, and D. S. Jeffries (1996), Regulation of nitrate-N release from temperate forests: A test of the N flushing hypothesis, Water *Resour. Res., 32*, 3337–

3354.

D.S. Jeffries (1996), Regulation of nitrate-N release from temperate forests: A test of the N flushing hypothesis, *Water Resour. Res., 32*, 3337-3354.

De Hoog, F. R., Knight, J. H., and Stokes, A. N. (1982). An improved method for numerical inversion of Laplace transforms. *S.I.A.M. J. Sci. and Stat. Comput., 3*, 357-366.

Dunne, T., and R. D. Black (1970), An experimental investigation of runoff production in permeable soils, *Water Resour. Res*., *6*, 478– 490.

Evans, C., and T. D. Davies (1998), Causes of concentration/discharge hysteresis and its potential as a tool for analysis of episode hydrochemistry, *Water Resour. Res., 34*, 129-137.

Gaskin, J. W., J. W. Dowd, W. L. Nutter and W. T. Swank (1989), Vertical and Lateral Components of Soil Nutrient Flux in a Hillslope, *J. Environ. Qual., 18*: 403-410.

Gelhar, L. W., C. Welty and K. R. Rehfeldt (1992), A critical review of data on field-scale dispersion in aquifers, *Water Resour. Res., 28*, 1955-1974.

Graham, C. B., W. J. van Verseveld, H. B. Barnard and J. J. McDonnell (in prep), Experimental Closing of the Water Balance.

Grieve I. C. (1991), A model of dissolved organic carbon concentration in soil and stream waters, *Hydrol. Processes 5*, 301–307.

Griffioen, J. W., D. A. Barry, and J.-Y. Parlange (1998), Interpretation of two-region model parameters, *Water Resour. Res., 34*, 373-384.

Haga, H., Y. Matsumoto, J. Matsutani, M. Fujita, K. Nishida, and Y. Sakamoto (2005), Flow paths, rainfall properties, and antecedent soil moisture controlling lags to peak discharge in a granitic unchanneled catchment, *Water Resour. Res*., *41*, W12410, doi:10.1029/2005WR004236.

Hagedorn, F., P. Schleppi, P. Waldner, and H. Fluhler (2000), Export of dissolved organic carbon and nitrogen from Gleysol dominated catchments—The significance of water flow paths, *Biogeochemistry, 50*, 137–161.

Haggerty, R., A. McKenna, and L. C. Meigs (2000), On the late-time behavior of tracer test breakthrough curves, *Water Resour. Res., 36*, 3467-3479.

Haggerty, R., C. F. Harvey, C. Freiherr von Schwerin, and L. C. Meigs (2004), What controls the apparent timescale of solute mass transfer in aquifers and soils? A comparison of experimental results, *Water. Resour. Res., 40*, W01510, doi:10.1029/2002WR001715.

Harr, R. D., (1977), Water flux in soil and subsoil on a steep forested slope, *J. Hydrol., 33*, 37-58.

Harvey, C. F., and S. M. Gorelick (1995), Temporal moment-generating equations: Modeling transport and mass transfer in heterogeneous aquifers, *Water Resour. Res., 37*, 1129-1142.

Hedin, L. O., J. C. von Fischer, N. E. Ostrom, B. P. Kennedy., M. G. Brown and G. P. Robertson (1998), Thermodynamic constraints on nitrogen transformations and other biogeochemical processes at soil-stream interfaces, *Ecology, 79*, 684-703.

Hedin, L. O., J. J. Armesto and A. H. Johnson (1995), Patterns of nutrient loss from unpolluted, old-growth temperate forests: evaluation of biogeochemical theory, *Ecology, 76,* 493-509.

Hendrickson, G. E., and R. A. Kreiger (1964), Geochemistry of natural waters of the Blue Grass region, Kentucky, *U.S. Geol. Surv. Water Supply Pap. 1700.*

Hewlett, J. D., and A. R. Hibbert (1963), Moisture and energy conditions within a sloping soil mass during drainage, *Journal of Geophysical Research, 68,* 1081-1087.

Hewlett, J. D., J. C. Fortson and G. B. Cunningham (1977), The effect of rainfall intensity on storm flow and peak discharge from forest land, *Water Resour. Res., 13,* 259-266.

Hill, A. R., (1993), Nitrogen dynamics of storm runoff in the riparian zone of a forested watershed, *Biogeochemistry, 20,* 19-44.

Hill, A. R., W. A. Kemp, J. M. Buttle, and D. Goodyear (1999), Nitrogen chemistry of subsurface storm runoff on forested Canadian Shield hillslopes, *Water Resour. Res., 35,* 811 –821.

Hinton M. J., S. L. Schiff and M. C. English (1997), The significance of storms for the concentration and export of dissolved organic carbon from two Precambrian Shield catchments, *Biogeochemistry, 36*: 67–88.

Hollenbeck, K. J. (1998) INVLAP.M: A matlab function for numerical inversion of Laplace transforms by the Hoog algorithm, http://wwww.isva.dtu.dk/staff/karl/invlap.htm

Hood, E., D. M. McKnight and M. W. Williams (2003), Sources and chemical character of dissolved organic carbon across an alpine/subalpine ecotone, Green Lakes Valley, Colorado Front Range, United States, *Water Resour. Res., 39(7),* 1188, doi:10.1029/2002WR001738.

Hood, E., M. N. Gooseff, and S. L. Johnson (2006), Changes in the character of stream water dissolved organic carbon during flushing in three small watersheds, Oregon, *J. Geophys. Res., 111,* G01007, doi:10.1029/2005JG000082.

Hood, E., M. W. Williams and D. M. McKnight (2005), Sources of dissolved organic matter (DOM) in a Rocky Mountain stream using chemical fractionation and stable isotopes, *Biogeochemistry, 74,* 231-255.

Hooper R. P, N. Christophersen and N. E. Peters (1990), Modelling streamwater chemistry as a mixture of soilwater endmembers—an application to the Panola Mountain catchment, Georgia, U.S.A., *J. Hydr., 116,* 321–343.

Hooper, R. B. (2001), Applying the scientific method to small catchment studies: a review of the Panola Mountain experience, *Hydr. Processes, 15,* 2039–2050

Hooper, R. P., (2003), Diagnostic tools for mixing models of stream water chemistry, *Water Resour. Res., 39(3),* 1055, doi:10.1029/2002WR001528.

Hornberger, G. M., K. E. Bencala, and D. M. McKnight (1994), Hydrological controls on dissolved organic carbon during snowmelt in the Snake River near Montezuma, Colorado, *Biogeochemistry, 25,* 147– 165.

Hursh, C. R., and E. F. Brater (1941), Separating storm-hydrographs from small

drainage-areas into surface- and subsurfaceflow, *Transactions of the American Geophysical Union, 3,* 863–871.

Inamdar, S. P., and M. J. Mitchell (2006), Hydrological and topographical controls on storm-event exports of dissolved organic carbon (DOC) and nitrate across catchment scales, *Water Resour. Res., 42*, W03421, doi:10.1029/2005WR004212.

Inamdar, S. P., O'Leary, N., Mitchell, M. J., and J. T. Riley (2006), The impact of storm events on solute exports from a glaciated forested watershed in western New York, USA, *Hydrol. Process. 20,* 3423–3439

Iorgulescu, I., and K. J. Beven (2004), Nonparametric direct mapping of rainfall-runoff relationships: An alternative approach to data analysis and modeling?, *Water Resour. Res.*, 40, W08403, doi:10.1029/2004WR003094.

Iverson R.M. (2000), Landslide triggering by rain infiltration, *Water Resour. Res., 36,* 1897-1910.

Jackson, C. R., (1992), Hillslope infiltration and lateral downslope unsaturated flow, *Water Resour. Res., 28,* 2533-2539.

James, A. L., and N. T. Roulet (2006), Investigating the applicability of end-member mixing analysis (EMMA) across scale: A study of eight small, nested catchments in a temperate forested watershed, *Water Resour. Res., 42,* W08434, doi:10.1029/2005WR004419.

James, M. E., (1978), Rock weathering in the central western Cascades, M.S., University of Oregon, Eugene.

Jardine, P. M., N. L. Weber and J. F. McCarthy (1989a), Mechanisms of dissolved organic carbon adsorption by soil, *Soil Sci. Soc. Am. J., 53,*1378–1385.

Jardine, P.M., G.V. Wilson, and R.J. Luxmoore (1990), Unsaturated solute transport through a forest soil during rain events, *Geoderma,* 46:103–118.

Jones, J. P., E. A. Sudicky, A. E. Brookfield, and Y.-J. Park (2006), An assessment of the tracer-based approach to quantifying groundwater contributions to streamflow, *Water Resour. Res., 42,* W02407, doi:10.1029/2005WR004130.

Kaiser, K., and G. Guggenbergers (2005), Storm flow flushing in a structured soil changes the composition of dissolved organic matter leached into the subsoil, *Geoderma, 127,* 177-187.

Kaplan, L. A., and J. D. Newbold (1993), Biogeochemistry of dissolved organic carbon entering streams, in *Aquatic Microbiology: An Ecological Approach,* edited by T. E. Ford, pp. 139 – 165, Blackwell Sci., Malden,Mass.

Katsuyama, M. and N. Ohte (2002), Determining the sources of stormflow from the fluorescence properties of dissolved organic carbon in a forested catchment, *J. of Hydr.,* 268, 192-202.

Keim, R. F., and A. E. Skaugset (2004), A linear system model of dynamic throughfall rates beneath forest canopies, *Water Resour. Res., 40,* W05208

Keim, R., H. J. Tromp-van Meerveld and J. J. McDonnell (2006), A virtual experiment on the effects of evaporation and intensity smoothing by canopy interception on subsurface stormflow generation, *J. Hydr., 327,* 352-364.

Kendall, K. A., J. B. Shanley and J. J. McDonnell (1999), A hydrometric and geochemical approach to test the transmissivity feedback hypothesis during snowmelt, *J. Hydr. 219*, 188–205.

Kienzler, P. M., and F. Naef (2007), Subsurface storm flow formation at different hillslopes and implications for the 'old water paradox', *Hydrol. Processes*, (in press).

Kim, Y., Darnault, C. J. G., Bailey, N. O., Parlange, J. Y., and T. S. Steenhuis (2005), Equation for describing solute transport in field soils with preferential flow paths, *Soil Sci. Soc. Am. J., 69*, 291-300.

Kirchner, J. W. (2003), A double paradox in catchment hydrology and geochemistry, *Hydrol. Processes, 17*, 871-874.

Kirchner, J. W. (2006), Getting the right answers for the right reasons: Linking measurements, analyses, and models to advance the science of hydrology, *Water Resour. Res., 42*, W03S04, doi:10.1029/2005WR004362.

Kirchner, J. W., X. Feng and C. Neal (2001), Catchment-scale advection and dispersion as a mechism for fractal scaling in stream tracer concentrations, *J. Hydr., 254*, 82-101.

Kirchner, J. W., X. Feng and C. Neal (2001), Catchment-scale advection and dispersion as a mechism for fractal scaling in stream tracer concentrations, *J. Hydr., 254*, 82-101.

Kirda, C., D. R. Nielsen and J. W. Biggar (1973), Simulateneous transport of chloide and water during water infiltration, Soil Sci. Soc. Amer. Proc., 37, 339-345.

Kreft, A., and A. Zuber, (1978), On the physical meaning if the dispersion equation and its solutions for different initial and boundary conditions, *Chem. Eng. Sci., 33*, 1471-1480.

Lajtha, K., Jarrell, W. M., Johnson, D. W., and P. Sollins (1999), Collection of Soil Solution. In: Robertson G. P., and others, Eds. Standard Soil Methods for Long-Term Ecological Research. New York: Oxford, University Press, p 166–182.

Lajtha, K., S. E. Crow, Y. Yano, S. S. Kaushal, E. Sulzman, P. Sollins and J. D. H. Spears (2005), Detrital controls on soil solution N and dissolved organic matter in soils: a field experiment, *Biogeochemistry, 76*, 261-281.

Leenheer, J. A., Brown, G. K., MacCarthy, P., and S. E. Cabaniss (1998), Models of metal binding structures in fulvic acid from the Suwannee River, Georgia, *Environmental Science and Technology, 32*, 2410-2416

Loh, W. Y. (2002), Regression trees with unbiased variable selection and interaction detection. *Statistica Sinica*, 12, 361-386

Loh, W. Y. (2006), Regression by Parts: Fitting Visually Interpretable Models with GUIDE, *Handbook of Computational Statistics*, vol. III, Springer, (in press)

Maraqa, M.A., Wallace, R.B., and T.C. Voice (1997), Effects of degree of water saturation on dispersivity and immobile water in sandy soil columns, *Journal of Contaminant Hydrol. 25*, 199–218.

Martinec, J. (1975), Subsurface flow from snowmelt traced by tritium, *Water Resour. Res., 11*, 496-498.

McCord, J. T., D. B. Stephens, and J. L. Wilson (1991), Hysteresis and state-dependent anisotropy in modeling unsaturated hillslope hydrologic processes, *Water Resour. Res., 27*, 1501–1518.

McDonnell, J. J., (1990), A rationale for old water discharge through macropores in a steep, humid catchment., *Water Resour. Res., 26*, 2821-2832.

McDowell, W. H., W. B. Bowden and C. E. Asbury (1992), Riparian nitrogen dynamics in two geomorphologically distinct tropical rain forest watersheds: subsurface solute patterns, *Biogeochemistry, 18*, 53-75.

McGlynn, B. L., and J. J. McDonnell, Role of discrete landscape units in controlling catchment dissolved organic carbon dynamics, *Water Resour. Res., 39(4),* 1090, doi:10.1029/2002WR001525, 2003.

McGlynn, B., J. J. McDonnell, J. Shanley and C. Kendall (1999), Riparian zone flowpath dynamics during snowmelt in a small headwater catchment, *J. Hydr., 222*,75-92.

McGuire, K. J., (2004), Water residence time and runoff generation in the western Cascades of Oregon, Ph.D., Oregon State University, Corvallis.

McGuire, K. J., and J. J. McDonnell (2006), A review and evaluation of catchment transit time modeling, *J. Hydr., 330*, 543-563.

McGuire, K. J., J. J. McDonnell and M. Weiler (2007), Integrating tracer experiments with modeling to infer water transit times, *Advances in Water Resources, 30,*

McGuire, K. J., McDonnell, J. J., and M. Weiler (2007), Integrating tracer experiments with modeling to infer water transit times, *Advances in Water Resources, 30,* 824-837.

McHale M. R., Mitchell M. J., McDonnell J. J. and C. P. Cirmo(2000), Nitrogen solutes in an Adirondack forested watershed: importance of dissolved organic nitrogen, *Biogeochemistry, 48,*165–184.

McHale, M. R., J. J. McDonnell, M. J. Mitchell, and C. P. Cirmo (2002), A field-based study of soil water and groundwater nitrate release in an Adirondack forested watershed, *Water Resour. Res., 38,*1031,doi:10.1029/2000WR000102.

McHale, M. R., J. J. McDonnell, M. J. Mitchell, and C. P. Cirmo (2002), A field-based study of soil water and groundwater nitrate release in an Adirondack forested watershed, *Water Resour. Res., 38,*1031,doi:10.1029/2000WR000102.

McKnight, D. M., E. W. Boyer, P. K. Westerhoff, P. T. Doran, T. Kulbe, and D. T. Anderson (2001), Spectrofluorometric characterization of dissolved organic matter for indication of precursor organic material and aromaticity, *Limnol. Oceanogr., 46*, 38– 48.

McKnight, D. M., G. M. Hornberger, K. E. Bencala and E. W. Boyer (2002), In-stream sorption of fulvic acid in an acidic stream: A stream-scale transport experiment *Water Resourc. Res. 38(1),* 10.1029/2001WR000269.

McKnight, D. M., R. Harnish, R. L. Wershaw, J. S. Baron, and S. Schiff (1997), Chemical characteristics of particulate, colloidal and dissolved organic material in Loch Vale Watershed, Rocky Mountain National Park, *Biogeochemistry, 36,* 99–124.

Meyer, J. L., B. J. Wallace and S. L. Eggert (1998), Leaf litter as a source of dissolved organic carbon in streams, *Ecosystems,1,* 240–249.

Meyer-Windel, S., B. Lennartz and P. Widmoser (1999), Bromide and herbicide transport under steady state and transient flow conditions, *European Journal of Soil Science, 50,* 23-33.

Michalzik, B., K. Kalbitz, J. H. Park, Solinger, S., and E. Matzner (2001), Fluxes and concentrations of dissolved organic carbon and nitrogen—A synthesis for temperate forests, *Biogeochemistry,* 52, 173–205.

Miller, A. E., Schimel, J. P., Meixner, T., Sickman, J. O. And J. M. Melack (2005), Episodic rewetting enhances carbon and nitrogen release from chaparral soils, *Soil Biology & Biochemistry, 37*, 2195-2204.

Miller, W. R., and J. I. Drever (1977), Water chemistry of a stream following a storm, Absaroka Mountains, Wyoming, *Geol. Soc. Am. Bull., 88,* 286–290.

Montgomery D.R., W. E. Dietrich and J. T. Heffner (2002), Piezometric response in shallow bedrockat CB1: Implications for runoff generation and landsliding, *Water Resour, Res., 38,* 101-1018.

Morris, D., H. Zagarese, C. E. Williamson, E. G. Balseiro, B. R. Hargreaves, B. Modenutti, R. Moeller and C. Queimalinos (1995), The attenuation of solar UV radiation in lakes and the role of dissolved organic carbon, *Limnol. Oceanogr., 40,* 1381–1391.

Mosley, M.P., (1979), Streamflow generation in a forested watershed, *Water Resour. Res., 15,* 795-806.

Mosley, M.P., (1982), Subsurface flow velocities through selected forest soils, South Island, New Zealand, *J. Hydrol., 55,* 65-92

Mulholland, P. J., and W. R. Hill (1997), Seasonal patterns in streamwater nutrient and dissolved organic carbon concentrations: Separating catchment flow path and in-stream effects, *Water Resour. Res., 33,,* 1297-1306.

Nash, J. E., and J. V. Sutcliffe (1970), River flow forecasting through conceptual models, I, A discussion of principles, *J. Hydrol., 10,* 282-290.

Nyberg, L., A. Rodhe and K. Bishop (1999) Water transit times and flow paths from two line injections of 3H and 36Cl in a microcatchment at Gårdsjön, Sweden. *Hydrol. Processes, 13,* 1557-1575.

Ocampo, C. J., C. E. Oldham, M. Sivapalan and J. V. Turner (2006), Hydrological versus biogeochemical controls on catchment nitrate export: a test of the flushing mechanism, *Hydrol. Processes, 20,* 4269 – 4286.

Park, J., J. Lee, S. Kang and S. Kim (2007), Hydroclimatic controls on dissolved organic matter (DOM) characteristics and implications for trace metal transport in Hwangryong River Watershed, Korea, during a summer monsoon period, *Hydrol. Processes, 21*.

Parker, J. C., and M. T. van Genuchten, Flux-averaged and volume averaged

concentrations in continuum approaches to solute transport, *Water Resour. Res., 20*, 866–872, 1984.

Pearce, A. J., M. K. Stewart, and M. G. Sklash (1986), Storm runoff generation in humid headwater catchments, 1, Where does the water come from?, *Water Resour. Res., 22*, 1263–1271.

Perakis S. S. and L. O. Hedin (2002), Nitrogen losses from temperate South American forests mainly as dissolved organic forms, *Nature, 415*, 416- 419.

Plummer, N., J. F. Busby, R. W. Lee and B. B. Hanshaw (1990), Geochemical modeling of the Madison aquifer in parts of Montana, Wyoming, and South Dakota, *Water Resour. Res., 26*, 1981-2014.

Porro, I., and P. J. Wierenga (1993), Transient and steady-state solute transport through a large undisturbed unsaturated column, *Groundwater, 31*, 193-200.

Ranken, D. W., (1974), Hydrologic properties of soil and subsoil on a steep, forested slope, M.S., Oregon State University, Corvallis.

Retter, M., P. Kienzler and P. F. Germann (2006), Vectors of subsurface stormflow in a layered hillslope during runoff initiation, *Hydrology and Earth System Sciences, 10*, 309-320.

Rubin, J. and R. Steinhardt (1963), "Soil water relation during rain infiltration: I. Theory." *Soil Sci. Soc. Am. Proc*., 27, 246–251

Rubin. J.. R. Steinhardt and P. Reiniger (1964), "Soil-water relations during rain infiltration II: moisture content profiles during rains of low intensities." *Proc., Soil Sci. Soc. of Am., 28*, 1-5.

Russo, D., W. A. Jury, and G. L. Butters (1989), Numerical of solute transport during transient irrigation. 1., *Water Resour. Res. 25*, 2109–2118.

Scully, N. M., and D. R. S. Lean (1994), The attenuation of ultraviolet light in temperate lakes, *Ergeb. Limnol., 43*, 101-114.

Sidle, R. C., Y. Tsuboyama, S. Noguchi, I. Hosoda, M. Fujieda, and T. Shimizu (1995), Seasonal hydrologic response at various spatial scales in a small forested catchment, Hitachi Ohta, Japan, *J. Hydrol., 168*, 227-250.

Sidle, S. (2006), Field observations and process understanding in hydrology: essential components in scaling, *Hydrol. Processes, 20*, 1439–1445.

Silver, W. L., D. J. Herman and M. K. Firestone (2001), Dissimilatory nitrate reduction to ammonium in upland tropical forest soils, *Ecology, 82(9)*, 2410-2416.

Sivapalan, M. (2003), Process complexity at hillslope scale, process simplicity at the watershed cale: is there a connection? *Hydrol. Processes, 17*, 1037-1041.

Sklash, M.G., M.K. Stewart, and A.J. Pearce (1986), Storm runoff generation in humid headwater catchments: A case study of hillslope and low-order stream response, *Water Resour. Res., 22*, 1273-1282.

Sollins P., C. C. Grier, F. M. McCorison, K. J. Cromack, R. Fogel and R. L. Fredriksen (1980), The internal element cycles of an oldgrowth Douglas-fir ecosystem in western Oregon. *Ecol. Monogr. 50*, 261–285.

Sollins, P., K. J. Cromack, F. M. McCorison, R. H. Waring, and R. D. Harr, (1981), Changes in nitrogen cycling at an old-growth Douglas-fir site after

disturbance, *J. Enivron. Qual.,, 10*, 37-42.

Solomatine, D. P. and Y. Xue (2004), M5 Model Trees and Neural Networks: Application to Flood Forecasting in the Upper Reach of the Huai River in China *Journal of Hydrologic Engineering, 9*, 491-501

Sudheer, K. P, A. K. Gosain, K. S. Ramasastri (2002), A data-driven algorithm for constructing artificial neural network rainfall-runoff models, *Hydrol. Process.*, 16, 1325–1330

Swank, W. T., J. W. Fitzgerald and J. T. Ash (1984), Microbial transformation of sulfate in forest soils, *Science, 223*, 182-184.

Swanson, F. J., and M. E. James, (1975), Geology and geomorphology of the H.J. Andrews Experimental Forest, western Cascades, Oregon., Res. Pap. PNW-188, U.S. Department of Agriculture, Forest Service, Pacific Northwest Forest and Range Experiment Station, Portland, OR.

Swistock, B. R., D. R. DeWalle, and W. E. Sharpe (1989), Sources of acidic storm flow in an Appalachian headwater stream, *Water Resour. Res., 25,* 2139–2147.

Tani, M. (1997), Runoff generation processes estimated from hydrological observations on a steep forested hillslope with a thin soil layer, *J. Hydrol.*, 200, 84-109.

Tiedje, J. M., (1988), Ecology of denitrification and dissimilatory nitrate reduction to ammonium, in: Zehnder AJB (ed) Biology of Anaerobic Microorganisms, pp 179–244. John Wiley and Sons, New York

Torres, R., W. E. Dietrich, D. R. Montgomery, S. P. Anderson, and K. Loague, (1998), Unsaturated zone processes and the hydrologic response of a steep, unchanneled catchment, *Water Resour. Res., 34*, 1865-1879.

Triska, F. J., J. R. Sedell, K. Cromack, S. V. Gregory, and F. M. McCorison, (1984), Nitrogen budget for a small coniferous forest stream, *Ecological Monographs, 54*, 119-140.

Triska, F. J., J. R. Sedell, K. Cromack, S. V. Gregory, and F. M. McCorison, (1984), Nitrogen budget for a small coniferous forest stream, *Ecological Monographs, 54*, 119-140.

Tromp-van Meerveld, H. J., and J. J. McDonnell (2006), Threshold relations in subsurface stormflow: 2. The fill and spill hypothesis, *Water Resour. Res., 42,* W02411, doi:10.1029/2004WR003800.

Tsuboyama Y, R. C. Sidle, S. Noguchi, and I. Hosoda (1994), Flow and solute transport through the soil matrix and macropores of a hillslope segment. *Water Resour. Res., 30,* 879–880.

Tymchak, M. P., and R. Torres (2007), Effects of variable rainfall intensity on the unsaturated zone response of a forested sandy hillslope, *Water Resour. Res., 43*, W06431, doi:10.1029/2005WR004584.

Uchida, T., I. Tromp-van Meerveld and J. J. McDonnell (2005), The role of lateral pipe flow in hillslope runoff response : an intercomparison of non-linear hillslope response, *J. Hydrol.*, 311, 117-133.

Uchida, T., Kosugi, K. and T. Mizuyama (2001), Effects of pipeflow on hydrological

process and its relation to landslide: a review of pipeflow studies in forested headwater catchments, *Hydrol. Processes*, *15*, 2151-2174

Uchida, T., Y. Asano, N. Ohte, and T. Mizuyama (2003), Seepage area and rate of bedrock groundwater discharge at a granitic unchanneled hillslope, *Water Resouces Research, 39*, 10.1029/2002WR001298.

Van Genuchten, M. T., and P. J. Wierenga (1976), Mass transfer studies in sorbing porous media I, Analytical solutions, *Soil Sci. Soc. Am. J., 410*, 473-480.

Van Genuchten, M. T., and P. J. Wierenga (1977), Mass transfer studies in sorbing porous media II, Experimental evaluation with tritium (^3H_2O), *Soil Sci. Soc. Am. J., 41*, 278-285.

Van Verseveld, W. J. (2007), Hydro-biogeochemical coupling at the hillslope and catchment scale, Ph.D., Oregon State University, Corvallis.

Vanderbilt, K. L., K. Lajtha and F. J. Swanson (2003), Biogeochemistry of unpolluted forested watersheds in the Oregon Cascades: temporal patterns of precipitation and stream nitrogen fluxes, *Biogeochemistry, 62*, 87–117.

Victory, N. I. (2007), Quantification of Advection and Dispersion in Lateral Subsurface Flowpaths at the Hillslope-scale, M.S.., Oregon State University, Corvallis.

Vidon, P. G. F., and A. R. Hill (2004), Landscape controls on nitrate removal in stream riparian zones, *Water Resour. Res., 40,* W03201, doi:10.1029/2003WR002473.

Vitousek, P.M., L. O. Hedin, P. A. Matson, J. H. Fownes and J. Neff (1998), Within-system element cycles, input-output budgets, and nutrient limitation. In: *Successes, Limitations, and Frontiers in Ecosystem Science.* Pace, M. and Groffman, P. (eds). p. 432–451.

Wagener, T., D. P. Boyle, M. J. Lees, H. S. Wheater, H. V. Gupta and S. Sorooshian (2001), A framework for development and application of hydrological models, *Hydrology and Earth System Sciences*, *5*(1), 13–26.

Walling, D. E., and I. D. L. Foster (1975), Variations in natural chemical concentration of river water during flood flows, and the lag effect: Some further comments, *J. Hydrol., 26*, 237–244.

Weiler, M. and J.J. McDonnell (2006), Testing nutrient flushing hypotheses at the hillslope scale: A virtual experiment approach. Journal of Hydrology, 319: 339–56.

Weiler, M., B. L. McGlynn, K. J. McGuire, and J. J. McDonnell (2003), How does rainfall become runoff? A combined tracer and runoff transfer function approach, *Water Resour. Res., 39,* 1315, doi:10.1029/2003WR002331.

Weiler, M., J. McDonnell, H. J. Tromp-van Meerveld and T. Uchida (2005), Subsurface Stormflow. Encyclopedia of Hydrological Sciences.Wiley and Sons.Whipkey.

Weishaar, J. L., G. R. Aiken, B. A. Bergamaschi, M. S. Fram, R. Fujii and K. Mopper (2003), Evaluation of Specific Ultraviolet Absorbance as an Indicator of the Chemical Composition and Reactivity of Dissolved Organic Carbon, *Environ. Sci. Technol., 37*, 4702-4708.

Weyman, D.R. (1973), Measurements of the downslope flow of water in a soil, *J. Hydrol., 20*, 267-288.

Whipkey, R.Z. (1965), Subsurface stormflow from forested slopes, *Int. Ass. Sci. Hydrol. Bull.,10*, 74-85.

Wierenga, P. J. (1977), Solute distribution profiles computed with steady-state and transient water movement models, *Soil Sci. Soc. Am. J. 41*, 1050–1055.

Williams, A. G., J. F. Dowd and E. W. Meyles (2002), A new interpretation of kinematic stormflow generation, *Hydrol. Process.,16*, 2791–2803.

Woods, R., and L. Rowe (1996), The changing spatial variability of subsurface flow across a hillside, *Journal of hydrology. New Zealand, 35*, 51-86.

Yano, Y., K. Lajtha, P. Sollins and B. A. Caldwell (2004), Chemical and seasonal controls on the dynamics of dissolved organic matter in a coniferous old-growth stand in the Pacific Northwest, USA, *Biogeochemistry, 71,* 197-223.

Yano, Y., K. Lajtha, P. Sollins and B. A. Caldwell (2005), Chemistry and Dynamics of Dissolved Organic Matter in a Temperate Coniferous Forest on Andic Soils: Effects of Litter Quality, *Ecosystems, 8,* 286-300.